

1984

# Effects of N-substituents on the Polymerization Properties of Maleimide

Dilip R. Abayasekara  
drdilip@centralpenn.edu

Follow this and additional works at: <http://scholarscompass.vcu.edu/etd>

 Part of the [Chemistry Commons](#)

© The Author

---

Downloaded from

<http://scholarscompass.vcu.edu/etd/4333>

This Dissertation is brought to you for free and open access by the Graduate School at VCU Scholars Compass. It has been accepted for inclusion in Theses and Dissertations by an authorized administrator of VCU Scholars Compass. For more information, please contact [libcompass@vcu.edu](mailto:libcompass@vcu.edu).

COLLEGE OF HUMANITIES AND SCIENCES  
VIRGINIA COMMONWEALTH UNIVERSITY

This is to certify that the dissertation prepared by DILIP RANJITHA ABAYASEKARA entitled EFFECTS OF N-SUBSTITUENTS ON THE POLYMERIZATION PROPERTIES OF MALEIMIDE has been approved by his committee as satisfactory completion of the dissertation requirements for the degree of Doctor of Philosophy.

[Redacted Signature]

Director of Dissertation

[Redacted Signature]

Committee Member

[Redacted Signature]

Committee Member

[Redacted Signature]

Committee Member

[Redacted Signature]

Committee Member

[Redacted Signature]

D

[Redacted Signature]

College Dean

October 12, 1984

Date



Dilip R. Abayasekara

1984

---

All Rights Reserved

TO

SHARON

Effects of N-Substituents on the  
Polymerization Properties of Maleimide

A dissertation submitted in partial fulfillment of the  
requirements for the degree of Doctor of Philosophy  
at Virginia Commonwealth University

by

Dilip R. Abayasekara

A.A. Palm Beach Junior College, 1975  
B.S. University of Florida, 1978

Director: Dr. Raphael M. Ottenbrite  
Professor of Chemistry  
Virginia Commonwealth University  
Richmond, Virginia  
December, 1984

ACKNOWLEDGMENTS

I would like to express my deep appreciation and gratitude to:

Dr. Raphael Ottenbrite for his help and guidance during the course of this research and for introducing me to the fascinating area of polymer chemistry.

The members of the faculty of the Department of Chemistry for their ready advice and assistance and the graduate students, particularly those in Dr. Raphael Ottenbrite's laboratory, for their friendship and help over the years.

Mrs. Susan Marsh and Dr. Albert Sneden for obtaining the NMR spectra.

Miss Linda Maillet for her help with the UV spectra.

Dr. Syang Yang Su and Ebenezer Asafu-Adjaye for their generous help with high pressure liquid chromatography.

Dr. Ryozo Takatsuka and Dr. Sarah Rutan for help with calculations and statistical analysis.

Dr. Billy Stump, who was as much concerned for my personal well-being as for my experimental results.

A special thank you goes to my wife, Sharon, for her patience, understanding, encouragement and sacrifices during the completion of this research project.

## Table of Contents

	Page
LIST OF TABLES . . . . .	vi
LIST OF FIGURES . . . . .	x
SCHEME 1 . . . . .	xv
LIST OF ABBREVIATIONS . . . . .	xvi
LIST OF SYMBOLS. . . . .	xviii
ABSTRACT . . . . .	xix
INTRODUCTION . . . . .	1
A. Heparinoids . . . . .	1
B. Pyran . . . . .	2
C. Amidated Polymers . . . . .	4
D. Amidated Polymers Containing Imide Rings.	7
E. Comparison of Copolymerization Behavior of Maleic Anhydride and Maleimide . . . . .	10
F. The Q-e Scheme and Role of Charge- Transfer Complexes . . . . .	13
G. Effects of N-Substituents on the Copolymerization Behavior of Maleimide . . . . .	15
H. Effect of N-Substituents on the Charge- Transfer Complexation of Maleimide . . . . .	23
RESEARCH AIM . . . . .	29
RESULTS AND DISCUSSION . . . . .	31
Complexation Studies . . . . .	41
Charge-Transfer Complexes . . . . .	41
Complexation Studies Utilizing Ultraviolet (UV) Spectroscopy . . . . .	42
Complexation Studies Utilizing $^1\text{H}$ NMR Spectroscopy . . . . .	52

## Table of Contents Continued

	Page
Copolymerizations and Homopolymerizations of N-Substituted Maleimides . . . . .	107
Effect of Electron-Withdrawing Groups on Maleimide Reactivity . . . . .	110
Copolymers of Maleic Anhydride with N-Substituted Maleimides . . . . .	112
<sup>13</sup> C NMR Spectroscopy of Polymers. . . . .	119
NMR Spectra . . . . .	122
N-Carbamylmaleimide-Styrene Copolymers .	122
N-Carbethoxymaleimide Copolymers . . . . .	125
Alternation in Copolymer Structure. . . . .	127
High Pressure Liquid Chromatography . . . . .	139
EXPERIMENTAL . . . . .	145
General . . . . .	145
Purification of Materials . . . . .	146
Monomer Syntheses . . . . .	147
N-Phenylmaleimide(1) . . . . .	147
A. Maleanilic Acid (2) . . . . .	148
B. N-Phenylmaleimide (1) . . . . .	148
N-Carbamylmaleimide (5). . . . .	149
A. N-Carbamylmaleamic acid (6) . .	149
B. N-Carbamylmaleimide (5) . . . . .	150
Maleimide (7). . . . .	151
N-Carbethoxymaleimide (8) . . . . .	152



## Table of Contents Continued

	Page
Copolymer Syntheses . . . . .	153
Copolymerizations of Electron-donor Monomers with Electron-acceptor Monomers . . . . .	153
Copolymerizations of N-Substituted Maleimides with Maleic Anhydride . . . . .	154
Homopolymer Syntheses . . . . .	155
Polymer Characterization . . . . .	157
Copolymers . . . . .	158
Homopolymers . . . . .	159
Rates of Conversion of Copolymers . . . . .	160
Complexation Studies . . . . .	162
Complex Study by $^1\text{H}$ NMR-Spectroscopy . . . . .	162
Complex Study by UV Spectroscopy . . . . .	165
High Pressure Liquid Chromatography . . . . .	168
Viscosities . . . . .	172
BIBLIOGRAPHY . . . . .	174
APPENDIX . . . . .	182
VITA . . . . .	207

## List of Tables

Table		Page
I	Ethylene/Maleic Anhydride Series (Hydrolysed Form).....	5
II	Polyacrylic and Polymethacrylic Series.....	6
III	$r$ , $Q$ , $e$ , Values for Some Maleimides....	16
IV	Carbonyl Absorption Bands in the Infrared Spectrum of N-alkylmaleimides .....	20
V	Monomer Reactivity Ratios for Styrene ( $M_1$ ) - N-(4-substituted phenyl) Maleimides ( $M_2$ ) and $Q_2$ , $e_2$ values of N-(4-substituted phenyl) Maleimides....	22
VI	Monomer Reactivity Ratios for Methyl Methacrylate ( $M_1$ ) - N-(4-substituted phenyl) Maleimides ( $M_2$ ) and $Q_2$ , $e_2$ Values of N-(4-substituted phenyl) Maleimides.....	22
VII	$^{13}\text{C}$ -NMR Chemical Shifts of Maleimide and N-Substituted Maleimides.....	35
VIII	IR Ring Carbonyl Stretching Frequencies of Maleic Anhydride, Maleimide, and N-Substituted Maleimides.....	36
IX	Summary of Charge-Transfer Absorptions Involving Styrene.....	44
X	Summary of Charge-Transfer Absorptions Involving Furan.....	47
XI	$^1\text{H}$ NMR Data for the Determination of Equilibrium Constant of Complexation of the Maleic Anhydride-Styrene System....	56
XII	$^1\text{H}$ NMR Data for the Determination of Equilibrium Constant of Complexation of the N-Carboethoxymaleimide-Styrene System.....	58

## List of Tables Continued

Table		Page
XIII	$^1\text{H}$ NMR Data for the Determination of Equilibrium Constant of Complexation of the N-Carbamylmaleimide-Styrene System .....	60
XIV	$^1\text{H}$ NMR Data for determination of Equilibrium Constant of Complexation of the N-Phenylmaleimide-Styrene System.....	62
XV	$^1\text{H}$ NMR Data for the Determination of Equilibrium Constant of the Maleimide Styrene System.....	64
XVI	$^1\text{H}$ NMR Data for Determination of Equilibrium Constant of Complexation for the Maleimide-Styrene System.....	65
XVII	Calculated Equilibrium Constants of Complexation (K) Based on $^1\text{H}$ NMR Data in $\text{CDCl}_3$ .....	67
XVIII	$^1\text{H}$ NMR Data for Determination of Equilibrium Constant of Complexation of the Maleic Anhydride-Furan System.....	71
XIX	$^1\text{H}$ NMR Data for Determination of Equilibrium Constant of Complexation of the N-Carbamylmaleimide-Furan System...	73
XX	$^1\text{H}$ NMR Data for Determination of Equilibrium of Constant of Complexation of the N-Carboethoxymaleimide-Furan System.....	75
XXI	$^1\text{H}$ NMR Data for Determination of Equilibrium Constant of Complexation of the N-Phenylmaleimide-Furan System.....	77
XXII	$^1\text{H}$ NMR Data for Determination of Equilibrium Constant of Complexation of the N-Ethylmaleimide-Furan System.....	79
XXIII	$^1\text{H}$ NMR Data for Determination of Equilibrium Constant of Complexation of the Maleimide-Furan System.....	81

## List of Tables Continued

Table		Page
XXIV	<sup>1</sup> H NMR Data for Determination of Equilibrium Constant of Complexation (K) of the Maleimide-Furan System.....	83
XXV	Calculated Equilibrium Constants of Complexation (K) Based on <sup>1</sup> H NMR Data in CDCl <sub>3</sub> .....	84
XXVI	<sup>1</sup> H NMR Data for Attempted Determination of Equilibrium Constant of Complexation of the Maleic Anhydride - 2-Chloroethyl Vinyl Ether System.....	88
XXVII	<sup>1</sup> H NMR Data for Attempted Determination of Equilibrium Constant of Complexation (K) of the Maleic Anhydride-Vinyl Ether System.....	89
XXVIII	Attempted Determination of Equilibrium Constants of Complexation (K) Based on <sup>1</sup> H NMR Data in CCl <sub>4</sub> .....	90
XXIX	<sup>1</sup> H NMR Data for Attempted Determination of Equilibrium Constant of Complexation of the N-Carbethoxymaleimide - 2-Chloroethyl Vinyl Ether System.....	93
XXX	<sup>1</sup> NMR Data for Attempted Determination of Equilibrium Constant of Complexation of the Maleimide - 2-Chloroethyl Vinyl Ether System.....	95
XXXI	<sup>1</sup> H NMR Data for Attempted Determination for Equilibrium Constant of Complexation of the N-Ethylmaleimide - 2-Chloroethyl Vinyl Ether System.....	97
XXXII	<sup>1</sup> H NMR Data for the Determination of Equilibrium Constant of Complexation of the Maleic Anhydride-Furan System.....	99
XXXIII	<sup>1</sup> H NMR Data for the Determination of Equilibrium Constant of Complexation of the N-Carbamylmaleimide-Furan System...	101

## List of Tables Continued

Table		Page
XXXIV	Effect of Solvent on the Chemical Shift of Maleic Anhydride Olefinic Protons and Effect of Concentration of Electron-Donor Species on Solvent Chemical Shifts.....	105
XXXV	Effect of Solvent on the Chemical Shift of N-Carbamylmaleimide Olefinic Protons and Effect of Concentration of Furan on Solvent Chemical Shifts.....	106
XXXVI	Data for NCMI-Styrene Copolymerization .....	108
XXXVII	Effect of Solvent on Rate of Conversion to Polymer for Homopolymerization of N-Carbamylmaleimide (NCMI) and Copolymerization of NCMI with Styrene (Sty).....	111
XXXVIII	Comparison of Rates of Conversion.....	113
XXXIX	Data for the Copolymerization of Maleic Anhydride (MA) and N-Phenylmaleimide...	114
XL	Data for the Copolymerization of Maleic Anhydride (MA) with N-Ethylmaleimide (NEMI) in Acetone at 65 C.....	116
XLI	Viscosities of N-Phenylmaleimide Maleic Anhydride Copolymers.....	120
XLII	<sup>1</sup> H NMR Integration Ratios of Aromatic Protons (H <sub>a</sub> ) to Aliphatic Protons (H <sub>o</sub> ) for NCMI-Styrene and NCEMI-Styrene Copolymers.....	135
XLIII	Elemental Analysis Data for NCMI-Styrene and NCEMI-Styrene Copolymers.....	136
XLIV	Copolymer Compositions of NCMI-Styrene and NCEMI-Styrene Copolymers.....	137
XLV	Decomposition Points of Homopolymers and Copolymers.....	184

## List of Figures

Figure		Page
1	Copolymerization diagram for Styrene-maleic anhydride, Styrene-N-phenylmaleimide, Styrene-maleimide...	12
2	A Proposed Charge-Transfer Complex.....	15
3	Comparison of X-ray Crystallography Structures of Maleic Anhydride and Maleimide.....	17
4	Resonance in Maleimide.....	18
5	Plots of $Q_2$ and $e_2$ obtained from the Copolymerization with MMA( $M_1$ ) vs $\sigma^*$ Constant for N-alkylmaleimide.....	20
6	Plot of $e_2$ value vs. $\sigma$ for R of N-(4-RP) MI.....	24
7	Plot of $\log 1/r_2$ vs $\sigma$ for R of N-(4-RP) MI.....	24
8	$K \epsilon^{295}$ vs. Hammett Constants for Various Para Substituted Maleimide-CEVE Complexes in Dichloromethane.....	26
9	Mole Fraction Cis Succinimide Units in N-Arylmaleimide-CEVE Copolymers vs. Hammett $\sigma$ Constant.....	28
10	$K \epsilon^{295}$ vs. Mole Fraction as Succinimide Units in N-Substituted Maleimide-CEVE Copolymers.....	28
11	Substituent Groups that were Utilized for Investigation of N-Substituent Effects on Polymerization Properties of Maleimides.....	33
12	H-Bonding in Maleimide (MI) and N-Carbamylmaleimide (NCMI).....	37
13	IR Spectrum of N-Carbamylmaleimide (NCMI) in Solid Phase (KBr Solvent)....	39
14	IR Spectrum of Maleimide (MI) in Solid Phase (KBr Solvent).....	40

## List of Figures Continued

Figure		Page
15	Continuous Variation Method Applied to the Charge Transfer Absorption of MA-Styrene; NCEMI-Styrene; NPMI-Styrene .....	45
16	Continuous Variation Method Applied to the Charge-Transfer Absorption of 291 nm in the MA-Furan System.....	48
17	Continuous Variation Method Applied to the Charge-Transfer Absorption in the MA-Furan System.....	49
18	Continuous Variation Method Applied to the Charge-Transfer Absorption in the NCMI-Furan System.....	50
19	Chemical Shifts of Protons on Acceptor (A) Molecules.....	53
20	<sup>1</sup> H NMR Chemical Shifts of Maleic Anhydride (MA) with Several Concentrations of Styrene.....	55
21	<sup>1</sup> H NMR Chemical Shifts of N-Carbethoxymaleimide (NCEMI) with Several Concentrations of Styrene.....	57
22	<sup>1</sup> H NMR Chemical Shifts of Olefinic Proton of N-Carbamylmaleimide (NCMI) with Several Concentrations of Styrene .....	59
23	<sup>1</sup> H NMR Shifts of Olefinic Proton of N-Phenylmaleimide (NPMI) with Several Concentration of Styrene.....	61
24	<sup>1</sup> H NMR Chemical Shifts of Maleimide (MI) with Several Concentrations of Styrene.....	63
25	<sup>1</sup> H NMR Determination of the Equilibrium Constant of Complexation between Styrene and Electron-Acceptors.....	66

## List of Figures Continued

Figure		Page
26	$^1\text{H}$ NMR Chemical Shifts of Maleic Anhydride (MA) with Several Concentrations of Furan.....	70
27	$^1\text{H}$ NMR Chemical Shifts of Olefinic Protons of N-Carbamylmaleimide (NCMI) with Several Concentrations of Furan...	72
28	$^1\text{H}$ NMR Chemical Shifts of Olefinic Protons of Maleimide (MI) with Several Concentrations of Furan.....	74
29	$^1\text{H}$ NMR Chemical Shifts of Olefinic Protons of N-Carbethoxymaleimide (NCEMI) with Several Concentrations of Furan.....	76
30	$^1\text{H}$ NMR Chemical Shifts of Olefinic Protons of N-Phenylmaleimide (NPMI) with Several Concentrations of Furan...	78
31	$^1\text{H}$ NMR Chemical Shifts of Olefinic Protons of N-Ethylmaleimide (NEMI) with Several Concentrations of Furan.....	80
32	$^1\text{H}$ NMR Determination of the Equilibrium Constant of Complexation between Furan and Electron-Acceptors.....	85
33	$^1\text{H}$ NMR Chemical Shifts of Olefinic Protons of Maleic Anhydride (MA) with Several Concentrations of 2-Chloroethyl Vinyl Ether (CEVE).....	87
34	$^1\text{H}$ NMR Chemical Shifts of Olefinic Proton of N-Carbethoxymaleimide (NCEMI) with Several Concentrations of 2-Chloroethyl Vinyl Ether (CEVE).....	92
35	$^1\text{H}$ NMR Chemical Shifts of Olefinic Protons of Maleimide (MI) with Several Concentrations of 2-Chloroethyl Vinyl Ether (CEVE).....	94



## List of Figures Continued

Figure		Page
36	$^1\text{H}$ NMR Chemical Shifts of Olefinic Protons of N-Ethylmaleimide (NEMI) with Several Concentrations of 2-Chloroethyl Vinyl Ether (CEVE).....	96
37	$^1\text{H}$ NMR Chemical Shifts of Maleic Anhydride with Several Concentrations of Furan.....	98
38	$^1\text{H}$ NMR Chemical Shifts of Olefinic Protons of N-Carbamylmaleimide (NCMI) with Several Concentrations of Furan...	100
39	Solvent effect on the NMR determination of the equilibrium constant of complexation between N-Carbamylmaleimide and Furan at 30.0 .....	103
40	Solvent effect in the NMR determination of the equilibrium constant of complexation between Maleic Anhydride and Furan of 30 C.....	104
41	Relationship between Mole Fraction of NCMI in Feed and Rate of conversion of the Copolymerization of NCMI with Styrene.....	109
42	90 MHz $^1\text{H}$ NMR Spectrum of Poly (N-Phenylmaleimide - co-maleic anhydride-13).....	117
43	60MHz NMR Spectrum of Poly (N-ethylmaleimide - co-maleic anhydride).....	118
44	Relationship between monomer feed and copolymer composition for NPMI and MA..	121
45	90 MHz $^1\text{H}$ NMR Spectrum of Poly (N-Carbamylmaleimide - co-styrene).....	123
46	Off-resonance $^{13}\text{C}$ NMR Spectrum of Poly (N-Carbamylmaleimide - co-styrene).....	124
47	90 MHz $^1\text{H}$ NMR Spectrum of Poly (N-Carbethoxymaleimide - co-styrene)...	126

## List of Figures Continued

Figure		Page
48	$^{13}\text{C}$ NMR Spectrum of Poly (N-Carboethoxymaleimide - co-styrene)...	128
49	Off-resonance $^{13}\text{C}$ NMR Spectrum of Poly (N-Carboethoxymaleimide -co-styrene)...	129
50	Calculated chemical Shift Values (ppm) for Internal Carbons of Possible Triads for NCEMI-Styrene Copolymers.....	132
51	Calibration curve for NCMI/Dioxane solutions at concentrations of $1.0 \times 10^{-3}$ - $5.0 \times 10^{-2}$ M.....	142
52	Calibration curve for NCMI in NCMI/- Styrene/Dioxane at NCMI concentration of $1.0 \times 10^{-3}$ - $5.0 \times 10^{-2}$ M .....	143

## Scheme 1

Page

Synthesis of EMA Copolymer Containing Imide, Amide, and Carboxylate Salt Functions . . . . .	8
---	---

## List of Abbreviations

A	-	Electron acceptor
AIBN	-	2,2'-Azobisisobutyronitrile
BPO	-	Benzoylperoxide
C	-	Concentration
CEVE	-	2-Chloroethyl vinyl ether
CT	-	Charge-transfer
CTC	-	Charge-transfer band
D	-	Electron donor
DMF	-	N,N-dimethylformamide
DMSO	-	Dimethylsulfoxide
dL	-	Deciliter
g	-	Gram
H <sub>a</sub>	-	Aromatic protons
H <sub>O</sub>	-	Aliphatic protons
HPLC	-	High Pressure Liquid Chromatography
Hz	-	Hertz
IR	-	Infrared
K	-	Equilibrium Constant
L	-	Liter
LD <sub>50</sub>	-	Dose that kills 50% of a test group as compared to a control group
mL	-	Milliliter
M	-	Monomer
MA	-	Maleic Anhydride

## List of Abbreviations Continued

MI	-	Maleimide
NBMI	-	N-bornylmaleimide
NCMI	-	N-carbamylmaleimide
NCEMI	-	N-carbethoxymaleimide
NEMI	-	N-ethylmaleimide
NPMI	-	N-phenylmaleimide
N-(4-RP)MI	-	N-(4-substituted phenyl) maleimide.
NMR	-	Nuclear Magnetic Resonance
ppm	-	Parts per million
r	-	Monomer reactivity ratio
UV	-	Ultraviolet
W/V	-	Weight of solute per volume of solvent
W/W	-	Weight of solute per weight of solvent

## List of Symbols

$\delta$	-	Chemical Shifts in parts per million
$\epsilon$	-	Molar absorptivity
$[\eta]$	-	Intrinsic viscosity
$\eta_{red}$	-	Reduced viscosity
$\eta_{sp}$	-	Specific viscosity
$\sigma$	-	Hammett sigma constant

## ABSTRACT

The effect of the amide function and the carbethoxy function on the polymerization properties of maleimide are reported. The effects of these functions on homopolymerization and copolymerization (with styrene) were examined. These electron-withdrawing groups appeared to decrease the rate of homopolymerization and increase the rate of copolymerization.

N-carbamylmaleimide and N-carbethoxymaleimide were copolymerized with styrene in 1,4-dioxane at 60.0° C at different feed ratios to high conversion. Copolymer composition, determined by elemental analysis and <sup>1</sup>H NMR, indicated that while 1:1 copolymers were obtained with an equimolar feed ratio, the two systems were not alternating. It is of note that the copolymerizations were carried out at a very low total monomer concentration of 0.2 mol/L due to the limited solubility of N-carbamylmaleimide in the reaction solvent. If higher concentrations had been possible, 1:1 copolymer formation would have been enhanced.

Investigation of the complexation of maleic anhydride, maleimide, N-carbethoxymaleimide, N-carbamylmaleimide, N-phenylmaleimide and N-ethylmaleimide with the electron-donors styrene, furan, and 2-chloroethyl vinyl-ether was accomplished by use of ultraviolet (UV)

spectroscopy and  $^1\text{H}$  NMR spectroscopy. It appeared generally that the electron-withdrawing groups increased the complexation of maleimide with the electron-donating comonomers. There was no evidence of complex formation with 2-chloroethyl vinyl ether for any of the compounds studied.

A continuous variation method using UV spectroscopy indicated that all observed charge-transfer complexes (maleic anhydride-styrene; N-carbethoxymaleimide-styrene; N-phenylmaleimide-styrene; maleic anhydride-furan; N-carbamylmaleimide-furan) had 1:1 stoichiometry. The formation constant of complexation between maleimide and styrene was increased towards the value of the complex formation constant for maleic anhydride-styrene when the electron-withdrawing groups  $-\text{CONH}_2$  and  $-\text{CO}_2\text{Et}$  were substituted on the maleimide N. The same effect was not observed for complexation with furan.

IR spectroscopy and  $^{13}\text{C}$  NMR spectroscopy indicate that the electron-withdrawing groups increase the double bond character of the maleimide carbonyl groups. The results of the complexation studies suggest that the carbonyl groups of maleimide may play a significant role in complex formation with styrene. The mechanism of complex formation with furan appears to be different from that of styrene.



It was also shown that when N-phenylmaleimide and maleic anhydride (both electron-accepting monomers) are copolymerized, a random copolymer results.

When reaction with styrene is considered, the results of this investigation indicate that electron-withdrawing N-substituents influence the polymerization properties of maleimide to be more like those of maleic anhydride.

## INTRODUCTION

Natural and synthetic polyanionic materials have been investigated for biological activity against tumors, viruses, bacteria, fungi, and enzymes (1,2). Many of these materials exhibit a broad spectrum of biological activity as well as prolonged prophylactic effects. Consequently, an impetus has developed for investigating the physico-chemical characteristics and modes of action of these macromolecules. By the investigation of synthetic polymers with defined structure and composition, it is hoped that meaningful structure-activity relationships can be obtained.

### A. Heparinoids

The first natural polyanion to receive considerable biological interest was heparin, a potent anti-coagulant. In 1962 Ascoli and Botre (3) found that the anti-coagulating activity of heparin was directly related to its calcium binding capacity. Calcium binding may also be a mechanism for heparin's antimitotic activity and inhibition of tumor growth (3,4). Attempts to develop synthetic or natural substituents similar to heparin have produced a number of polyanions that exhibit antimitotic activity (4,5).

One of the earliest synthetic polyelectrolytes to be studied for biological activity was sodium poly(ethylene-sulfonate) by Breslow and Hulse in 1954 (6). Subsequent

work by Regelson and Holland (7) established that in mice, this polyanion is an effective antineoplastic agent against Adenocarcinoma 775, L1210 lymphoid leukemia, Krebs 2 carcinoma (ascites), L5178 lymphatic leukemia, Ehrlich (ascites) and Sarcoma 180. Unfortunately, the tumor inhibitory activity was too low and the toxicity was too great in man for clinical applications (8).

## B. Pyran

The synthetic polymer that has received the most interest is divinyl ether-maleic anhydride copolymer, commonly referred to as pyran copolymer due to the tetrahydrofuran ring that was reported to form during polymerization (9). In the literature it is also referred to by the acronym DIVEMA (divinyl ether-maleic anhydride copolymer) and, more recently, as MVE (maleic anhydride-vinyl ether copolymer). Pyran was first reported by Butler in 1960 (9) and was submitted to the National Institutes of Health (NIH) for screening for biological activity. Independently, Breslow of Hercules Corporation also synthesized pyran and submitted it to the NIH screen. Pyran showed significant activity and was designated as NSC 46015 by the National Cancer Institute. It has been under investigation for use in cancer chemotherapy and has been found to have a wide range of other biological activities (2). Pyran has interferon inducing capacity (10-13); it is active against a number of viruses (10-18) including Friend

leukemia, Rauscher leukemia, Maloney sarcoma, polyoma, vesicular stomatitis, mengo, encephalomyocarditis, and foot-and-mouth disease; it has antibacterial (19-21) and antifungal activity (19); it stimulates immune response (19-25) and is a blood anticoagulant (26). Pyran inhibits adjuvant disease (27,28), a hypersensitive reaction to mycobacterial antigens, similar to rheumatoid arthritis and also shows potential for removing plutonium from the liver (29).

In early clinical trials, pyran NSC 46015 was too toxic in human patients (2,30). Specifically, it caused thrombocytopenia, a condition characterized by a decrease in the absolute number of thrombocytes in the blood circulation. Its other toxic effects involved cytoplasmic inclusions throughout the blood as well as in liver and spleen cells of the reticuloendothelial system (RES), inhibition of microsomal enzymes, sensitization to endotoxin and enlargement of the liver (hepatomegaly) and spleen (splenomegaly) (28). At high dosages (12 mg/kg/day), pyran NSC 46015 induced fever and blocked the conversion of fibrinogen to fibrin. Although the toxicity of pyran NSC 46015 was initially too high for further clinical investigations, it has recently been shown (2,31) that these toxicities are less prevalent for lower molecular weight material and when 6-7% calcium is included with the sodium salt of pyran. These findings have

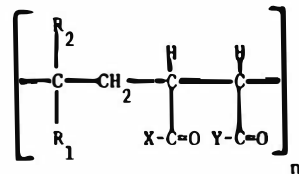
prompted a detailed phase I clinical study of MVE-2, a low molecular weight, narrow polydispersed form of the drug.

### C. Amidated Polymers

Regelson et al. (32) investigated the hypothesis that the inhibition of tumor growth may be a function of the density and distribution of ionic charges on the polyelectrolyte molecule. Polycarboxylates of ethylene-maleic anhydride (EMA) copolymers and those derived from polyacrylic acid were evaluated. The charge density and solution configuration of these compounds were varied over a wide range by placing substituents on the backbone of the molecule and by substituting other groups for some of the carboxyl groups, as shown in Table I and Table II. The hydrolyzed ethylene maleic anhydride copolymer (HEMA) has the dicarboxylic structure and the ammoniated EMA copolymer (AEMA) has the half amide- half acid form. The principle tumor in the study was sarcoma 180. When activity was observed with sarcoma 180, a wider range of tumor systems such as Krebs 2 carcinoma, Leukemia L-1210, and carcinoma 755 were evaluated. Also the monomeric units of HEMA and AEMA; succinic acid, succinamic acid, succinimide, and succinamide were evaluated and were found to be inactive.

The observations from this study were that (1) polymeric structure is necessary for tumor inhibition; (2) the completely amidated product (diamide form) had negligible antitumor activity but had lower toxicity than carboxyl

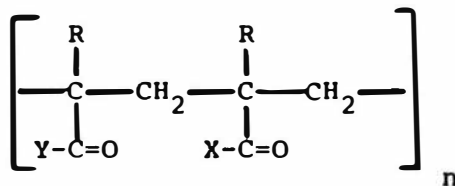
Table I. Ethylene/Maleic Anhydride Series (Hydrolysed Form)



Molecular Weight	Hydrolyzed Ethylene	Ammoniated Ethylene	Ethylene Amide-Acid	Diamide Ethylene	Hydrolyzed Propylene	Ammoniated Propylene	Hydrolyzed Isobutylene	Ammoniated Isobutylene
$R_1$	H	H	H	H	H	H	CH <sub>3</sub>	CH <sub>3</sub>
$R_2$	H	H	H	H	CH <sub>3</sub>	CH <sub>3</sub>	CH <sub>3</sub>	CH <sub>3</sub>
X	CH	NH <sub>2</sub>	NH <sub>2</sub>	NH <sub>2</sub>	O(Na)	NH <sub>2</sub>	O(Na)	NH <sub>2</sub>
Y	OH	ONH <sub>4</sub>	OH	NH <sub>2</sub>	O(Na)	ONH <sub>4</sub>	O(Na)	ONH <sub>4</sub>
Dose mg/kg	200	300	400			400	19	50
2-3,000 Average % Inhibition	54	80	70			59	13	79
20-30,000	100	50	100	800	9	50		40
	72	81	78	38	15	67		77
60-70,000	10	50	100		19	50	9	25
	55	65	69		38	59	23	65
80-100,000	4	75	25					
	46	83	58					
120,000 and up	4	75	25					5
	61	72	51					46

Inhibition of Subcutaneous Sarcoma 180

Table II. Polyacrylic and Polymethacrylic Series



Molecular Weight		Polyacrylic Acid	Polymethacrylic Acid	Acrylamide
	R	H	CH <sub>3</sub>	H
	X	OH	OH	NH <sub>2</sub>
	Dose mg/kg	50	50	
2-3,000	Average % Inhibition	50	54	
20-30,000		25	19	
		37	26	
60-70,000		19	25	800
		50	58	-1
120,000 and up		10	40	400
		72	61	19

Inhibition of Subcutaneous Sarcoma 180

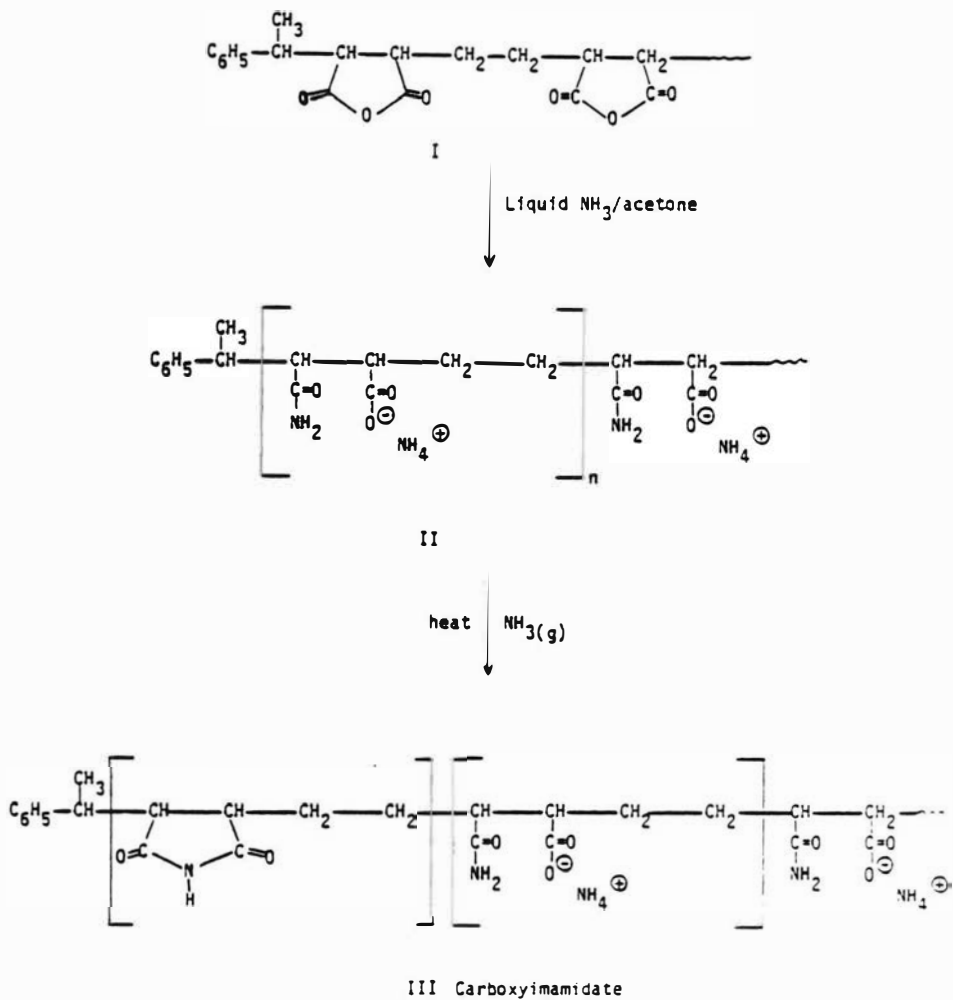
containing compounds (HEMA and AEMA) of similar molecular weight; (3) when the activity of low molecular weight (2,000-3,000) HEMA and AEMA were compared, the half amide-half acid AEMA form was clearly more effective as an antitumor agent and showed a broader spectrum of biological activity; polymers of MW 20,000-30,000 displayed the same pattern of tumor inhibition; (4) as the molecular weight increased, toxicity of the dicarboxylic acid HEMA increased; (5) the difference between the two series is the position of carboxyl groups on the polymer backbone which did not greatly alter the antitumor activity of the compound (both have the same charge density per repeating unit).

These observations indicate that carboxylic functions are necessary for significant tumor inhibition. They also indicate that the presence of the amide function on the polyelectrolyte increases its antitumor activity while decreasing its toxic effects.

#### D. Amidated Polymers Containing Imide Rings

Fields et al. have prepared carboxyimamide, a low molecular weight ethylene-maleic anhydride copolymer derivatized to contain both a half-amide, half-carboxylate salt function and an imide function (33,34). The synthesis was carried out by first preparing a low molecular weight alternating copolymer of ethylene and maleic anhydride (I in scheme 1) in equimolar ratio, with ethyl benzene serving





Scheme 1. Synthesis of EMA copolymer containing imide, amide, and carboxylate salt functions.

as the chain transfer solvent. The anhydride groups of the copolymer were converted to half-amide, half-ammonium salt functions (II in scheme 1) by reacting a solution of the polymer in acetone with a liquid ammonia-acetone mixture. This ammoniated copolymer was then converted to the partial imide (III in Scheme 1) by heating a xylene slurry under reflux for 20-30 minutes while maintaining a flow of ammonia through the reaction vessel (34). The product was recovered by filtration and vacuum drying. It was shown to have 14-25 weight percent of the succinimide rings. Carboxyimamidate, variously referred to in publications as N-137 and NED-137, was evaluated for biological activity against several transplantable tumors (34). It inhibited Lewis lung carcinoma and several other murine solid tumors. It was found to have relatively low acute toxicity in mice and rats with an LD<sub>50</sub> of approximately 2500 mg/kg body weight. This study indicated that the antitumor activity of ammoniated ethylene-maleic anhydride copolymers could be increased by the formation of 14-25% imide rings in a low molecular weight (1200-1500) preparation.

Carboxyimamidate has been found to be a potent tumor inhibitor and has prevented metastases of a methylcholanthrene-induced carcinoma of the bladder (FBCa) in F344 rats (35). This tumor is known to metastasize to the lung within one week of tumor implantation. Animals treated with carboxyimamidate at 30 mg/kg showed prolonged survival as compared to control animals. All the treated

animals were found to be free of pulmonary metastases when autopsied, while all the control animals had extensive pulmonary metastases. The effect of this copolymer as an adjuvant to surgical excision of the FBCa tumor was examined (35,36). The treated animals were observed for tumor recurrence and survival time after excision versus untreated control animals. Tumor recurrence was 100% in the control animals with subsequent death 35 days after surgical excision. Autopsy after 60 days indicated that carboxyimamidate treated animals were free of pulmonary metastases (35). Indefinite survival in these animals could be obtained with repeated administration of the drug. The investigators showed that the active antitumor effect was due to a component of the serum and was coprecipitable with the serum immunoglobins (35,36). This response was transferred to normal animals by the serum of animals treated with carboxyimamidate. It was also noted that the experimental animals showed no acute or chronic toxicity to carboxyimamidate.

#### E. Comparison of Copolymerization Behavior of Maleic Anhydride and Maleimide

Maleic anhydride (MA) and its nitrogen analogue, maleimide (MI) (1 H-pyrrole-2,5-dione), although similar in structure, do not show identical polymerization behavior. For example, the homopolymerization of maleic anhydride has been achieved only with high initiator and monomer

concentrations and high reaction temperatures (37,38) while maleimide and some of its derivatives have been shown to be far more reactive towards self-polymerization. Homopolymers of maleimide (39,40), N-butyl and N-dodecylmaleimide (41) and N-Phenylmaleimide (42,43) have been readily prepared.

Some maleimides have demonstrated a tendency, similar to maleic anhydride, to form alternating copolymers with electron-donating monomers. Curve (a) of Figure 1 is a copolymerization diagram for the maleic anhydride-styrene copolymer system (44) and represents a doubly alternating system. Here the reactivity ratio of each monomer is zero with the composition of the copolymer being 50% in each comonomer regardless of the initial monomer feed. Both N-phenylmaleimide (NPMI) (45) and maleimide (MI) (40) form nearly alternating copolymers with styrene, as illustrated in Figure 1, curves (b) and (c), respectively. However, unlike the maleic anhydride-styrene copolymer, these were not doubly alternating systems, but singly alternating ones, meaning that the reactivity ratio of only one comonomer is zero and that of the other comonomer is greater than zero. Variation of the mole fraction of the maleimide in the monomer feed (singly alternating system) does have a small effect on the mole fraction of maleimide present in the copolymer. Similar single alternations have been observed in the copolymerization of styrene with N-butylmaleimide (41), N-bornylmaleimide (46),

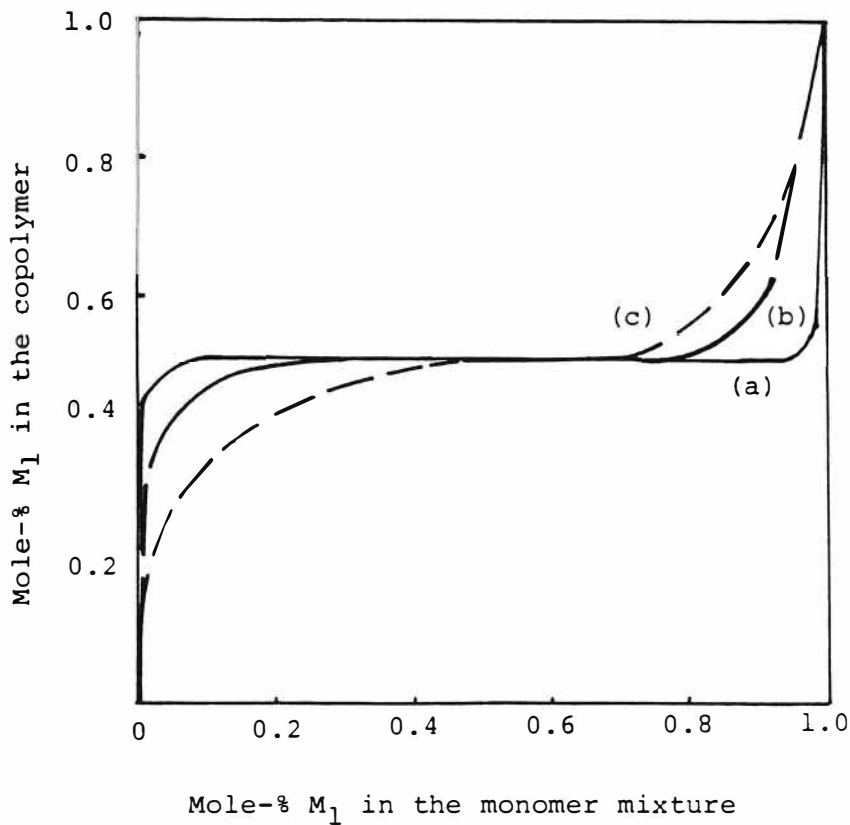


FIGURE 1. Copolymerization diagram for

- a. Styrene-maleic anhydride  
( $r_1=0.0095$ ,  $r_2=0$ ) (44)
- b. Styrene-N-phenylmaleimide  
( $r_1=0.012$ ,  $r_2=0.047$ ) (45)
- c. Styrene-maleimide  
( $r_1=0.1$ ,  $r_2=0.1$ ) (40)

N-(p-chloro-phenyl)maleimide (47), and N-(p-carboxyphenyl)-maleimide (47).

The copolymers of maleimide and its derivatives have been demonstrated to be significantly different from maleic anhydride (MA) copolymers. For example, the copolymerization of 2-allylphenol (2AP) with maleic anhydride, maleimide, and N-phenylmaleimide was studied both neat and in a variety of solvents (48) and only the MA-2AP copolymers were equimolar for all starting feed ratios.

#### F. The Q-e Scheme and Role of Charge-Transfer Complexes

The Q-e scheme proposed by Alfrey and Price (49) has proved to be useful in correlating the structures of monomers with their reactivities in copolymerization. The specific reactivity of a monomer (determined by the resonance effect) is denoted by Q, and the polar character of the radical adduct is denoted by e. According to this semi-quantitative scheme, the copolymerization ratios can be given by the following equations:

$$r_1 = \frac{k_{11}}{k_{12}} = \frac{Q_1}{Q_2} \exp [-e_1(e_1 - e_2)]$$

$$r_2 = \frac{k_{22}}{k_{21}} = \frac{Q_2}{Q_1} \exp [-e_2(e_2 - e_1)]$$

Relatively large  $Q$  values are associated with relatively large reactivities. Electron donating monomers have negative  $e$  values whereas electron accepting monomers have positive  $e$  values. Hence  $r$ ,  $Q$ , and  $e$  values which are determined from copolymerization data give valuable information about the reactivities of the monomers and the nature of the mechanism(s) involved in the copolymerization reaction.

Van Paesschen and Timmerman (40) copolymerized maleimide with styrene, vinylidene chloride, and methyl methacrylate and determined the reactivity ratios and the  $Q$ - $e$  values. Of the three systems, only the maleimide-styrene copolymer was alternating in composition. Also, in the maleimide-styrene system, maleimide was found to have an extremely large  $Q$  value relative to the maleimide-vinylidene chloride system and the maleimide-methyl methacrylate systems. This large  $Q$  value is indicative of a large monomer reactivity. Since in the case of maleic anhydride charge-transfer complexes are considered to be more reactive to polymerization than either one of the comonomers (50) and charge-transfer complex formation can lead to the formation of an alternating copolymer, it was postulated that the large  $Q$  value for maleimide in the maleimide-styrene system was indicative of charge-transfer complex formation in the transition state. Thus, a complex (figure 2) could be

formed by the transfer of an electron from the styrene double bond to the maleimide.

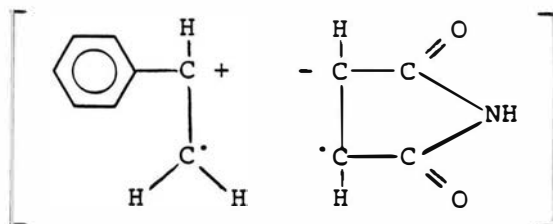


Figure 2. A Proposed Charge-Transfer Complex

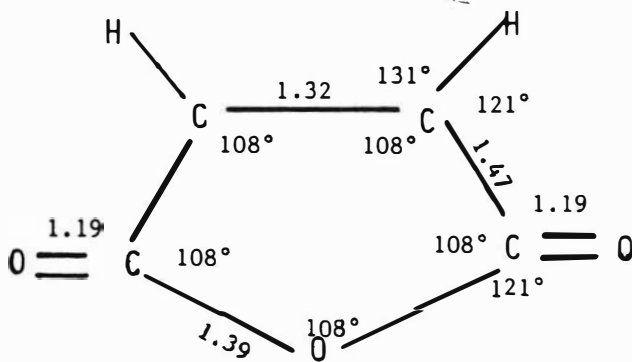
### G. Effects of N-Substituents on the Copolymerization Behavior of Maleimide

Yamaguchi and Minoura (46) investigated the radical copolymerization of N-bornylmaleimide (NBMI) with styrene, methyl methacrylate, and vinylidene chloride; only the N-bornylmaleimide-styrene system gave results similar to the maleimide-styrene system that Van Paesschen and Timmerman (40) had reported. In this study too, it was postulated that the large  $Q$  value of N-bornylmaleimide obtained for the N-bornylmaleimide-styrene system was due to the formation of an intermediate molecular complex between the electron-accepting N-bornylmaleimide and the electron-donating styrene. Listed in Table III (46) are the  $r$ ,  $Q$ , and  $e$  values determined for several maleimide copolymers. It was postulated that the  $Q_2$  values of the N-substituted maleimides tend to become large because of the resonance effects of the phenyl groups. The trend in  $e_2$  values suggested that electron-withdrawing

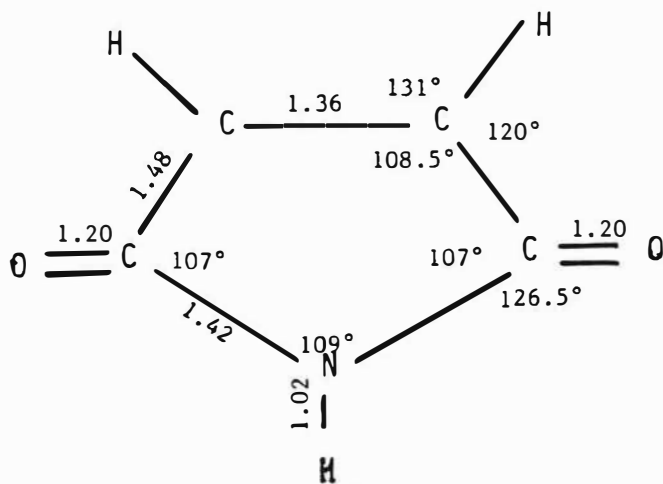


TABLE III  $r, Q, e$  Values for Some Maleimides

$M_1$	$M_2$	$r_1$	$r_2$	$Q_2$	$e_2$	$Q_2$	average $e_2$	reference
St	NBMI	0.13	0.05	1.09	1.44			
MMA	NBMI	2.02	0.16	0.58	1.46	0.48	1.47	46
VCl <sub>2</sub>	NBMI	1.15	0.47	0.48	1.47			
St	Maleimide	0.1	0.1	1.8	1.34			
MMA	Maleimide	2.50	0.17	0.43	1.33	0.41	1.33	40
VCl <sub>2</sub>	Maleimide	0.71	0.48	0.39	1.33			
Isobutyl vinyl ester	NPMI	0	0.32	0.33	1.41			
MMA	NPMI	1.38	0.20	0.83	1.76	0.57	1.57	42
Vinyl acetate	NPMI	0.03	0.66	0.56	1.53			
St	N-n-Butyl-maleimide	1.33	0.12	3.08	1.75			41
St	p-Chloro-phenyl-maleimide	0.01	0.05	11.6	1.89			
MMA	p-Chloro-phenyl-maleimide	1.08	0.17	1.15	1.70			47, 43
Vinyl acetate	p-Chloro-phenyl-maleimide	0.02	0.60	0.73	1.80			
St	N-(Carboxy p-phenyl) maleimide	0.02	0.1	6.3	1.19			
MMA	N-(Carboxy p-phenyl) maleimide	1.18	0.11	1.11	1.83			47, 43
Vinyl acetate	N-(Carboxy p-phenyl) maleimide	0.02	0.18	0.67	2.07			



(a) Bond Lengths (Å) and Bond Angles of Maleic Anhydride



(b) Bond Lengths (Å) and Bond Angles of Maleimide

FIGURE 3. Comparison of X-ray Crystallography Structures of Maleic Anhydride and Maleimide

N-substituents increase the  $e_2$  value of the monomer, indicative of an increase in the monomer's electron-accepting ability.

In Figure 3 is a representation of the MA molecule (51) and of the MI molecule (52). Although these molecules appear to have similar structures, electronically they differ in that, the lone pair of electrons on the nitrogen atom of maleimide can interact with the carbonyl groups on either side thus creating partial single bond character in the carbonyl groups of maleimide (Figure 4).

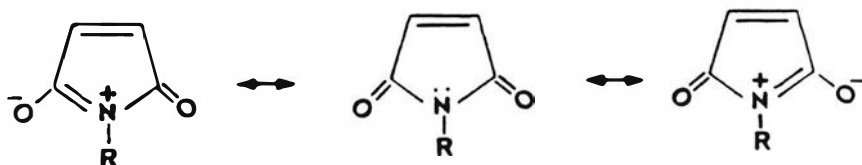
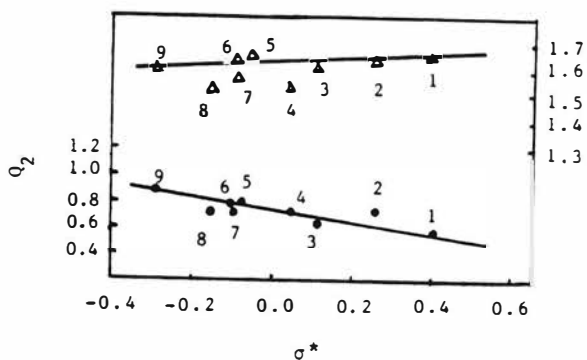


Figure 4. Resonance in Maleimide

Since the O atom is more electronegative than the N atom, the lone pair of electrons on the O atom of maleic anhydride would not interact with the carbonyl functions as readily as the lone pair of electrons on the N atom of maleimide. Therefore, the C=O groups of MA would have greater double bond character than the C=O groups of MI. The C=O group with greater double bond character should

have higher electron affinity. This postulate was borne out by Matsuo (53), who found that on analysis of the  $^1\text{H}$  NMR chemical shifts of the ethylenic protons, the specific interaction between benzene and maleic anhydride is much greater than that between benzene and several N-substituted maleimides. Furthermore, he observed that in benzene there existed no appreciable differences between chemical shift for N-ethylmaleimide and N-ethylsuccinimide and little difference between maleic anhydride and succinic anhydride. Hence in such benzene-solute interactions the ethylenic double bond did not seem to play an important role. He concluded that the specific intermolecular interactions are due primarily to the nature of the carbonyl groups.

Takase et al. (54) investigated the effects of alkyl substituents of N-alkylmaleimides in radical copolymerization. It appeared that as the electron-donating power of the alkyl substituent increased, so did the reactivity ratio ( $r_2$ ) of the maleimide. In Figure 5 are plots of Q and e of the N-alkylmaleimides versus  $\sigma^*$ , the Taft's polar substituent constant. It is apparent that as the electron-donating power of the N-substituent increases the Q value (reactivity) increases and e value (polarity) decreases. As indicated by the data in Table IV, the carbonyl absorption band frequency of the maleimides decreased concomittant with an increase in the electron donating ability of the alkyl substituent. These results suggest that electron-donating substituents increase the



Substituent (R)  
 1.  $\text{ClCH}_2\text{CH}_2$  2.  $\text{C}_6\text{H}_5\text{CH}_2$  3.  $\text{C}_6\text{H}_5\text{CH}_2\text{CH}_2$   
 4.  $\text{CH}_3$  5.  $\text{C}_2\text{H}_5$  6.  $i\text{C}_4\text{H}_9$  7.  $n\text{C}_4\text{H}_9$   
 8.  $i\text{C}_3\text{H}_7$  9.  $t\text{C}_4\text{H}_9$

FIGURE 5. Plots of  $Q_2$  and  $e_2$  obtained from the copolymerization with  $\text{MMA}(\text{M}_1)$  vs.  $\sigma^*$  constant for N-alkylmaleimide

TABLE IV. Carbonyl absorption bands in the infrared spectra of N-alkylmaleimides.

No.	N-alkylmaleimide	(a) $\nu_{\text{C=O}}$ (cm <sup>-1</sup> )
1	CEMI	1716
2	BZMI	1713
3	PEMI	1715
4	MMI	1713
5	EMI	1712
6	i-BMI	1710
7	n-BMI	1710
8	i-PMI	1706
9	t-BMI	1709
10	PhMI	1722
11	MI	1732

(a) Measured in  $\text{CHCl}_3$  solution at conc. of  $4.28 \times 10^{-2} \text{ mol.L}^{-1}$

single bond character of the carbonyl double bond. The concomitant decrease of the  $e$  values indicates that the acceptor character (electron affinity) of the alkylmaleimides decreases with electron donation into the imide ring. These results suggest that if a N-substituted maleimide with electron accepting ability which is similar to maleic anhydride is to be prepared, then the N-substituent should be electron withdrawing in nature so as to disrupt the nitrogen lone pair electrons from interacting with the carbonyl groups.

Yamada et al. (55) carried out free radical copolymerizations of N-(4-substituted phenyl)maleimide [N-(4-RP)MI] ( $M_2$ ) with styrene ( $M_1$ ) and methyl methacrylate ( $M_1$ ). Copolymerization with styrene gave a copolymer of 1:1 alternating composition, independent of monomer feed ratios. The calculated  $r$ ,  $Q$ , and  $e$  values are shown in Table V. For the relative reactivities of [N-(4-RP)MI] ( $r_2$  values) with polystyryl radical no order was obtained for all substituents. The authors postulated that in this reaction system the electrostatic interaction between the two monomers is much stronger than the effects of the 4-substituent in [N-(4-RP)MI]. The one observation that was not made is that there is a trend for  $r_1 \cdot r_2$  to approach zero as the electron withdrawing ability of the 4-substituent increases. In terms of copolymer composition, the electron withdrawing group ( $-\text{COCH}_3$ ) at the

TABLE V. Monomer Reactivity Ratios for styrene ( $M_1$ )-N-(4-substituted phenyl) maleimides ( $M_2$ ) and  $Q_2, e_2$  values of N-(4-substituted phenyl) maleimides,



R group in $M_2$	Monomer reactivity ratio					
	$r_1$	$r_2$	$r_1$	$r_2$	$Q_2$	$e_1$
$CH_2$	0.25	0.08	0.02	0.02	0.8	1.18
H	0.05	0.13	0.0065	0.0065	3.3	1.45
Cl	0.01	0.05	0.0005	0.0005	11.6	1.89
$OCOCH_3$	0.1	0.01	0.001	0.001	1.2	1.83
$COOC_2H_5$	0.02	0.1	0.0002	0.0002	6.3	1.79
$COCH_3$	0.04	0.0	0.000	0.000	---	----

TABLE VI. Monomer reactivity ratios for methyl methacrylate ( $M_1$ )-N-(4-substituted phenyl) maleimides ( $M_2$ )  $Q_2, e_2$  values of N-(4-substituted phenyl)maleimides.



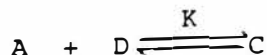
R group in $M_2$	Monomer reactivity ratio					$Q_2$	$e_2$
	$r_1$	$r_2$	$\frac{1}{r_1}$	$\frac{1}{r_2}$			
$CH_3$	0.93	0.41	1.08	2.44	1.17	1.38	
H	0.98	0.30	1.02	3.33	1.18	1.51	
Cl	1.08	0.17	0.93	5.88	1.15	1.70	
$OCOCH_3$	1.14	0.13	0.88	7.46	1.12	1.77	
$COOC_2H_5$	1.18	0.11	0.85	9.09	1.11	1.83	

4-position approximates the results obtained from the copolymerization of maleic anhydride with styrene.

The  $r$ ,  $Q$ , and  $e$  values determined for the copolymerization of [N-(4-RP)MI] with methylmethacrylate are listed in Table VI. The relative reactivities of [N-(4-RP)MI] toward the poly(methyl methacrylate) radical ( $1/r_2$ ) clearly increased with the electron withdrawing ability of the 4-substituent. As illustrated in Figures 6 and 7, Hammett's  $\sigma$  values bore a linear relationship with both the  $e_2$  values and  $\log (1/r_2)$ . It was concluded that the radical reactivities of [N-(4-RP)MI] are influenced by the polar characteristics of the 4-substituents.

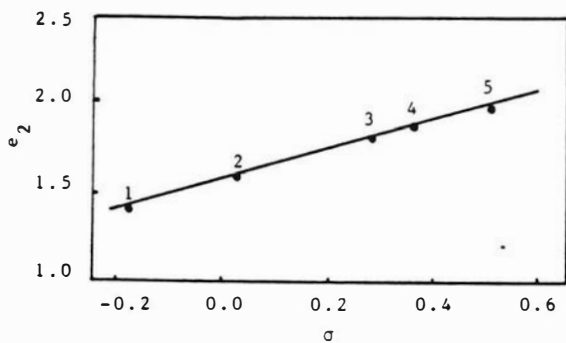
#### H. Effect of N-Substituents on the Charge-Transfer Complexation of Maleimide

Olson and Butler (55,56) recently investigated the role of a charge-transfer complex in the alternating copolymerization of N-substituted maleimides and vinyl ethers. Two methods were employed for this study. The first method involved utilization of UV spectroscopy to detect charge-transfer bands. The complex equilibrium can be described by:



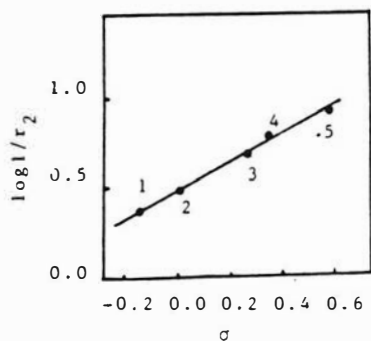
where A is the acceptor concentration, D is the donor concentration, C is the complex concentration and K is the





Substituent (R)  
 1.  $\text{CH}_3$  2. H 3. Cl 4.  $\text{OCOCH}_3$   
 5.  $\text{COOC}_2\text{H}_5$

FIGURE 6. Plot of  $e_2$  value vs.  $\sigma$  for  
 R of N-(4-RP)MI



Substituent (R)  
 1.  $\text{CH}_3$  2. H 3. Cl 4.  $\text{OCOCH}_3$   
 5.  $\text{COOC}_2\text{H}_5$

FIGURE 7. Plot of  $\log 1/r_2$  vs.  $\sigma$  for  
 R of N-(4-RP)MI

equilibrium constant. Olson investigated the complex formation of 2-chloroethyl vinyl ether (CEVE) with N-aryl-maleimides with electron-donating and electron-withdrawing groups in the para position of the phenyl ring. The intensity of the charge transfer band was measured for five different CEVE concentrations with each maleimide. Absorbance measurements were made at 295 nm since neither CEVE nor the substituted maleimides exhibited any significant absorption at this wavelength. It was found that the  $K\epsilon^{295}$  values are relatively small for those N-aryl maleimides substituted with electron donating groups in the para position, and large for those with para electron withdrawing groups. This relationship is shown in a plot of  $K\epsilon^{295}$  values versus the Hammett substituent constants ( $\sigma$ ) for the para substituents (Figure 8). If the  $\epsilon^{295}$  values are similar within the series of N-arylmaleimides, then the differences in  $K\epsilon^{295}$  are due to differences in the equilibrium constants (K) for complex formation. This would mean that electron withdrawing para substituents enhance formation of the charge-transfer complex. One could extrapolate this reasoning further to say that it is possible that the increase in complexation with electron withdrawing ability of the para substituents is due to an increase in the acceptor character of the maleimide.

The second method utilized by Olson to investigate charge-transfer complex formation was to study the  $^{13}\text{C}$  NMR spectra of copolymers of the N-arylmaleimides with CEVE.

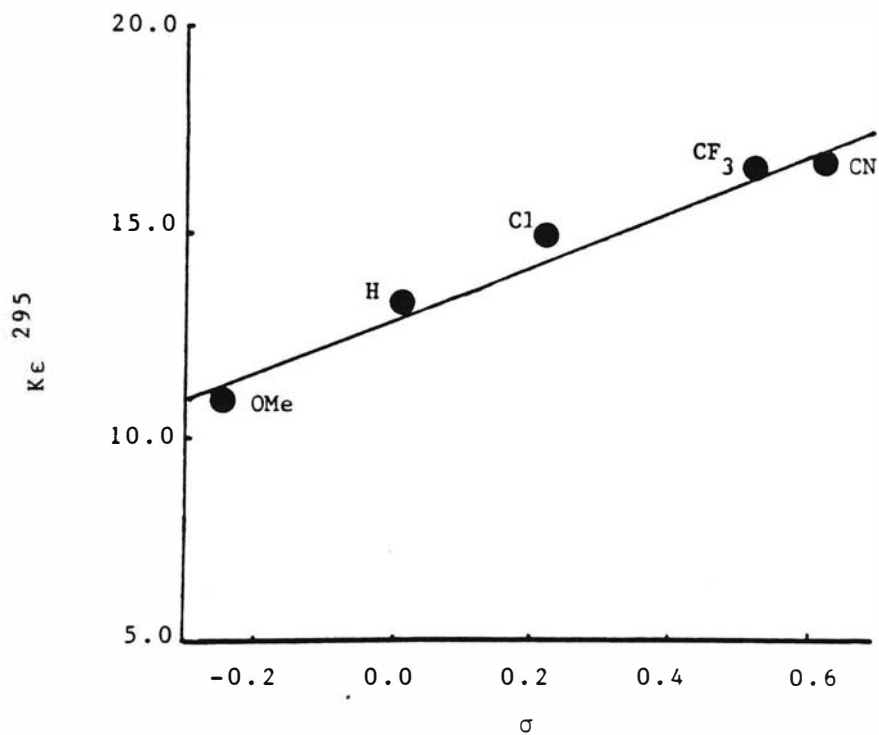


FIGURE 8.  $K_c^{295}$  vs. Hammett  $\sigma$  Constants  
for Various Para Substituted Maleimide-  
CEVE Complexes in Dichloromethane

It was found that there is a greater preference for cis stereochemistry at the succinimide units when the maleimide is substituted with an electron withdrawing group (-CN), relative to substitution with an electron donating group (-OMe). Since conditions that were expected to increase the fraction of maleimide monomers in the complexed state produced copolymers with a higher cis:trans ratio at the succinimide units, it was postulated that the copolymer stereochemistry was related to the maleimide-CEVE complex. The correlation between the mole fraction of cis succinimide units found in the N-substituted maleimide-CEVE copolymers with the Hammett  $\sigma$  constants of the substituents is shown in Figure 9. A similar relationship of the copolymer stereochemistry with  $K_e^{295}$  values was observed (Figure 10). It was concluded that the comonomer complex was participating in the propagating steps and that the succinimide stereochemistry is dependent on the fraction of maleimide monomer in complexed form.

These studies conducted by Matsuo (52), Takase (53), Yamada (54), and Olson (55) of N-substituted maleimides indicate that the electronic nature of maleimide could be altered with an electron withdrawing substituent to enable it to react similarly to maleic anhydride during radical copolymerizations.

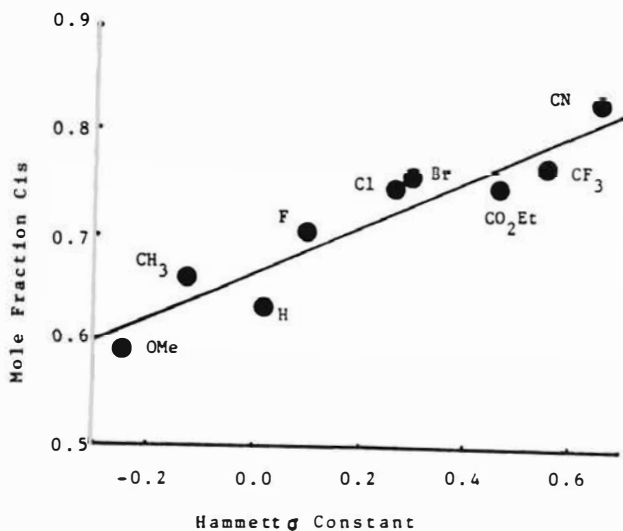


FIGURE 9. Mole Fraction Cis Succinimide Units in N-Arylmaleimide-CEVE Copolymers vs. Hammett  $\sigma$  Constant

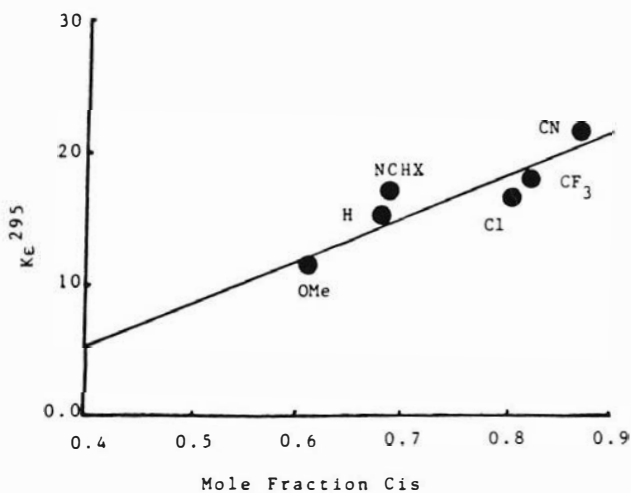


FIGURE 10.  $K_c^{295}$  vs. Mole Fraction Cis Succinimide Units in N-Substituted Maleimide-CEVE Copolymers

## RESEARCH AIM

The general aim of these investigations was to evaluate the effects of N-substituents on the polymerization behavior of maleimide. More specifically, the question of whether electron-withdrawing N-substituents on maleimide influence it to approximate the copolymerization properties of maleic anhydride was to be answered.

The electron-withdrawing N-substituents of maleimide used were the amide group (N-carbamylmaleimide) and the carbethoxy group (N-carbethoxymaleimide). The electron donating N-substituents used were the phenyl group (N-phenylmaleimide) and the ethyl group (N-ethylmaleimide).

N-carbamylmaleimide (NCMI) and N-phenylmaleimide (NPMI) were prepared by an addition reaction on maleic anhydride of urea and aniline, respectively, to yield the maleamic acid, which was then cyclized with loss of water to the imide form. Maleimide (MI) was prepared by degradation of NCMI in N,N-dimethylformamide. N-carbethoxymaleimide (NGEMI) was prepared by reaction of maleimide with ethylchloroformate in the presence of triethylamine.

Since maleic anhydride is known to readily form charge-transfer complexes with electron-donating comonomers, the complexation properties of maleic anhydride, maleimide and N-substituted maleimides with the electron-donating systems styrene, furan and 2-chloroethyl

vinyl ether were evaluated and compared. Charge-transfer complexation was investigated by the use of ultraviolet (UV) spectroscopy and  $^1\text{H}$  NMR spectroscopy. When charge-transfer bands were observed by UV spectroscopy, a continuous variation method, which involved monitoring the absorption of the charge-transfer band while varying the mole fraction of a component, was utilized to determine the stoichiometry of complexation. The formation constants of complexation were determined by  $^1\text{H}$  NMR experiments using Hanna and Ashbaugh's adaptation of the Benesi-Hildebrand equation.

Homopolymerization rates and copolymerization rates of MI, NCMI, and NCEMI were compared. The electron-donating monomer used for the copolymerizations was styrene. High yield copolymerizations with varied feed ratios of the NCMI-styrene system and NCEMI-styrene system were performed in order to determine whether NCMI and NCEMI form 1:1 alternating copolymers with styrene.

It was also investigated whether a NPMI-MA 1:1 copolymer could be prepared. Variation of copolymer composition with variation of monomer feed was determined by  $^1\text{H}$  NMR spectroscopy and elemental nitrogen analysis.

High pressure liquid chromatography was evaluated for suitability as a technique for monitoring monomer concentrations during NCMI-styrene copolymerization.

## RESULTS AND DISCUSSION

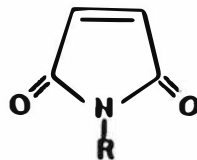
The thrust of this research was to investigate whether the electronic properties of maleimide (MI) could be altered such that it would display properties similar to maleic anhydride in its polymerization behavior. Maleic anhydride (MA) is known to form alternating copolymers with electron-donating monomers. Maleimide does not show as strong a propensity for alternation in its copolymerization with electron-donors. The alternation of comonomers in the copolymer structure of MA copolymers has been attributed (48) to its ability to form charge-transfer complexes with electron-donor species.

Olson and Butler (56,57) reported that electron-withdrawing substituents on the para position of N-phenylmaleimide (NPMI) increased the complexing ability of NPMI with the electron-donating 2-chloroethyl vinyl ether (CEVE). Matsuo indicated (53) that the interaction between electron-donating benzene and electron-accepting MA is significantly greater than the interaction between benzene and N-substituted maleimides. Furthermore, in the interaction with benzene, he concluded that these intermolecular interactions were controlled by the nature of the carbonyl groups whereas the olefinic double bond did not seem to play a significant role. We postulated that the reason para-electron-withdrawing substituents of NPMI increased its complexation with CEVE (57) was because such

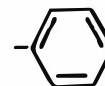


substituents, by induction and resonance, tied up the lone pair of electrons on the N atom of maleimide, thus preventing or reducing the frequency of the N lone pair electrons from resonating with the carbonyl groups of the imide ring (Figure 4). If the resonance within the maleimide ring was inhibited, the carbonyl bond strength would more closely approximate the carbonyl bond strength of maleic anhydride. If the carbonyl bond played a significant role in complexation with electron-donors, then the charge-transfer interaction between electron-donor and electron-acceptor would be enhanced, leading to an increase in complexation between the two species and ultimately to an increase in the alternation of the two components in the copolymers.

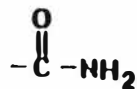
Figure 11 indicates the structures of the maleimides used in this study. Two electron-withdrawing groups, the amide and carbethoxy groups, and two weakly electron-donating groups, the phenyl and ethyl groups, were used to compare the effects of electron-withdrawing and electron-donating N-substituents on the complexing and polymerization properties of maleimide. Besides being a weak electron-donor, the phenyl group could also have an effect on the maleimide carbonyl bond strength similar to an electron-acceptor by tying up the lone pair of electrons on the maleimide N atom (by resonance with the pi electrons in the phenyl ring) and thus decreasing resonance within the maleimide ring. Any effects due to mass of the substituents



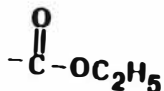
R = -H      Maleimide (MI)



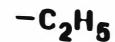
N-Phenylmaleimide  
(NPMI)



N-Carbamylmaleimide (NCMI)



N-Carbethoxymaleimide (NCEMI)



N-Ethylmaleimide  
(NEMI)

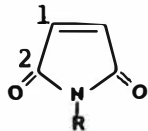
Figure 11. Substituent Groups That Were Utilized for Investigation of N-Substituent Effects on Polymerization Properties of Maleimide.

were assumed to be insignificant since the two electron-donating substituents had the smallest and largest molecular weights and the molecular weights of the two electron-withdrawing substituents fell in-between.

The  $^{13}\text{C}$  NMR chemical shifts in  $\text{DMSO-d}_6$  of maleimide and some of the N-substituted maleimides are summarized in Table VII. It can be seen that the  $^{13}\text{C}$  chemical shifts of the olefinic and carbonyl carbons do not change very much with variation of the electronic nature of the substituent. However, a trend is observed for the carbonyl carbon chemical shifts. The carbonyl NMR resonances appearing farthest upfield are those contained in maleimides with electron-withdrawing groups. Changes in  $^{13}\text{C}$  chemical shift have often been related to changes in electron density about that carbon (58,59). If the electron-withdrawing N-substituents did increase the electron density around the carbonyl group, an upfield shift would be expected.

IR spectroscopy of the maleimides was performed in KBr at 1% or lower concentrations. The imide ring carbonyls give two bands which are believed to be due to resonance between the symmetric and asymmetric stretching modes (50). The less intense higher frequency band was denoted  $\nu_H$  and the more intense lower frequency band was denoted  $\nu_L$ . The observed carbonyl stretching frequencies are summarized in Table VIII. Hydrogen bonding in maleimide and N-carbamylmaleimide (NCMI) (Figure 12) could decrease the force constant of the carbonyl bond; hence low

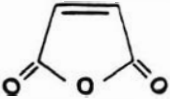
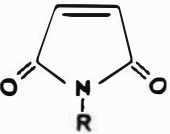
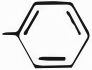
Table VII  
 $^{13}\text{C}$ -NMR Chemical Shifts of Maleimide and N-Substituted  
 Maleimide (DMSO- $d_6$ , TMS reference)



R	1	2	3	4	5	6	7
-H	135.13	172.61					
$\begin{array}{c} \text{O} \\ \parallel \\ -\text{C}-\text{NH}_2 \\ 3 \end{array}$	135.13	168.50	147.81				
$\begin{array}{c} \text{O} \\ \parallel \\ -\text{C}-\text{O}-\text{CH}_2\text{CH}_3 \\ 3 \quad 4 \quad 5 \end{array}$	135.13	165.68	165.68	63.83	13.98		
$\begin{array}{c} -\text{CH}_2\text{CH}_3 \\ 6 \quad 7 \end{array}$	134.24	170.67				31.97	13.56

Table VIII

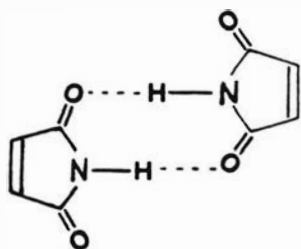
IR Ring Carbonyl Stretching Frequencies of Maleic Anhydride, Maleimide, and N-Substituted Maleimides

Compound	CONC. <sup>a</sup> (%)	$\nu_H^b$	$\nu_L^c$
	0.50	1857	1780
			
$-\overset{\text{O}}{\parallel}{\text{C}}-\text{OC}_2\text{H}_5$	0.25	1800	1770
$-\overset{\text{O}}{\parallel}{\text{C}}-\text{NH}_2$	0.10	1797	1745
-H	0.10	1773	1710
	0.25	1742	1710
$-\text{C}_2\text{H}_5$	1.0	1740	1707

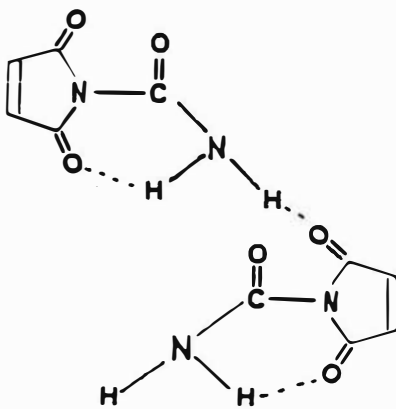
a) KBr pellets

b) high frequency ring carbonyl stretch

c) low frequency ring carbonyl stretch



MI



NCMI

Figure 12. H-Bonding in Maleimide (MI) and N-Carbamylmaleimide (NCMI).

concentrations were used in determining their carbonyl stretching frequencies. Primary amides show free N-H stretching modes near 3500 to 3400  $\text{cm}^{-1}$  and bonded N-H stretching modes near 3350 to 3180  $\text{cm}^{-1}$  (60). As shown in Figure 13, the IR spectra of NCMI, in 0.1% and 1% concentrations showed that there were free and bonded N-H stretching present. Secondary amides show free N-H stretching modes at 3460-3420  $\text{cm}^{-1}$  and bonded N-H stretching modes at 3320-3140  $\text{cm}^{-1}$  (60). As indicated in Figure 14, the solid solutions of MI gave an N-H stretching frequency at 3200  $\text{cm}^{-1}$  indicative that there was hydrogen bonding present. The carbonyl frequencies of maleic anhydride, maleimide, and the N-substituted maleimides are summarized in Table VIII. While keeping in mind that the H-bonding in MI and NCMI would have lowered the carbonyl stretching frequencies of the two moieties, it is seen that there is a definite trend for the carbonyl frequencies to shift toward the frequencies exhibited by maleic anhydride when the N-substituents are electron-withdrawing. The electron-donating N-substituents appeared to decrease the force constant of the carbonyl bond. These observations are consistent with the postulates that (1) the lone pair of electrons on the imide N atom is in resonance with the carbonyl groups, creating a partial positive charge on the N atom, (2) electron-withdrawing groups would destabilize the positive charge by inductive effect or tie up the lone-pair of electrons of the N atom by engaging in resonance with it,

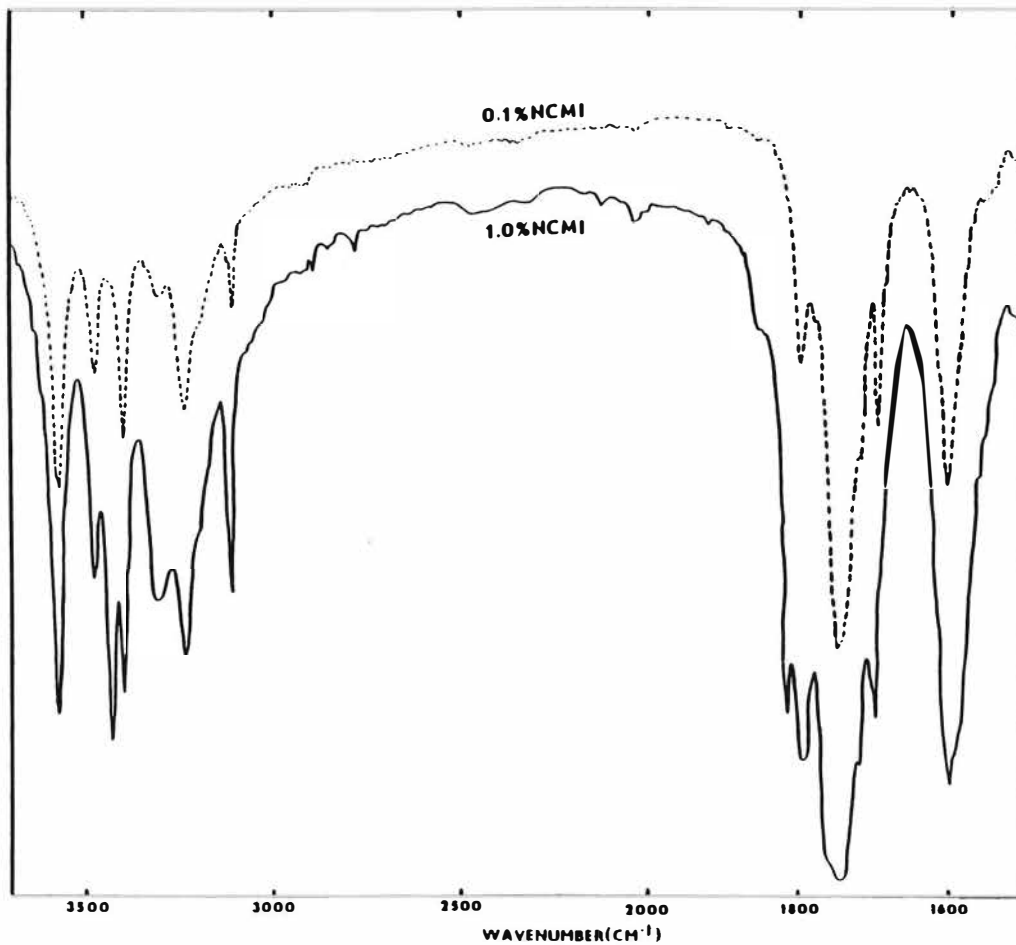


Figure 13. IR Spectrum of N-carbamylmaleimide (NCMI) in Solid Phase (KBr Solvent).



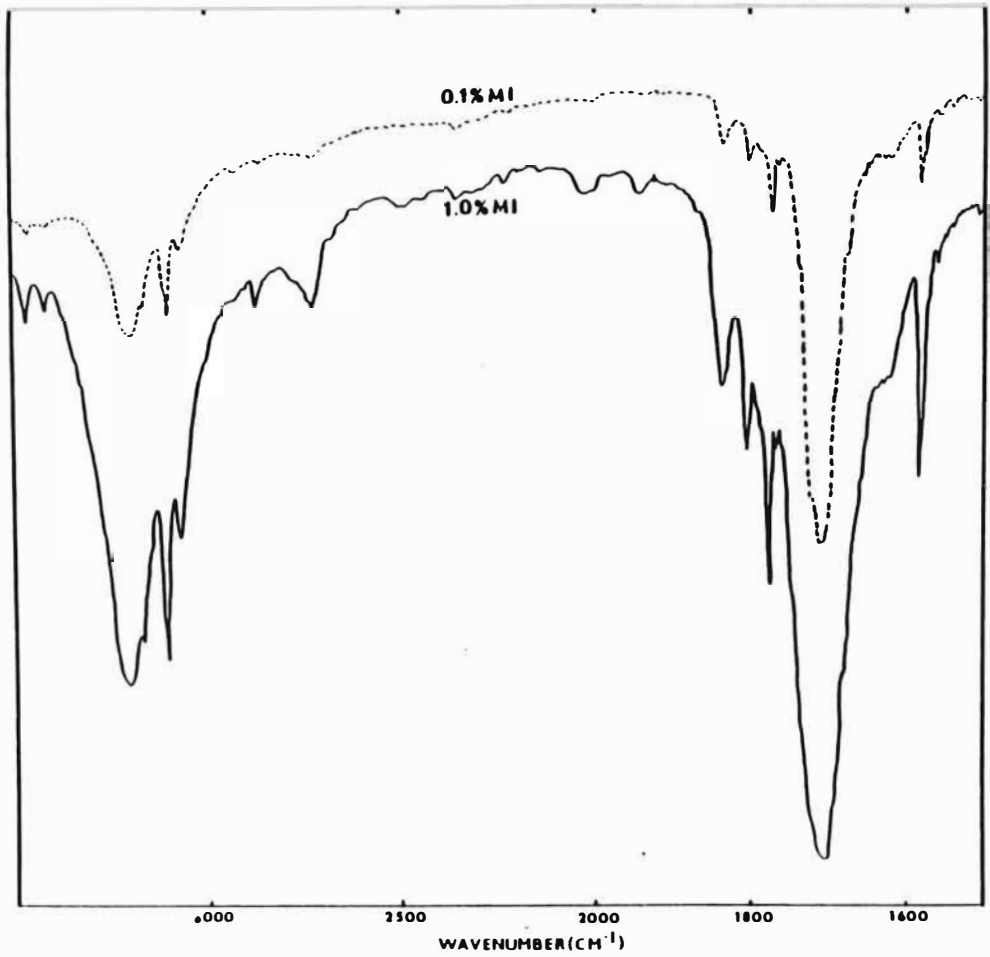


Figure 14 . IR Spectrum of Maleimide (MI) in Solid Phase (KBr Solvent).

and (3) electron-donating groups would stabilize the positive charge on the N atom and hence enhance maleimide ring resonance.

Resonance within the MI ring would decrease the force constant of the carbonyl bond. The electron-withdrawing groups would decrease the MI ring resonance and thus increase the carbonyl bond strength, making it more similar to the carbonyl bond strength of maleic anhydride. Electron-donating groups would have the opposite effect, making the maleimide carbonyl bond strength more dissimilar to that of maleic anhydride.

The trends shown in the carbonyl  $^{13}\text{C}$  NMR chemical shifts and the IR carbonyl resonance frequencies indicate that the carbonyl bond strengths of maleimide are altered in a direction toward the carbonyl bond strength of maleic anhydride in the case of NCMI and NCEMI and in a direction away from MA in the case of NEMI and NPMI.

### Complexation Studies

#### Charge-Transfer Complexes

Formation of charge-transfer or electron-donor-acceptor complexes between monomers has been proposed as a step in the mechanism of formation of alternating copolymers (48). The charge-transfer resonance model was first formulated by Mulliken (61,62) in 1950 to account for the striking spectral features of many donor-acceptor complexes. There

is as yet no clear agreement on the limitations of the definition of charge-transfer complexes. The most general interpretation includes all complexes in which one component is a potential Lewis base (electron-donor) and the other a potential Lewis acid (electron-acceptor) (63). This broad definition can include polarization-bonded complexes at the weak end of the interaction energy scale and complexes of transition metal ions at the strong end of the scale (63).

Charge-transfer complexes (CTCs) have been studied by a variety of methods including optical techniques (ultraviolet, Raman, microwave, optical rotatory dispersion, polarimetry) diffraction (electron, neutron, x-ray), resonance (electron spin, nuclear magnetic, nuclear quadrupole, Mossbauer), dipole moments, conductance, and colligative properties (64). (For a general discussion of these methods see references 61-68.)

#### Complexation Studies Utilizing Ultraviolet (UV) Spectroscopy

The classical method for the determination of the equilibrium constant of complexation is that of Benesi and Hildebrand (69) which involves determination of the charge-transfer absorbance of an electron-donor-acceptor combination for several electron-donor concentrations while the electron-acceptor concentration is kept constant and very much less than that of the electron-donor. Effective modifications of this method, such as the Scott method (70) and the Scatchard method (71), have been reported.

The UV studies of this investigation focused upon determining whether an absorption band attributable to a charge-transfer complex could be observed and, if so, the stoichiometry of complex formation. A change in the absorption spectrum of the mixture when compared to the spectra of the individual components is considered to be due to complex formation. The complex absorption is greatest at the optimum stoichiometry for complexation, meaning that if a 1:1 complex forms, its absorbance should be greatest in a 1:1 mixture of the electron-donor and electron-acceptor. Such 1:1 complex absorptions have been reported for complexes of maleic anhydride with styrene, cyclohexene, 2,5-dihydrofuran, naphthalene (72), 1,2-dimethoxy ethylene (73), p-dioxene, isobutyl vinyl ether, divinyl ether (74), p-oxathiene (75), furan (76), dimethyldivinylsilane and trimethylvinylsilane (77). UV charge transfer bands attributable to electron-donor interactions with maleimide or N-substituted maleimides have not been reported to the best of our knowledge. The results of our charge-transfer (CT) absorption studies involving styrene are summarized in Table IX. MA-styrene and N-carbethoxymaleimide-styrene (NCEMI-styrene) had distinct CT bands at 340 nm in benzene (Figure 15). Due to the insolubility of N-carbamylmaleimide (NCMI) in benzene and most other organic solvents, complex studies involving NCMI were limited to dioxane solvent. CT bands for NCMI-styrene were not observable though a very weak complex absorption was observed for N-phenylmaleimide-

TABLE IX

## Summary of Charge-Transfer Absorptions Involving Styrene

System	Total Concentration (mol.L <sup>-1</sup> )	Solvent	Wave Length of Absorption (nm)	Maximum Absorbance (at nm)	Complex Stoichiometry
MA-Styrene	0.1	Benzene	340	0.071	1:1
NCEMI-Styrene	0.1	Benzene	340	0.071	1:1
NCMI-Styrene	0.001,0.1	Dioxane	---	---	---
NPMI-Styrene	0.1	CHCl <sub>3</sub>	---	---	---
NPMI-Styrene	0.1	Benzene	340,350,360	0.018 (350 nm)	1:1
MI-Styrene	0.1	Dioxane	---	---	---

List of abbreviations is on page xvi.

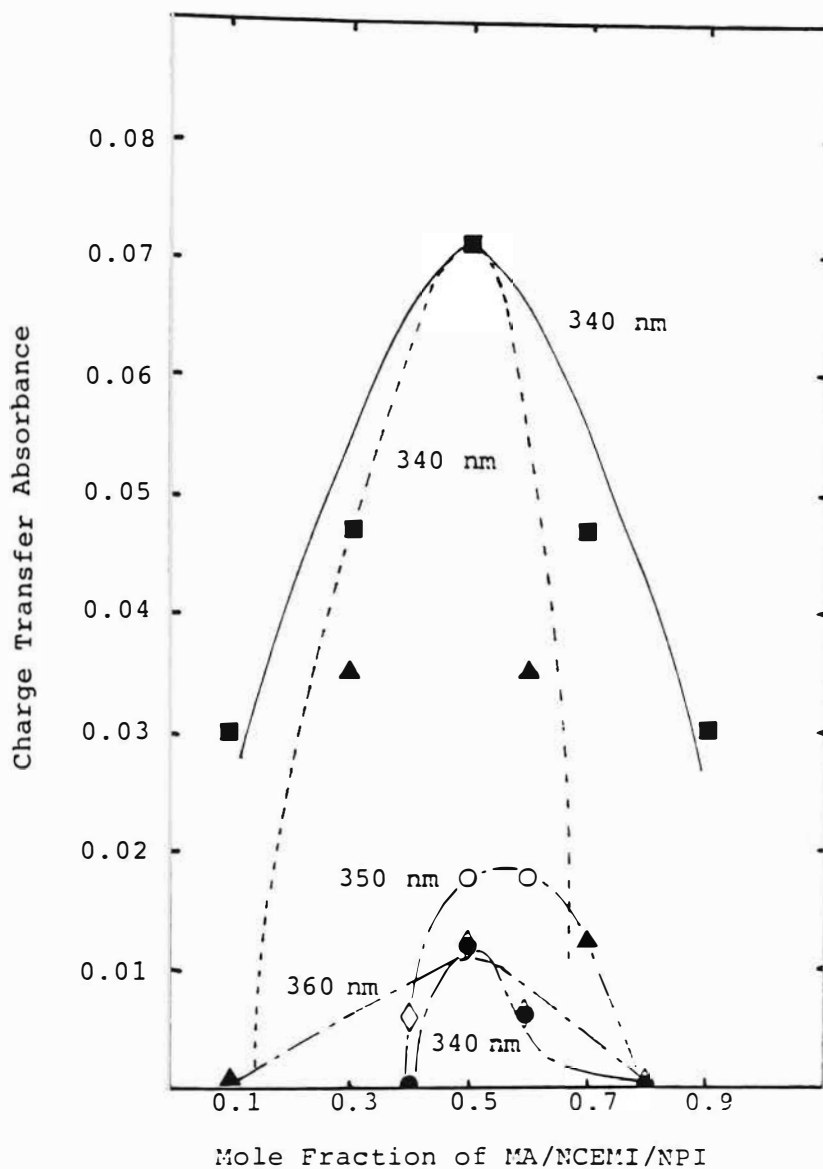


Figure 15. Continuous Variation Method Applied to the Charge Transfer Absorption of MA-Styrene (—); NCEMI-Styrene (----); NPMI-Styrene (- - -).  $[M]_T = 0.1$ ; Solvent: 1,4-dioxane.

styrene (NPMI-styrene) (Figure 15) having a maximum absorbance about 25% of that of the MA-styrene and NCEMI-styrene complex absorbances. As summarized in Table X, complexation with furan was observed for MA and NCMI in dioxane (Figures, 16, 17, 18) whereas MI, NPMI, and NEMI displayed no charge-transfer bands. The polarity of the solvent seems to play a role in complexation. NCMI-furan displayed CT absorption in dioxane (dielectric constant 2.209 at 25 C) but not in the more polar  $\text{CHCl}_3$  (dielectric constant 4.806 at 20 C). MA-furan had an opposite trend; the CT absorption being less in dioxane than in  $\text{CHCl}_3$ . A polar solvent would have a tendency to separate charged species of opposite charge and thus inhibit or retard charge-transfer complexation. Furthermore,  $\text{CHCl}_3$  is known to be a weak electron-acceptor molecule (79). It could compete with the electron-acceptor solute (i.e., NCMI or MA) for complexation sites on the electron-donor furan, thereby lowering the concentration of solute-solute complex. This could explain the absence of a CT band for NCMI-furan in  $\text{CHCl}_3$  but does not account for the increased CT absorption of MA-furan.

No evidence of CT absorption was observed for mixtures of 2-chloroethyl vinyl ether (CEVE) with maleic anhydride (in  $\text{CHCl}_3$  and in benzene), NCMI (in dioxane), NCEMI (in benzene), and MI (in benzene) at a total monomer concentration of 0.1M. Kokubo et al (80) have determined the formation constant of complexation of MA-CEVE by use of UV

TABLE X

## Summary of Charge-Transfer Absorptions Involving Furan

System	Total Concentration (mol.L <sup>-1</sup> )	Solvent	Wave Length of Absorption (nm)	Maximum Absorbance (at nm)	Complex Stoichiometry
MA-Furan	0.1	Dioxane	290,315,325 330,335	0.068 (315)	1:1
MA-Furan	0.1	CHCl <sub>3</sub>	291	0.220	1:1
NCMI-Furan	0.1	Dioxane	325,330,335	0.053 (325)	1:1
NCMI-Furan	0.1	CHCl <sub>3</sub>	---	---	---
MI-Furan	0.1	Dioxane	---	---	---
NPMI-Furan	0.1	Dioxane	---	---	---
NEMI-Furan	0.1	Dioxane	---	---	---

List of abbreviations is on page .



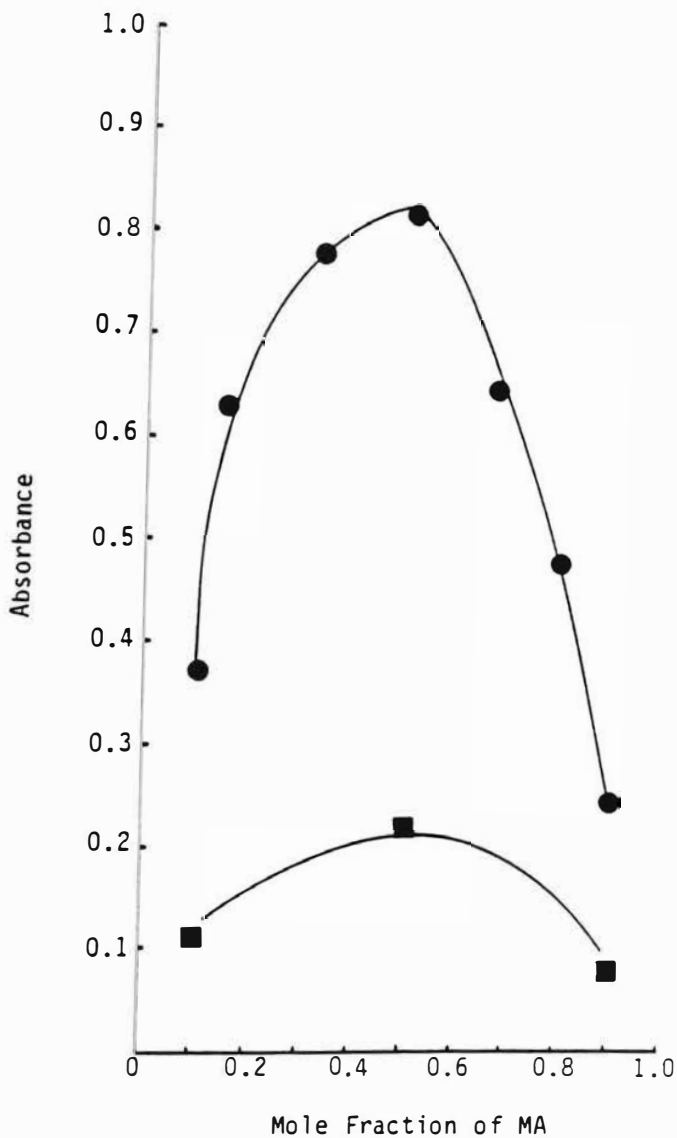


Fig.16. Continuous variation method applied to the charge-transfer absorption at 291 nm in the MA-Furan system. Solvent:  $\text{CHCl}_3$ . (●) reported by Butler et. al. for unspecified concentrations; (■)  $[\text{MA}] + [\text{Furan}] = 0.1 \text{ M}$ .

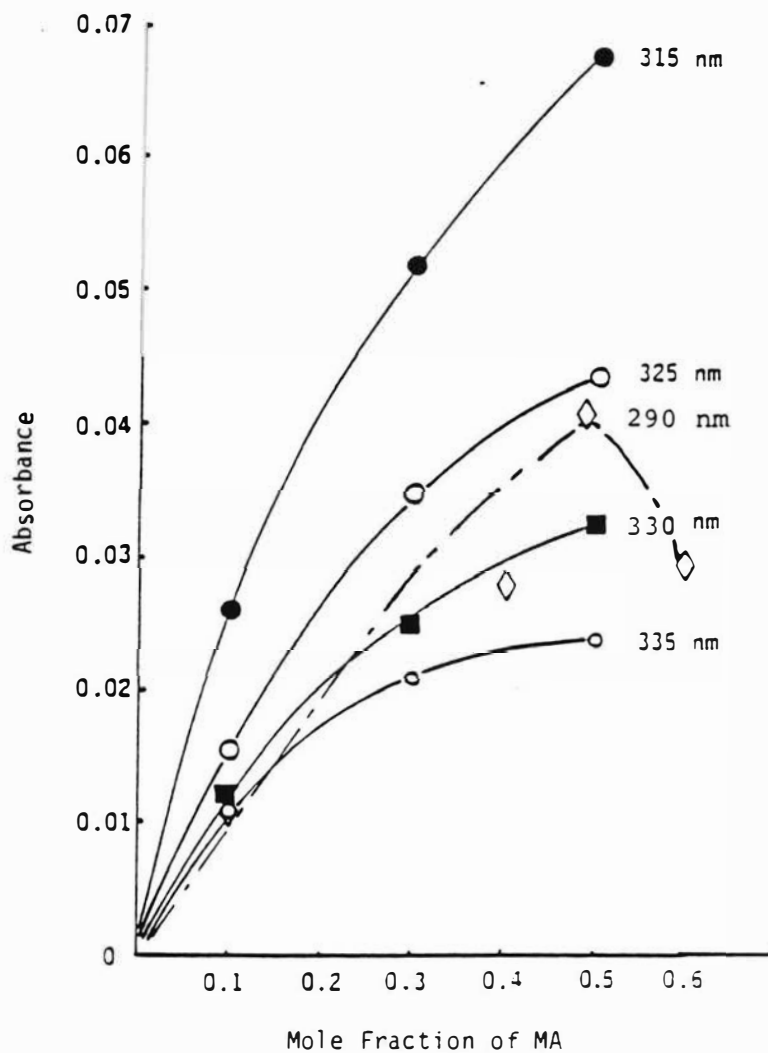


Fig.17. Continuous variation method applied to the charge-transfer absorption in the MA-Furan system.  $[MA] + [Furan] = 0.1 M$ ; solvent: dioxane.

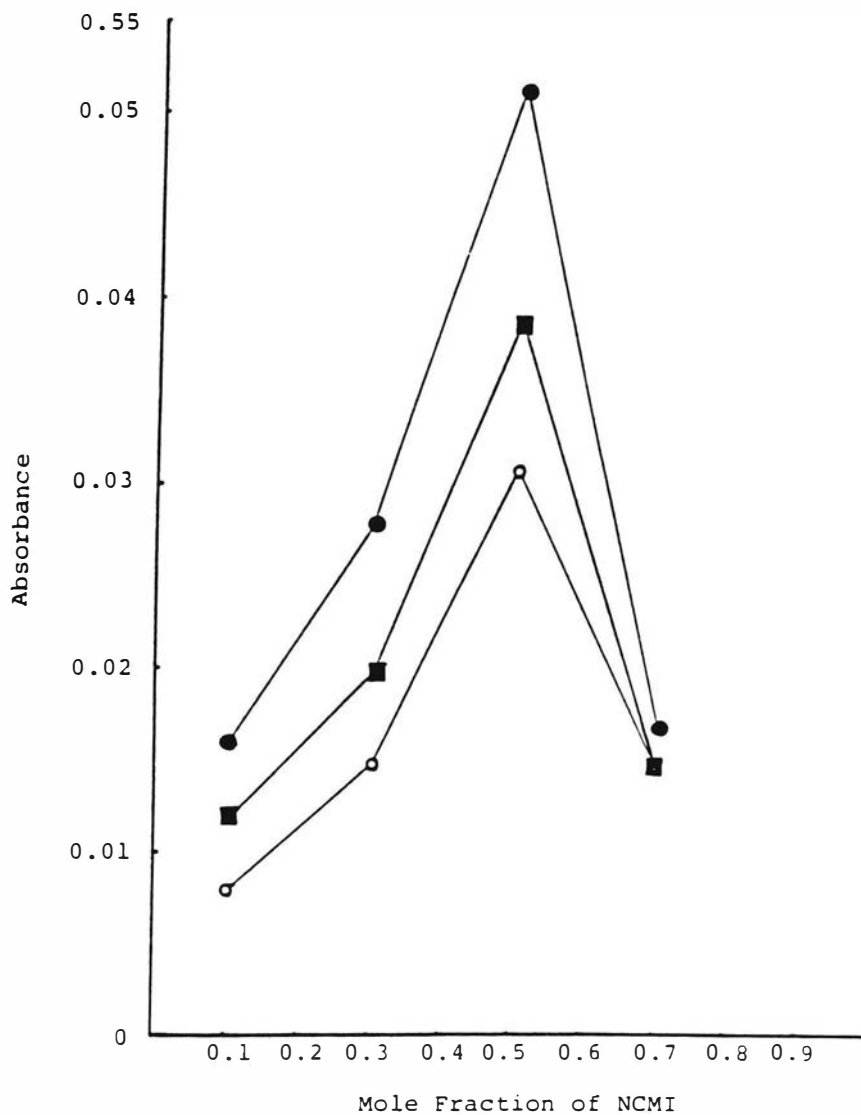


Fig.18. Continuous variation method applied to the charge-transfer absorption in the NCMI-Furan system. NCMI + Furan = 0.1 M; solvent:dioxane. (●) measured at 325 nm; (■) at 330 nm; (○) at 335 nm.

spectroscopy and application of the Benesi-Hildebrand equation. They kept the MA concentration constant at 0.025M while the CEVE concentration was varied from 0.5 to 1.90M. CT absorption was observed at 340 and 350 nm in benzene and  $\text{CHCl}_3$ . Since the Benesi-Hildebrand equation gives a linear plot only in the case of 1:1 complexes, it appears that MA-CEVE does form a 1:1 complex. The reason that no CT band for MA-CEVE was observed in our investigations may be due to the fact that the total monomer concentration was too low for a sufficient amount of CT complexation to occur for appearance of a CT band.

It is significant that except for NPMI-styrene, all charge-transfer absorptions for complexes with styrene and with furan were observed only for MA and for maleimides substituted with electron-withdrawing groups (NCMI and NCEMI). Barrales-Rienda *et al* reported (45) that no CT band was observed for NPMI-styrene at an unspecified total monomer concentration. The CT band we observed was extremely weak but nevertheless appears to be real, having an absorbance maximum at 0.5 mole fraction, indicative of 1:1 complexation. As mentioned earlier, the phenyl substituent could tie-up the lone pair of electrons on the N atom of maleimide by resonance with its pi electrons. This would decrease maleimide ring resonance (Figure 4) and increase the electron density of the maleimide carbonyl groups, leading to an enhancement in CT interaction with the electron-donor styrene.

## Complexation Studies Utilizing $^1\text{H}$ NMR Spectroscopy

Hanna and Ashbaugh (80) developed a technique similar to that of Benesi and Hildebrand (69) whereby shifts of NMR resonances in solutions of donors and acceptors relative to the resonances of the components themselves are used to evaluate the equilibrium constant for complex formation. Hanna and Ashbaugh's method (69) has been elaborated upon by Tsuchida et al (79).

### Theory

Consider the equilibrium:



Where A and D represent acceptor and donor molecules, respectively, and where CTC represents the charge-transfer complex. The equilibrium constant K is then given by:

$$K = [\text{CTC}] / ([\text{A}_0] - [\text{CTC}])([\text{D}_0] - [\text{CTC}]) \quad (1)$$

where  $[\text{A}_0]$  and  $[\text{D}_0]$  are the total concentrations of acceptor and donor, both complexed and uncomplexed. In the weak CTC, the chemical shift of protons in the A (or D) molecules are undergoing a rapid exchange between the complexed and uncomplexed states (81). Hence, the chemical shift of protons on A molecules is observed as a peak which

corresponds to the weighted average of the shift due to the free molecules of A and that due to the complex. This relationship is indicated (79) in Figure 19 and equation (2).

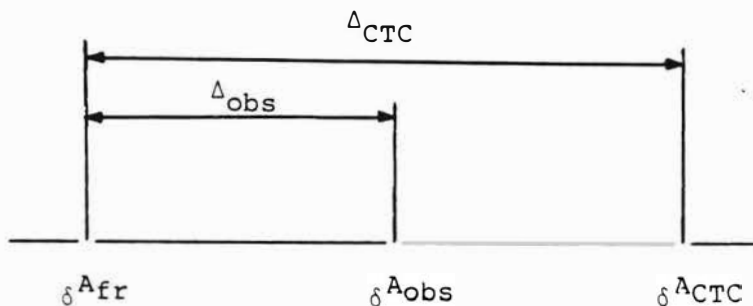


Figure 19. Chemical Shifts of Protons on Acceptors (A) Molecules

$\delta^{A_{Obs}} = \delta^{A_{Fr}}([A]/([A] + [CTC]) + \delta^{A_{CTC}}([CTC]/([A] + [CTC]))$  (2) where  $\delta^{A_{Fr}}$  is the shift of acceptor protons in the free or uncomplexed form,  $\delta^{A_{Obs}}$  is the observed shift of acceptor protons in the complexing media, and  $\delta^{A_{CTC}}$  is the shift of acceptor protons in the pure complex.

$$\Delta_{obs} = \delta^{A_{Fr}} - \delta^{A_{Obs}} \quad (3)$$

$$\Delta_{CTC} = \delta^{A_{Fr}} - \delta^{A_{CTC}} \quad (4)$$

When  $[D]_0 \gg [A]_0$ , equations (1) and (2) are transformed into equation (5) (cf. equations (3) and (4)):

$$1/[D]_0 = (\Delta_{CTC}) (K) (1/\Delta_{obs}) - K \quad (5)$$

Equation (5) is analogous to the Benesi-Hildebrand equation (69) which applies to UV spectra, except that the concentration of the A molecule does not appear, and  $\Delta_{\text{obs}}$  and  $\Delta_{\text{CTC}}$  are used instead of the absorbance and molar absorptivity, respectively.

Hanna and Ashbaugh (62) expressed equation (5) in the form of equation (6):

$$1/\Delta_{\text{obs}} = (1/K \Delta_{\text{CTC}}) (1/[D_0]) + (1/\Delta_{\text{CTC}}) \quad (6)$$

Thus, a plot of  $1/\Delta_{\text{obs}}$  versus  $1/[D_0]$  gives a straight line with a slope of  $1/K \Delta_{\text{CTC}}$  and an intercept of  $1/\Delta_{\text{CTC}}$  from which  $K$  and  $\Delta_{\text{CTC}}$  can be determined.

When mixed with several different concentrations of styrene, the electron acceptors MA, MI, and the N-substituted maleimides showed definite chemical shift dependence of the olefinic protons upon the concentration of styrene (Figures 20-25 and Tables XI-XVI) showing linear relationships between  $1/[D_0]$  and  $1/\Delta_{\text{obsd}}$ . Computer linear regression analysis of the data was performed and the reliability of the least squares parameters was checked (82,83) using the following equations:

$$S_R^2 = \frac{\sum_{i=1}^N (R_a - R_c)^2}{N-2} \quad (7)$$

[Styrene]	0.0	0.8000	2.4000	3.2000	4.0000
mol/L					
[MA]	<0.05	<0.05	<0.05	<0.05	<0.05
cps	628.90	610.83	579.58	564.45	551.75
ppm	7.018	6.817	6.468	6.299	6.157

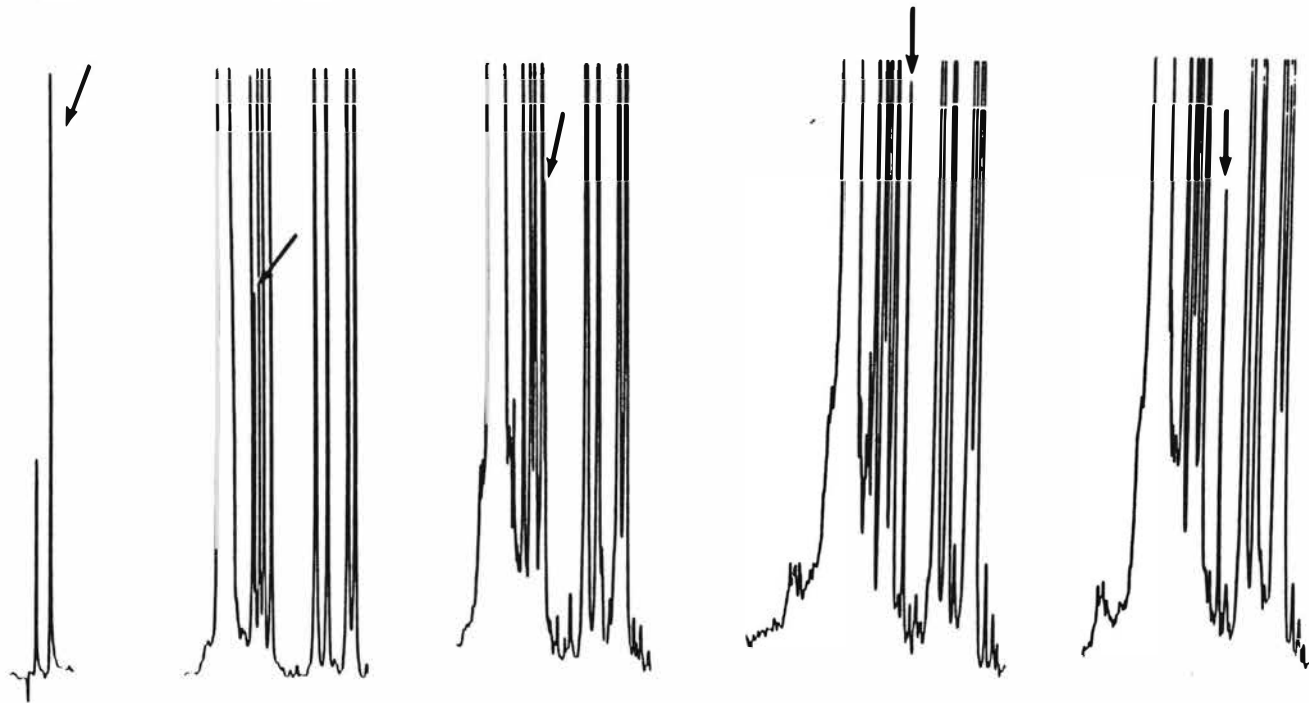


Figure 20.  $^1\text{H}$  NMR Chemical Shifts of Maleic Anhydride (MA) with Several Concentrations of Styrene (in  $\text{CDCl}_3$  at  $33.0^\circ\text{C}$ ).



Table XI

$^1\text{H}$  NMR DATA FOR THE DETERMINATION OF EQUILIBRIUM CONSTANT OF COMPLEXATION OF THE  
MALEIC ANHYDRIDE-STYRENE SYSTEM (in  $\text{CDCl}_3$  at  $33.0^\circ\text{C}$ )

[MA] $\text{mol}\cdot\text{L}^{-1}$	[STYRENE] $\text{mol}\cdot\text{L}^{-1}$	$\delta_{\text{obsd}}^A$ cps	$\Delta_{\text{obsd}}^A$ cps	$1/[\text{STYRENE}]$ $\text{L}\cdot\text{mol}^{-1}$	$1/\Delta_{\text{obsd}}^A$ $\text{cps}^{-1}$
<0.0500	-	$628.90 = \delta_0^A$	-	-	-
<0.0500	0.8000	610.83	18.07	1.2500	0.0553
<0.0500	1.6000	a	a	0.6250	a
<0.0500	2.4000	579.58	49.32	0.4167	0.0203
<0.0500	3.2000	564.45	64.45	0.3125	0.0155
<0.0500	4.0000	551.75	77.15	0.2500	0.0130

a) MA peak was hidden behind a styrene peak

correlation coefficient = 0.9999; slope = 0.0423; intercept = 0.0025

[Styrene]	0.0	1.6002	2.4003	3.2004	4.0005	4.8006
mol/L						
[NCEMI]	0.0500	0.0500	0.0500	0.0500	0.0500	0.0500
cps	611.32	peak	571.77	560.54	549.31	539.06
ppm	6.822	hidden	6.381	6.256	6.130	6.016

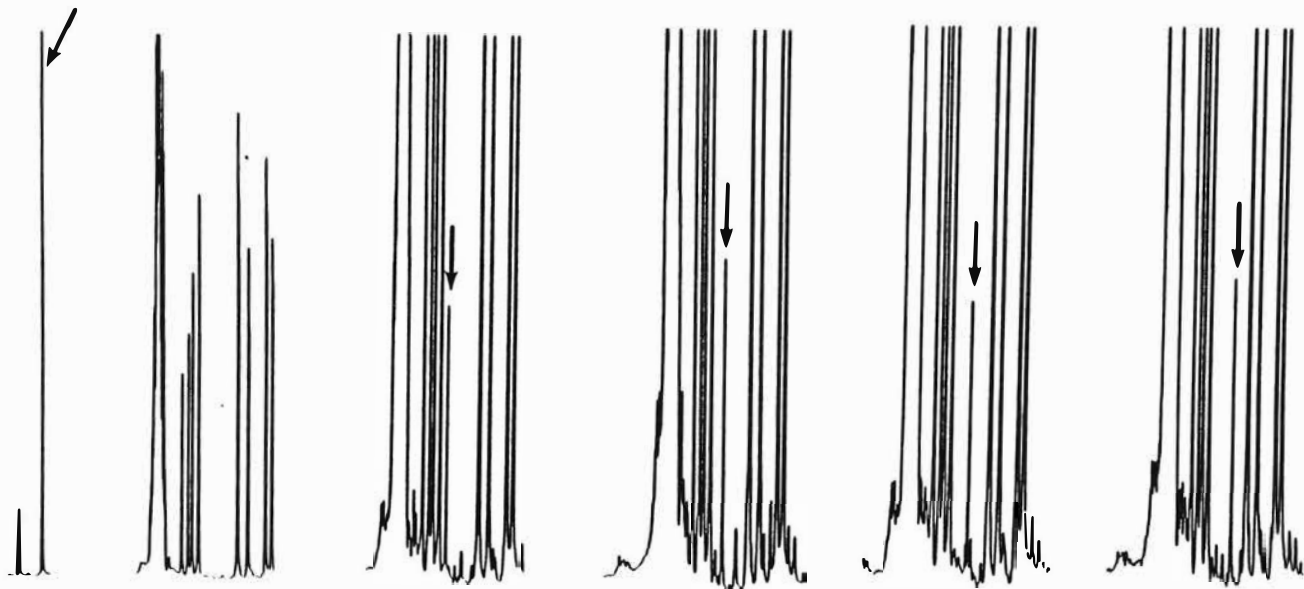


Figure 21.  $^1\text{H}$  NMR Chemical Shifts of N-carbethoxymaleimide (NCEMI) with Several Concentrations of Styrene (in  $\text{CDCl}_3$  at  $32.3^\circ\text{C}$ ).

Table XII  
 $^1\text{H}$  NMR DATA FOR THE DETERMINATION OF EQUILIBRIUM CONSTANT OF COMPLEXATION  
 OF THE N-CARBETHOXYMALEIMIDE-STYRENE SYSTEM (in  $\text{CDCl}_3$  at  $32.3^\circ\text{C}$ )

[NCEMI] $\text{mol}\cdot\text{L}^{-1}$	[Styrene] $\text{mol}\cdot\text{L}^{-1}$	$\delta_{\text{obsd}}^{\text{A}}$ cps	$\Delta_{\text{obsd}}^{\text{A}}$ cps	$1/[\text{Styrene}]$ $\text{L}\cdot\text{mol}^{-1}$	$1/\Delta_{\text{obsd}}^{\text{A}}$ $\text{cps}^{-1}$
0.0500	-	$611.32 = \delta_0^{\text{A}}$	-	-	-
0.0500	1.6002	a	a	0.6249	a
0.0500	2.4003	571.77	39.55	0.4166	0.0253
0.0500	3.2004	560.54	50.78	0.3125	0.0197
0.0500	4.0005	549.31	62.01	0.2500	0.0161
0.0500	4.8006	539.06	72.26	0.2083	0.0138

a) olefinic proton resonance of NCEMI was hidden behind a styrene peak.

correlation coefficient = 0.9999; slope = 0.0553; intercept = 0.0023

[Styrene]	0.0	0.8001	1.6002	2.4003	3.2004	4.0005	4.8006
mol/L							
[NCMI]	0.02	0.02	0.02	0.02	0.02	0.02	0.02
cps	614.25	peak	peak	569.33	555.66	542.96	532.22
ppm	6.855	hidden	hidden	6.354	6.201	6.059	5.939

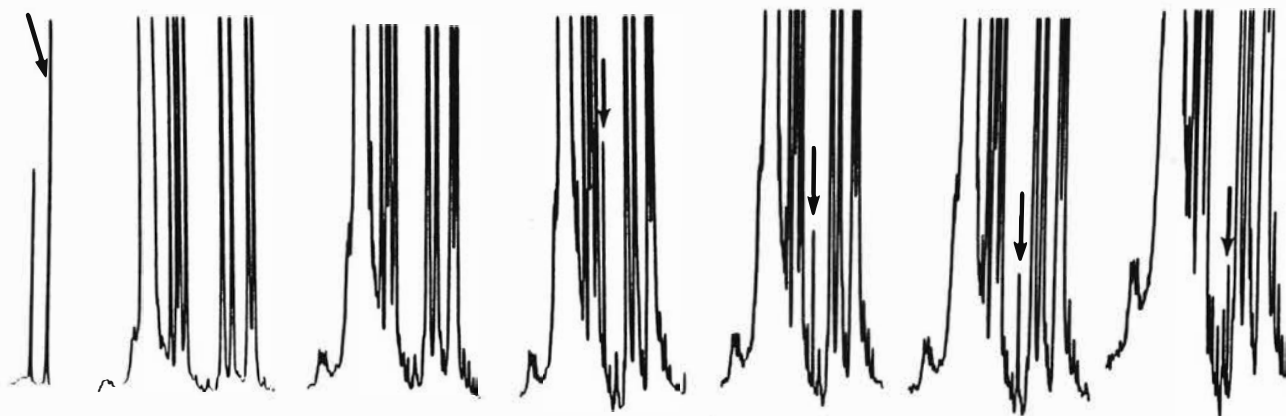


Figure 22.  $^1\text{H}$  NMR Chemical Shifts of Olefinic Protons of N-carbamylmaleimide (NCMI) with Several Concentrations of Styrene (in  $\text{CDCl}_3$  at  $32.9^\circ\text{C}$ ).

Table XIII

$^1\text{H}$  NMR DATA FOR THE DETERMINATION OF EQUILIBRIUM CONSTANT OF COMPLEXATION  
OF THE N-CARBAMYLMALEIMIDE-STYRENE SYSTEM (in  $\text{CDCl}_3$  at  $32.9^\circ\text{C}$ )

[NCMI] $\text{mol}\cdot\text{L}^{-1}$	[Styrene] $\text{mol}\cdot\text{L}^{-1}$	$\delta_{\text{obsd}}^{\text{A}}$ cps	$\Delta_{\text{obsd}}^{\text{A}}$ cps	$1/[\text{Styrene}]$ $\text{L}\cdot\text{mol}^{-1}$	$1/\Delta_{\text{obsd}}^{\text{A}}$ $\text{cps}^{-1}$
0.02	-	$614.25 = \delta_0^{\text{A}}$	-	-	
0.02	0.8001	a	a	0.1250	a
0.02	1.6002	a	a	0.6249	a
0.02	2.4003	569.33	44.92	0.4166	0.0223
0.02	3.2004	555.66	58.59	0.3125	0.0171
0.02	4.0005	542.96	71.29	0.2500	0.0140
0.02	4.8006	532.22	82.03	0.2083	0.0122

a) olefinic proton resonance of NCMI was hidden behind a styrene peak.

correlation coefficient = 0.9997; slope = 0.0488; intercept = 0.0019

[Styrene]	0.0	0.8000	1.6000	2.4000	3.2000	4.0000
mol/L						
[NPMI]	0.0500	0.0500	0.0500	0.0500	0.0500	0.0500
cps	612.79	602.53	peak	peak	573.73	564.45
ppm	6.839	6.724	hidden	hidden	6.403	6.299

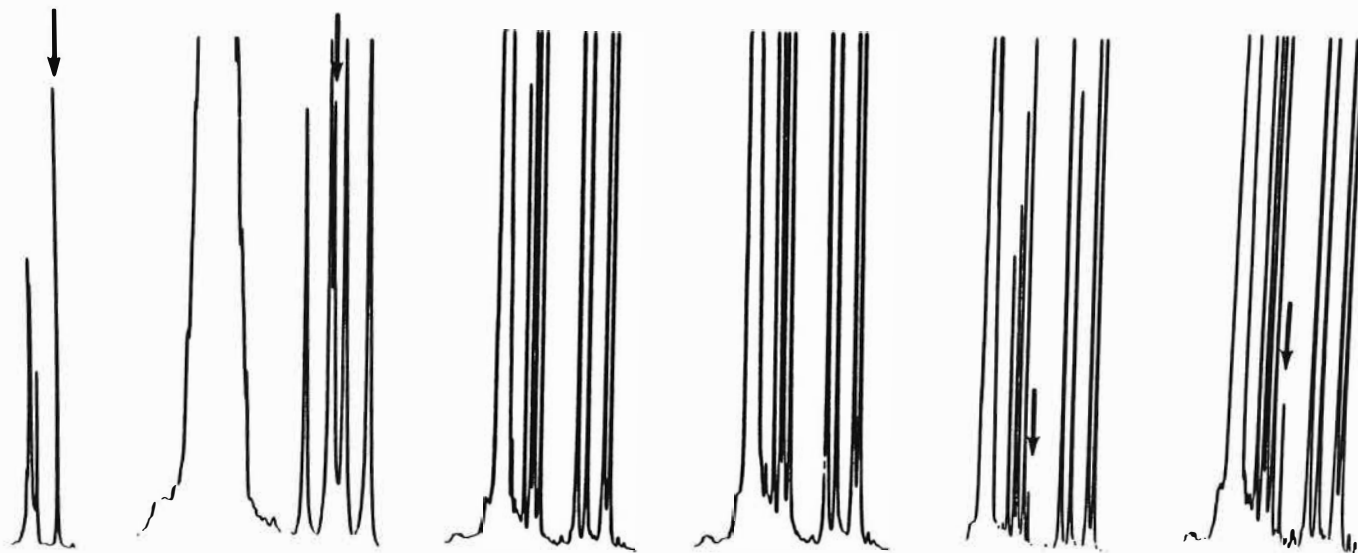


Figure 23.  $^1\text{H}$  NMR Chemical Shifts of Olefinic Protons of N-Phenylmaleimide (NPMI) with Several Concentrations of Styrene (in  $\text{CDCl}_3$  at  $33.0^\circ\text{C}$ ).

Table XIV

$^1\text{H}$  NMR DATA FOR DETERMINATION OF EQUILIBRIUM CONSTANT OF COMPLEXATION  
OF THE N-PHENYLMALIMIDE-STYRENE SYSTEM (in  $\text{CDCl}_3$  at  $33.0^\circ\text{C}$ )

[NPMI] $\text{mol}\cdot\text{L}^{-1}$	[STYRENE] $\text{mol}\cdot\text{L}^{-1}$	$\delta_{\text{obsd}}^{\text{A}}$ cps	$\Delta_{\text{obsd}}^{\text{A}}$ cps	$1/[\text{STYRENE}]$ $\text{L}\cdot\text{mol}^{-1}$	$1/\Delta_{\text{obsd}}^{\text{A}}$ $\text{cps}^{-1}$
0.0500	-	$612.79 = \delta_0^{\text{A}}$	-	-	-
0.0500	0.8000	602.53	10.06	1.2500	0.0994
0.0500	1.6000	a	a	0.6250	a
0.0500	2.4000	a	a	0.4167	a
0.0500	3.2000	573.73	39.06	0.3125	0.0256
0.0500	4.0000	564.45	48.34	0.2500	0.0207

a) NPMI olefinic proton peak was hidden behind a styrene peak

correlation coefficient = 1.0000; slope = 0.0787; intercept = 0.0010

[Styrene]	0.0	1.6000	2.4000	3.2000	4.0000
mol/L					
[MI]	0.0500	0.0500	0.0500	0.0500	0.0500
cps	600.58	579.10	568.35	554.68	550.29
	599.12	577.63	567.38	553.22	548.82
ppm	6.702	6.463	6.343	6.190	6.141
	6.686	6.446	6.332	6.174	6.125

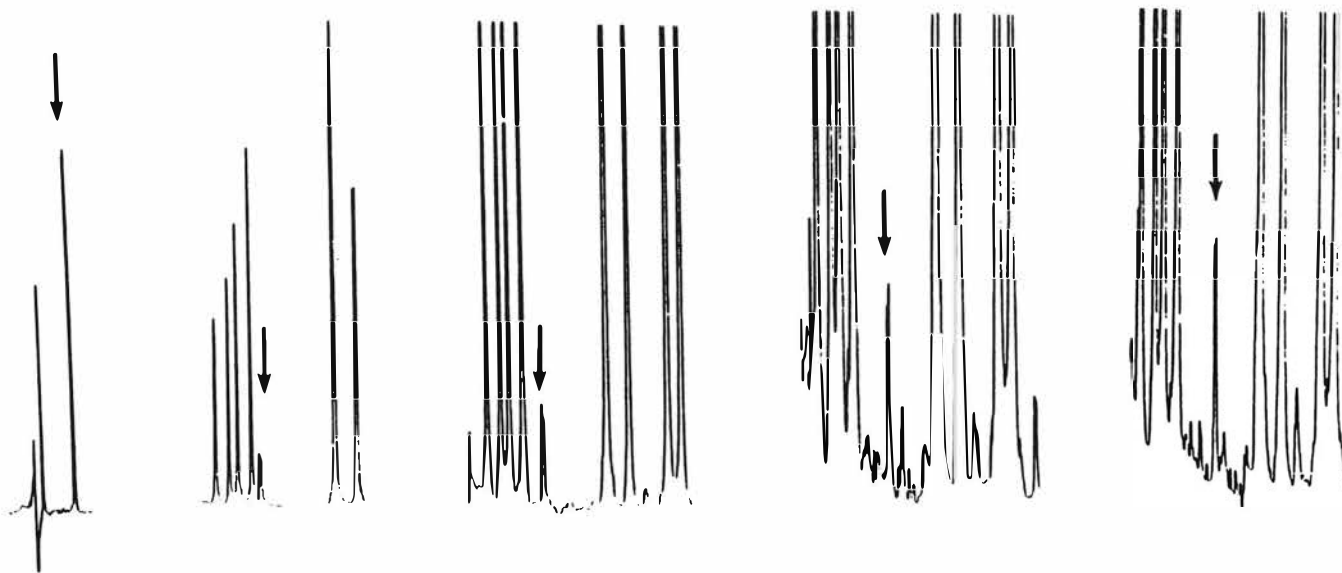


Figure 24.  $^1\text{H}$  NMR Chemical Shifts of Maleimide (MI) with Several Concentrations of Styrene (in  $\text{CDCl}_3$  at  $32.9^\circ\text{C}$ ).



Table XV  
<sup>1</sup>H NMR DATA FOR THE DETERMINATION OF EQUILIBRIUM CONSTANT OF THE  
MALEIMIDE-STYRENE SYSTEM (in CDCl<sub>3</sub> at 32.9°C)

[MI] mol.L <sup>-1</sup>	[STYRENE] mol.L <sup>-1</sup>	δ <sup>A</sup> <sub>obsd</sub> cps	Δ <sup>A</sup> <sub>obsd</sub> cps	1/[STYRENE] L.mol <sup>-1</sup>	1/Δ <sup>A</sup> <sub>obsd</sub> cps <sup>-1</sup>
0.0500	-	600.58=δ <sup>A</sup> <sub>obsd</sub> 599.12	-	-	-
0.0500	0.8000	a	a	1.2500	a
0.0500	1.6000	579.10 577.63	21.48 21.49	0.6250	0.0466 0.0465
0.0500	2.4000	568.35 567.38	32.23 31.74	0.4167	0.0310 0.0315
0.0500	3.2000	554.68 553.22	45.90 45.90	0.3125	0.0218 0.0218
0.0500	4.0000	550.29 548.82	50.29 50.30	0.250	0.0199 0.0199

a) MI peaks were hidden behind styrene peaks

downfield peak - correlation coefficient = 0.9958; slope = 0.0738; intercept = 0.0002  
upfield peak - correlation coefficient = 0.9955; slope = 0.0737; intercept = 0.0004

TABLE XVI

$^1\text{H}$  NMR Data for Determination of Equilibrium Constant of  
Complexation for the Maleimide - Styrene System (in  $\text{CDCl}_3$  at  $32.9^\circ\text{C}$ )

[MI] mol.L <sup>-1</sup>	[Styrene] mol.L <sup>-1</sup>	$\delta^A$ obsd (a) cps	$\Delta^A$ obsd cps	1/[Styrene] L.mol <sup>-1</sup>	1/ $\Delta^A$ obsd cps <sup>-1</sup>
0.0500	---	599.85 = $\delta_0^A$	---	---	---
0.0500	1.6000	578.37	21.48	0.6250	0.0466
0.0500	2.4000	567.87	31.98	0.4167	0.0313
0.0500	3.2000	553.95	42.90	0.3125	0.0218
0.0500	4.0000	549.56	50.29	0.2500	0.0199

a) mean values of chemical shifts of the MI doublet are given.

correlation coefficient = 0.9957; slope = 0.0738; intercept = 0.0003

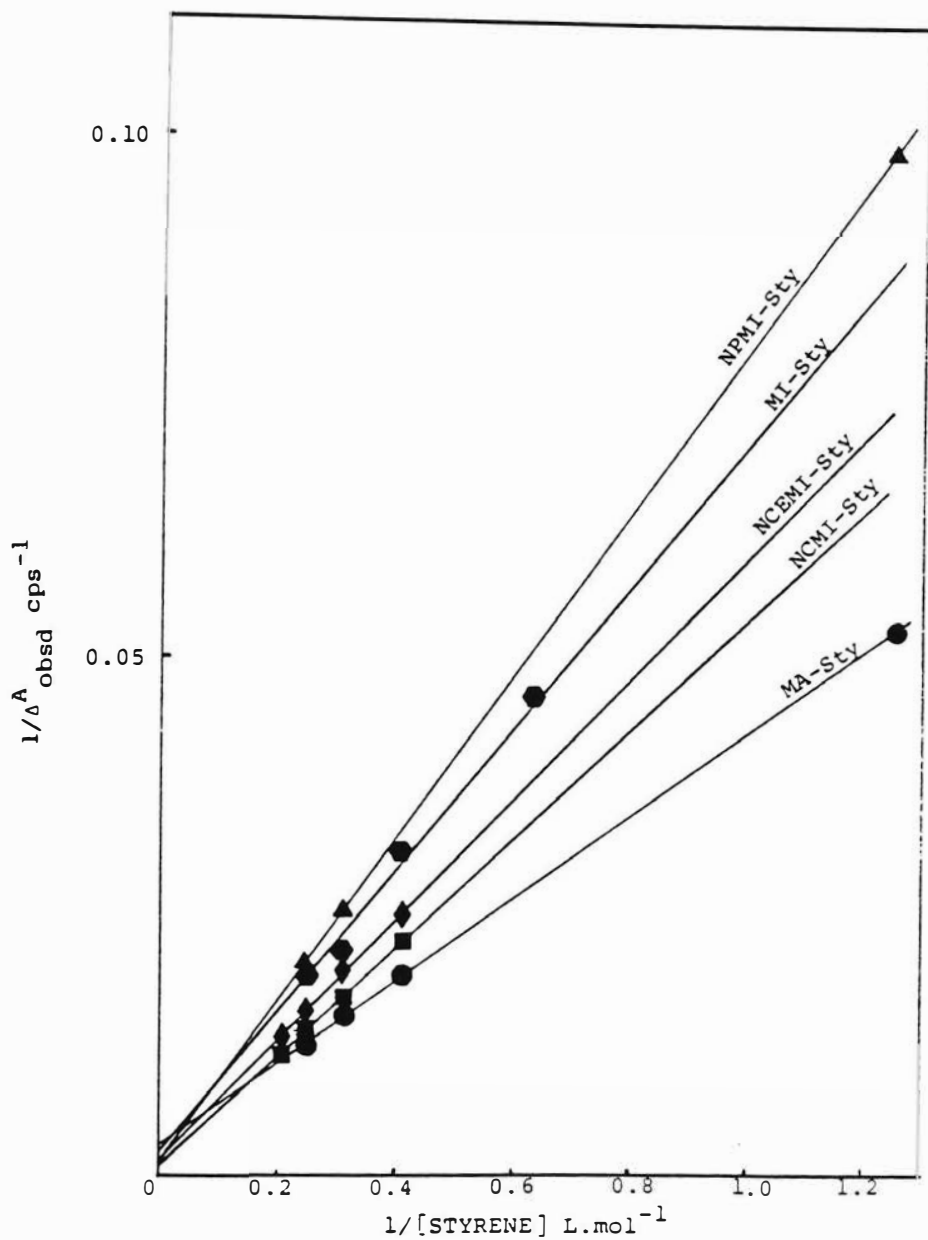


Fig.25.  $^1\text{H}$  NMR Determination of the Equilibrium Constant of Complexation between Styrene and Electron-acceptors.

TABLE XVII

Calculated Equilibrium Constants of Complexation (K) Based on  
 $^1\text{H}$  NMR Data in  $\text{CDCl}_3$

System	Temperature ( C )	K (L.mol <sup>-1</sup> )	Relative Standard Deviation of K (%)	Limits of K at 90% Confidence
MA-Styrene	33.0	0.0591 $\pm$ 0.0025	4	0.0562-0.0620
NCEMI-Styrene	32.3	0.0416 $\pm$ 0.0036	9	0.0374-0.0458
NCMI-Styrene	32.9	0.0389 $\pm$ 0.0062	15	0.0316-0.0462
NPMI-Styrene	33.0	0.0127 $\pm$ 0.0004	3	0.0120-0.0134
MI-Styrene	33.0	0.0038 $\pm$ 0.0266	700	-0.0588-0.0664

Abbreviations are listed on page xvi.

$$D = N \left[ \sum_{i=1}^N (C_i)^2 - \left( \sum_{i=1}^N C_i \right)^2 \right] \quad (8a)$$

or,

$$D = N \sum_{i=1}^N (C_i - \bar{C}_i)^2 \quad (8b)$$

where  $R_a$  is the actual measurement and  $R_c$  is the calculated measurement for  $R = mC+b$  ( $Y=R$ ;  $X=C$ ). By establishing the limits of the  $K$  values at a 90% confidence interval (84) a range in the formation constants of complexation was determined (Table XVII). As expected MA-styrene had the largest  $K$  value. The two maleimides with electron-withdrawing substituents, NCEMI and NCMI had the next largest  $K$  values and their ranges of  $K$  indicate that the difference in  $K$  values between them is not significant. Since the olefinic protons of MI appeared as a doublet (Figure 24), the mid-point of the doublet was used for equilibrium constant calculations (Table XVI). The  $K$  value determined for MI-styrene appears to be statistically unreliable (Table XVII) which could mean that the degree of complexation between MI and styrene is negligible. As noted by the weak CT band in the UV spectrum of NPMI-styrene, the phenyl moiety appears to very slightly enhance the complexing ability of MI with styrene.

Furan complexes also showed olefinic proton shifts of acceptor in the presence of several donor concentrations

(Figures 26-31) and linearity of plots (Tables XVIII - XXIV and Figure 32) which enabled the determination of formation constants (Table XXV). Again, MA had the largest formation constant. NCEMI-furan and MI-furan yielded approximately similar K values. The K values of NCEMI-furan and NPMI-furan too were approximately similar. As predicted, NEMI, the maleimide with the most strongly electron-donating substituent, yielded the smallest K value. All ranges of formation constants were at the 90% confidence limit. The trend of K values determined for complexes involving styrene is not followed in the case of the complexes involving furan. In the furan complexes, the electron-withdrawing groups do not appear to enhance complex formation (lower K value in NCEMI-furan than in MI-furan). However, electron-donating groups appear to have a deleterious effect on complexation (lowest K value was for NEMI-furan).

A  $^1\text{H}$  NMR complexation study of 2-chloroethyl vinyl ether (CEVE) with MA in  $\text{CDCl}_3$  was carried out using a MA concentration of 0.045 M and CEVE concentrations ranging from 0.7458 M to 3.7288 M. Unlike the earlier studies with styrene and furan, the MA olefinic protons showed no change in chemical shift, staying constant at 7.028 ppm (629.39 Hz). However, the isotopic proton chemical shift of  $\text{CDCl}_3$  displayed a downfield shift with increasing CEVE concentration. No formation constant of complexation for  $\text{CDCl}_3$ -CEVE could be calculated, indicating that it was unlikely that a complexation mechanism was causing the  $\text{CDCl}_3$

[Furan]	0.0	1.0000	2.0000	4.0000	6.0000	8.0000
mol/L						
[MA]	0.01	0.01	0.01	0.01	0.01	0.01
cps	628.90	620.11	613.28	598.63	585.44	574.70
ppm	7.018	6.920	6.844	6.681	6.533	6.414

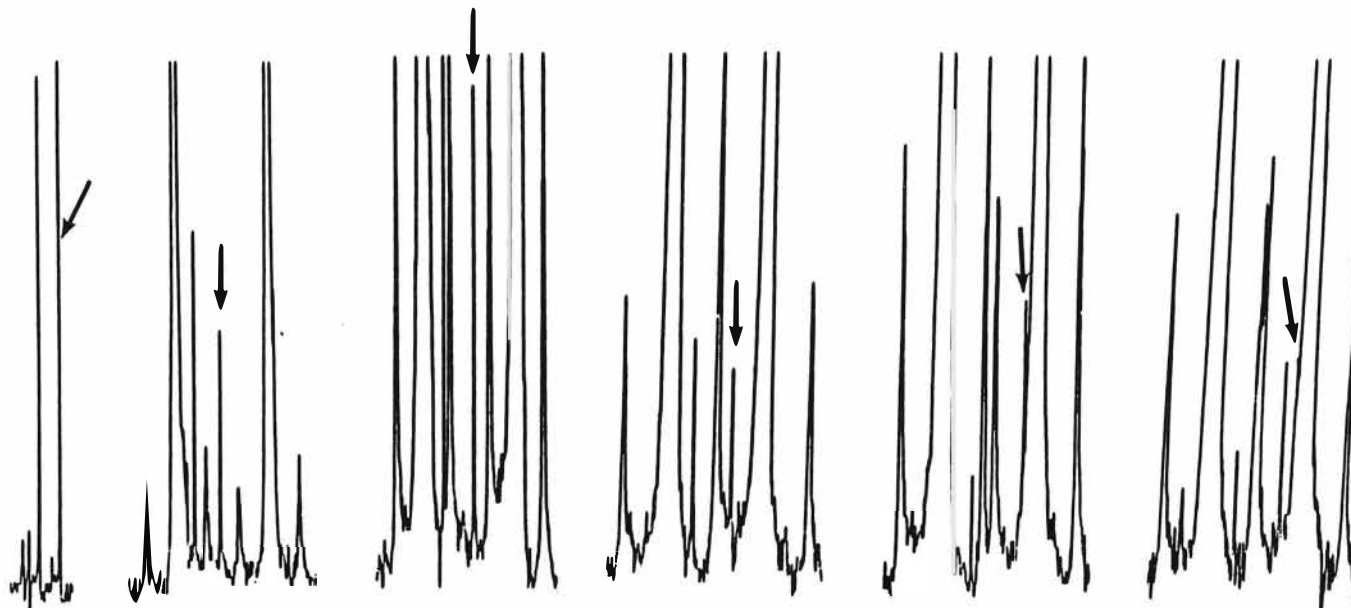


Figure 26.  $^1\text{H}$  NMR Chemical Shifts of Maleic Anhydride (MA) with Several Concentrations of Furan (in  $\text{CDCl}_3$  at  $30.0^\circ\text{C}$ ).

Table XVIII

$^1\text{H}$  NMR DATA FOR DETERMINATION OF EQUILIBRIUM CONSTANT OF COMPLEXATION OF THE  
MALEIC ANHYDRIDE-FURAN SYSTEM (in  $\text{CDCl}_3$  at  $30.0^\circ\text{C}$ )

$[\text{MA}]$ $\text{mol}\cdot\text{L}^{-1}$	$[\text{Furan}]$ $\text{mol}\cdot\text{L}^{-1}$	$\delta^{\text{A}}_{\text{obsd}}$ cps	$\Delta^{\text{A}}_{\text{obsd}}$ cps	$1/[\text{Furan}]$ $\text{L}\cdot\text{mol}^{-1}$	$1/\Delta^{\text{A}}_{\text{obsd}}$ $\text{cps}^{-1}$
0.01	--	$628.90 = \delta^{\text{A}}_0$	--	--	--
0.01	1.0000	620.11	8.79	1.0000	0.114
0.01	2.0000	613.28	15.62	0.5000	0.0640
0.01	4.0000	598.63	30.27	0.2500	0.0330
0.01	6.0000	585.44	43.46	0.1667	0.0230
0.01	8.0000	574.70	54.20	0.1250	0.0185

correlation coefficient = 0.9987; slope = 0.1097; intercept = 0.0057



[Furan]	0.0	1.0000	2.0000	4.0000	6.0000
mol/L					
[NCMI]	0.01	0.01	0.01	0.01	0.01
cps	614.25	606.93	599.60	587.40	576.66
ppm	6.855	6.773	6.691	6.555	6.435

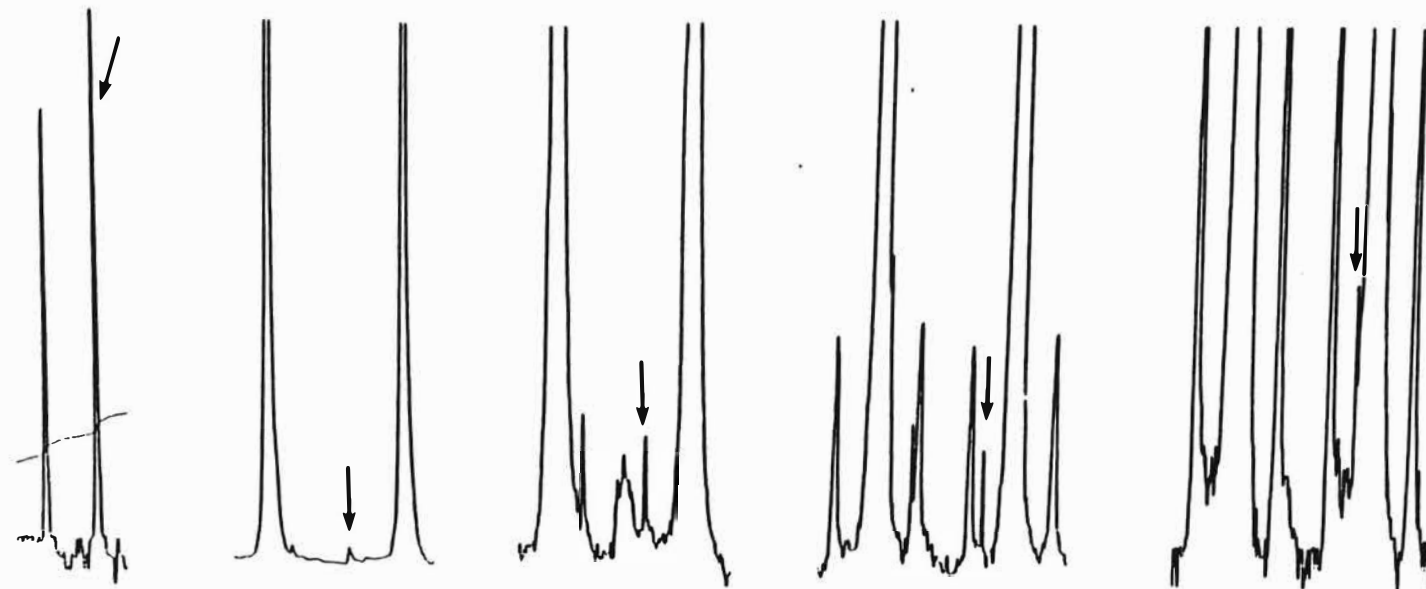


Figure 27.  $^1\text{H}$  NMR Chemical Shifts of Olefinic Protons of N-carbamylmaleimide (NCMI) with Several Concentrations of Furan (in  $\text{CDCl}_3$  at  $30.0^\circ\text{C}$ ).

Table XIX

$^1\text{H}$  NMR DATA FOR DETERMINATION OF EQUILIBRIUM CONSTANT OF COMPLEXATION OF THE  
N-CARBAMYLMALEIMIDE-FURAN SYSTEM (in  $\text{CDCl}_3$  at  $30.0^\circ\text{C}$ )

[NCMI] $\text{mol}\cdot\text{L}^{-1}$	[Furan] $\text{mol}\cdot\text{L}^{-1}$	$\delta^{\text{A}}$ obsd cps	$\Delta^{\text{A}}$ obsd cps	$1/[\text{Furan}]$ $\text{L}\cdot\text{mol}^{-1}$	$1/\Delta^{\text{A}}$ obsd $\text{cps}^{-1}$
0.01	--	614.25	--	--	--
0.01	1.0000	606.93	7.32	1.0000	0.137
0.01	2.0000	599.60	14.65	0.5000	0.0683
0.01	4.0000	587.40	26.85	0.2500	0.0372
0.01	6.0000	576.66	37.59	0.1667	0.0266

correlation coefficient = 0.9997; slope = 0.1326; intercept = 0.0037

[Furan]	0.0	2.3993	3.5990	4.7986	5.9983
mol/L					
[NCEMI]	0.0500	0.0500	0.0500	0.0500	0.0500
cps	611.32	596.67	589.35	583.00	577.63
ppm	6.822	6.659	6.577	6.506	6.446

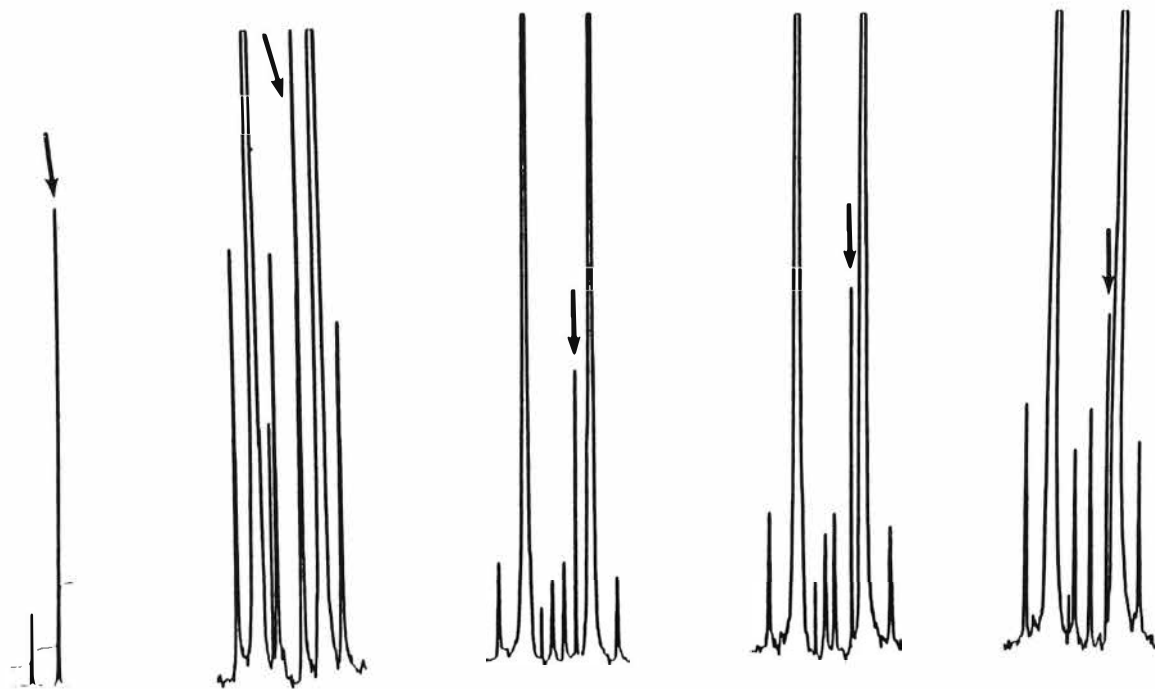


Figure 28.  $^1\text{H}$  NMR Chemical Shifts of Olefinic Protons of N-carbethoxymaleimide (NCEMI) with Several Concentrations of Furan (in  $\text{CDCl}_3$  at  $32.3^\circ\text{C}$ ).

Table XX

$^1\text{H}$  NMR DATA FOR DETERMINATION OF EQUILIBRIUM CONSTANT OF COMPLEXATION OF THE  
N-CARBETHOXYMALEIMIDE-FURAN SYSTEM (in  $\text{CDCl}_3$  at  $32.9^\circ\text{C}$ )

[NCEMI] $\text{mol.L}^{-1}$	[Furan] $\text{mol.L}^{-1}$	$\delta_{\text{obsd}}^{\text{A}}$ cps	$\Delta_{\text{obsd}}^{\text{A}}$ cps	$1/[\text{Furan}]$ $\text{L.mol}^{-1}$	$1/\Delta_{\text{obsd}}^{\text{A}}$ $\text{cps}^{-1}$
0.0500	--	$611.32 = \delta_0^{\text{A}}$	--	--	--
0.0500	2.3993	596.67	14.65	0.4168	0.0683
0.0500	3.5990	589.35	21.97	0.2779	0.0455
0.0500	4.7986	583.00	28.32	0.2084	0.0353
0.0500	5.9983	577.63	33.69	0.1667	0.0297

correlation coefficient = 0.9992; slope = 0.1553; intercept = 0.0032

[Furan] mol/L	0.0	1.0000	2.0000	2.5000	3.0000	4.0000
[NPMI]	0.0500	0.0500	0.0500	0.0500	0.0500	0.0500
cps	613.28	608.39	604.00	601.56	599.12	594.72
ppm	6.844	6.790	6.741	6.713	6.686	6.637

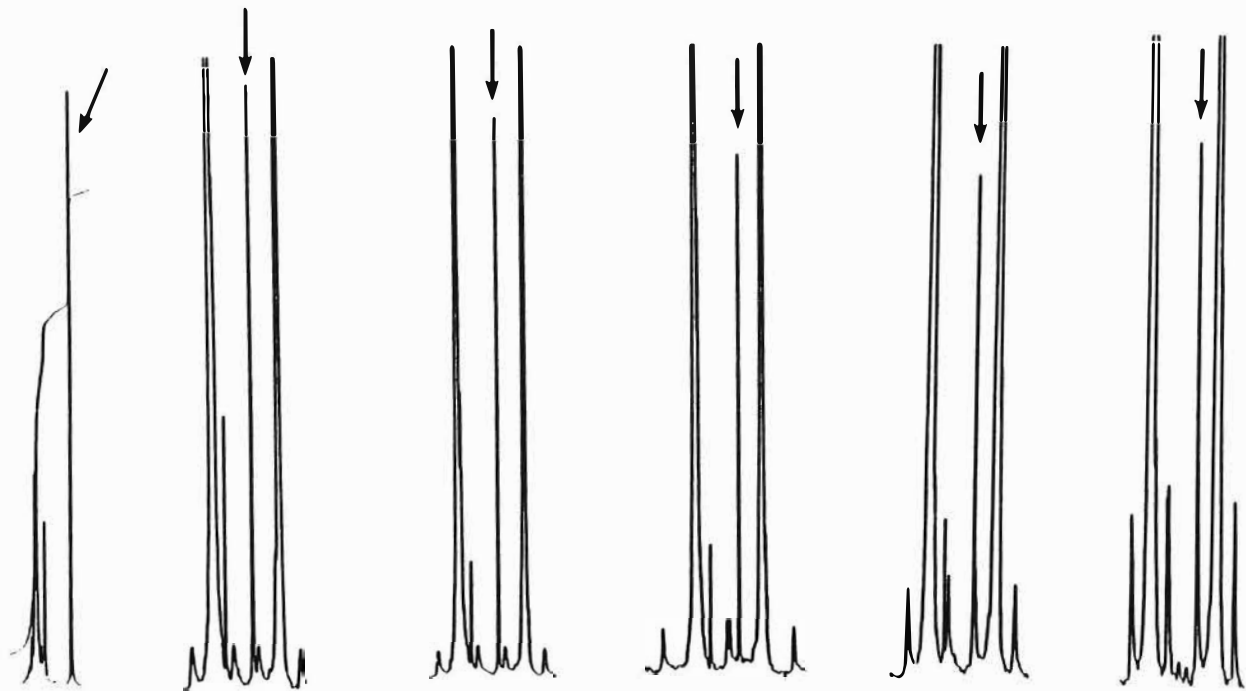


Figure 29.  $^1\text{H}$  NMR Chemical Shifts of Olefinic Protons of N-phenylmaleimide (NPMI) with Several Concentrations of Furan (in  $\text{CDCl}_3$  at  $32.0^\circ\text{C}$ ).

Table XXI

$^1\text{H}$  NMR DATA FOR DETERMINATION OF EQUILIBRIUM CONSTANT OF COMPLEXATION OF  
THE N-PHENYLMALIMIDE-FURAN SYSTEM (in  $\text{CDCl}_3$  at  $32.0^\circ\text{C}$ )

[NPMI] $\text{mol}\cdot\text{L}^{-1}$	[FURAN] $\text{mol}\cdot\text{L}^{-1}$	$\delta^{\text{A}}$ obsd cps	$\Delta^{\text{A}}$ obsd cps	$1/[\text{FURAN}]$ $\text{L}\cdot\text{mol}^{-1}$	$1/\Delta^{\text{A}}$ obsd $\text{cps}^{-1}$
0.0500	--	$613.28 = \delta^{\text{A}}_0$	--	--	--
0.0500	1.0000	608.39	4.89	1.0000	0.204
0.0500	2.0000	604.00	9.28	0.5000	0.108
0.0500	2.5000	601.56	11.72	0.4000	0.0853
0.0500	3.0000	599.12	14.16	0.3333	0.0706
0.0500	4.0000	594.72	18.56	0.2500	0.0539
0.0500	5.0000	587.89	25.39	0.2000	0.0394

correlation coefficient = 0.9990; slope = 0.2031; intercept = 0.0027

[Furan] mol/L	0.0	1.0007	2.0014	2.4017	4.0000
[NEMI]	0.0500	0.0500	0.0500	0.0500	0.0500
cps	598.63	594.23	589.84	588.38	581.54
ppm	6.681	6.632	6.583	6.567	6.490

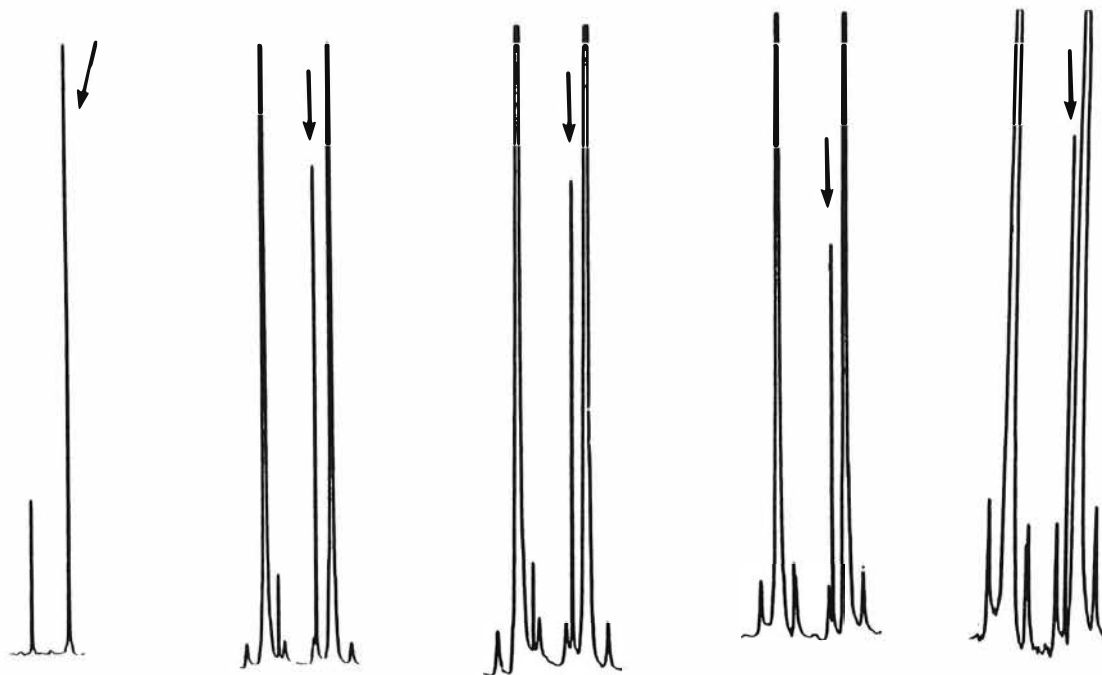


Figure 30.  $^1\text{H}$  NMR Chemical Shifts of Olefinic Protons of N-ethylmaleimide (NEMI) with several Concentrations of Furan (in  $\text{CDCl}_3$  at  $32.0^\circ\text{C}$ ).

Table XXII

$^1\text{H}$  NMR DATA FOR DETERMINATION OF EQUILIBRIUM CONSTANT OF COMPLEXATION OF THE  
N-ETHYLMALIMIDE-FURAN SYSTEM (in  $\text{CDCl}_3$  at  $32.0^\circ\text{C}$ )

[NEMI] $\text{mol}\cdot\text{L}^{-1}$	[Furan] $\text{mol}\cdot\text{L}^{-1}$	$\delta_{\text{obsd}}^{\text{A}}$ cps	$\Delta_{\text{obsd}}^{\text{A}}$ $\text{cps}^{-1}$	$1/[\text{Furan}]$ $\text{L}\cdot\text{mol}^{-1}$	$1/\Delta_{\text{obsd}}^{\text{A}}$ $\text{cps}^{-1}$
0.0500	--	$598.63 = \delta_{\text{A}_0}^{\text{A}}$	--	--	--
0.0500	1.007	594.23	4.40	0.9993	0.227
0.0500	2.0014	598.84	8.79	0.4997	0.114
0.0500	2.4017	588.38	10.25	0.4164	0.0976
0.0500	4.0000	581.54	17.09	0.2500	0.0585

correlation coefficient = 0.9999; slope = 0.2243; intercept = 0.0028



[Furan] mol/L	0.0	1.0000	2.0000	3.0000	4.0000	5.0000	6.0000	7.0000
[MI]	<0.05	<0.05	<0.05	<0.05	<0.05	<0.05	<0.05	<0.05
cps	601.07 599.60	595.70 594.23	591.30 590.33	585.93 584.47	581.05 579.58	577.14 575.68	573.24 571.77	569.82 568.35
ppm	6.708 6.691	6.648 6.632	6.599 6.588	6.539 6.523	6.484 6.468	6.441 6.425	6.397 6.381	6.359 6.343

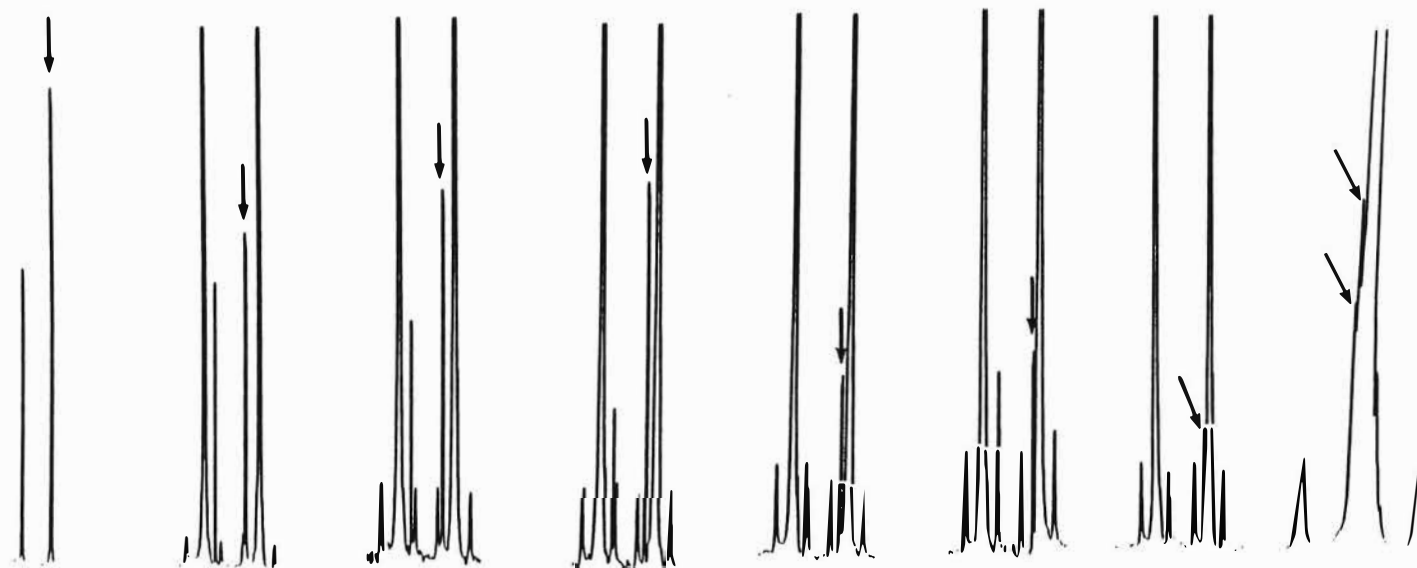


Figure 31.  $^1\text{H}$  NMR Chemical Shifts of Olefinic Protons of Maleimide (MI) with Several Concentrations of Furan (in  $\text{CDCl}_3$  at  $32.0^\circ\text{C}$ ).

Table XXIII

$^1\text{H}$  NMR DATA FOR DETERMINATION OF EQUILIBRIUM CONSTANT OF COMPLEXATION OF THE  
MALEIMIDE-FURAN SYSTEM (in  $\text{CDCl}_3$  at  $32.0^\circ\text{C}$ )

[MI] $\text{mol}\cdot\text{L}^{-1}$	[FURAN] $\text{mol}\cdot\text{L}^{-1}$	$\delta_{\text{obsd}}^{\text{A}}$ cps	$\Delta_{\text{obsd}}^{\text{A}}$ cps	$1/[\text{FURAN}]$ $\text{L}\cdot\text{mol}^{-1}$	$1/\Delta_{\text{obsd}}^{\text{A}}$ $\text{cps}^{-1}$
<0.0500	-	$601.07 = \delta_0^{\text{A}}$ 599.60	-	-	-
<0.0500	1.0000 1.0000	595.70 594.23	5.37 5.37	1.0000 1.0000	0.186 0.186
<0.0500	2.0000 2.0000	591.30 590.33	9.77 9.27	0.5000 0.5000	0.102 0.108
<0.0500	3.0000 3.0000	585.93 584.47	15.14 15.13	0.3333 0.3333	0.0661 0.0661
<0.0500	4.0000 4.0000	581.05 579.58	20.02 20.02	0.2500 0.2500	0.0500 0.0500
<0.0500	5.0000 5.0000	577.14 575.68	23.93 23.92	0.2000 0.2000	0.0418 0.0418
<0.0500	6.0000 6.0000	573.24 571.77	27.83 27.83	0.1667 0.1667	0.0359 0.0359

Table XXIII (Cont.)

$^1\text{H}$  NMR DATA FOR DETERMINATION OF EQUILIBRIUM CONSTANT OF COMPLEXATION OF THE  
THE MALEIMIDE-FURAN SYSTEM (in  $\text{CDCl}_3$  at  $32.0^\circ\text{C}$ ) (continued)

[MI] $\text{mol}\cdot\text{L}^{-1}$	[FURAN] $\text{mol}\cdot\text{L}^{-1}$	$\delta^{\text{A}}$ obsd cps	$\Delta^{\text{A}}$ obsd cps	$1/[\text{FURAN}]$ $\text{L}\cdot\text{mol}^{-1}$	$1/\Delta^{\text{A}}$ obsd $\text{cps}^{-1}$
<0.0500	7.0000	569.82	31.25	0.1429	0.0320
	7.0000	568.35	31.25	0.1429	0.0320
<0.0500	8.0000	a	a	0.1250	a
	8.0000			0.1250	

a) MI peaks were hidden behind styrene peak

downfield peak - correlation coefficient = 0.9991, slope = 0.1816; intercept = 0.0061

upfield peak - correlation coefficient = 0.9967; slope = 0.1830; intercept = 0.0065

TABLE XXIV

$^1\text{H}$  NMR Data for Determination of Equilibrium Constant of  
Complexation (K) of the Maleimide - Furan System (in  $\text{CDCl}_3$  at  $32.0^\circ\text{C}$ )

[MI] $\text{mol}\cdot\text{L}^{-1}$	[Furan] $\text{mol}\cdot\text{L}^{-1}$	$\delta^{\text{A}}$ obsd (a) cps	$\Delta^{\text{A}}$ obsd cps	$1/[\text{Furan}]$ $\text{L}\cdot\text{mol}^{-1}$	$1/\Delta^{\text{A}}$ obsd $\text{cps}^{-1}$
0.05	---	$600.34 = \delta_u^{\text{A}}$	---	---	---
0.05	1.0000	594.97	5.37	1.0000	0.1862
0.05	2.0000	590.82	9.52	0.5000	0.1050
0.05	3.0000	585.20	15.14	0.3333	0.0661
0.05	4.0000	580.32	20.02	0.2500	0.0450
0.05	5.0000	576.41	23.93	0.2000	0.0418
0.05	6.0000	572.51	27.83	0.1667	0.0359
0.05	7.0000	569.09	31.25	0.1429	0.0320

a) mean values of chemical shifts of the MI doublet are given.

correlation coefficient = 0.9971; slope = 0.1836; intercept = 0.0051

TABLE XXV

Calculated Equilibrium Constants of Complexation (K) Based on  
<sup>1</sup>H NMR Data in CDCl<sub>3</sub>

System	Temperature ( C )	K (L.mol <sup>-1</sup> )	Relative Standard Deviation (%)	Limits of K at 90% Confidence
MA-Furan	30.0	0.052 ± 0.017	33	0.036-0.068
NCMI-Furan	30.0	0.028 ± 0.007	25	0.020-0.036
MI-Furan	32.0	0.0278 ± 0.0009	3	0.0271-0.0285
NCEMI-Furan	32.9	0.021 ± 0.004	19	0.016-0.026
NPMI-Furan	32.0	0.024 ± 0.014	58	0.011-0.037
NEMI-Furan	32.0	0.013 ± 0.004	31	0.008-0.018

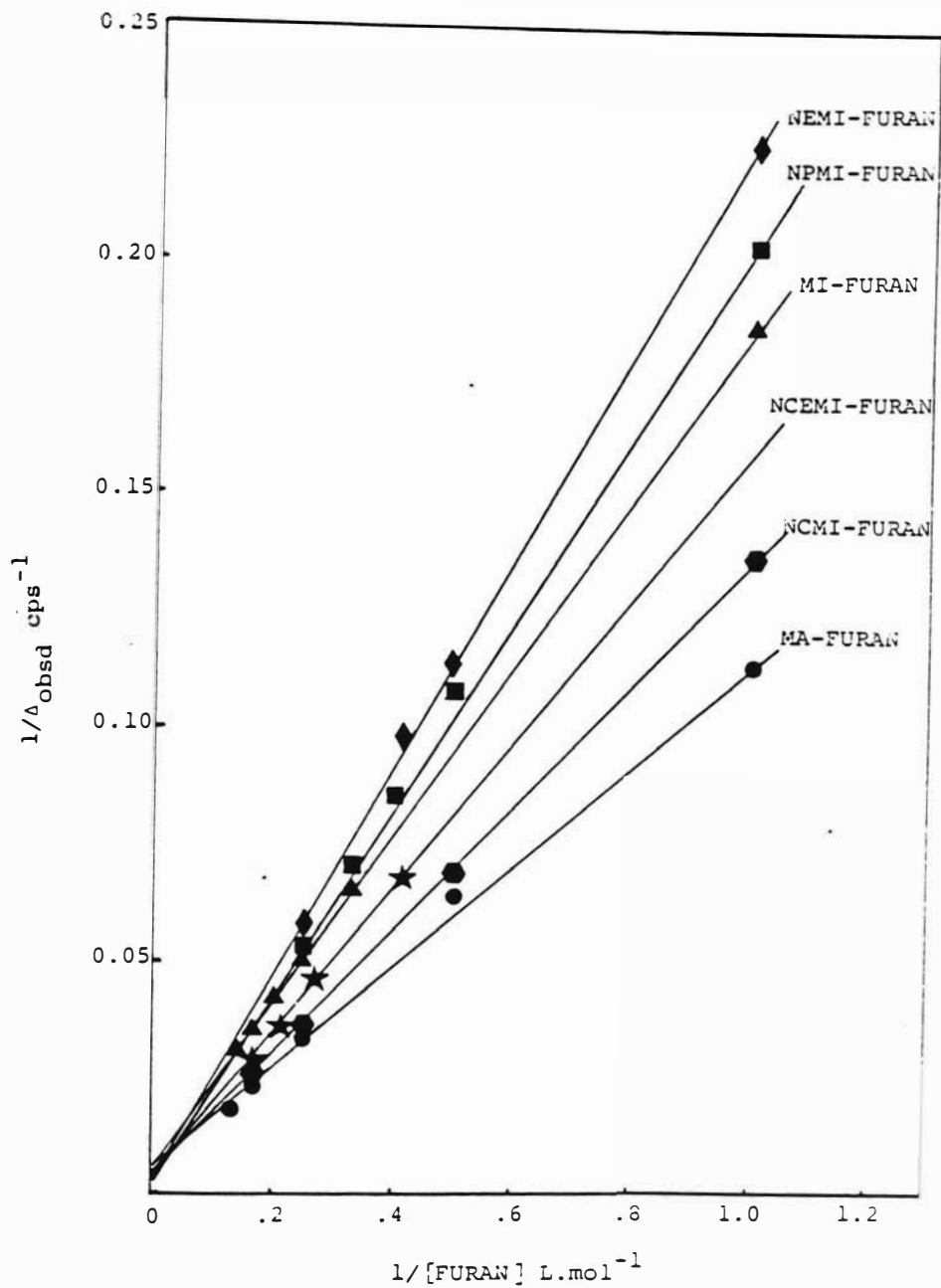


Fig.32.  $^1\text{H}$  NMR Determination of the Equilibrium Constant of Complexation between Furan and Electron-acceptors.

proton chemical shift. Tsuchida et al. reported (79) the determination of a formation constant of  $0.33 \text{ L}\cdot\text{mol}^{-1}$  for the MA-CEVE complex in n-hexane using the  $^1\text{H}$  NMR technique. Their experimental procedure involved using the chemical shift of  $\text{CHCl}_3$  as a calibration mark assuming that it had a constant shift value of 436 cps from TMS AT 60 MHz. The change in chemical shift for the  $\text{CDCl}_3$  resonance at 90 MHz that we observed indicates that Tsuchida et al.'s determination of the K value for MA-CEVE is in error because the point of reference used ( $\text{CHCl}_3$  resonance) has a variable chemical shift with different concentrations of CEVE. In our investigation, a plot of  $1/[\text{CEVE}]$  versus the reciprocal of the difference in chemical shift value between MA and  $\text{CDCl}_3$  for the corresponding CEVE concentration did not yield a reasonable K value. Since there was no evidence of MA-CEVE complexation in  $\text{CDCl}_3$  (at the concentrations used), a less polar solvent,  $\text{CCl}_4$ , was used for investigation of CEVE complexes. The MA protons displayed a doublet (Figure 33 and Table XXVI) and the mid-point of the doublet was used to measure chemical shift changes in MA for determination of the K value of MA-CEVE (Table XXVII). Unlike the styrene and the furan complexation experiments, the chemical shift changes of the electron-acceptors with increasing CEVE concentration were very small. As summarized in Table XXVIII, only MA-CEVE and MI-CEVE  $^1\text{H}$  NMR studies yielded a calculable value for a complex formation constant but their large standard deviations and the exceptionally large value

[CEVE] mol/L	0.0	0.7993	1.5986	2.3980	3.1973	3.9966
[MA]	0.0218	0.0218	0.0218	0.0218	0.0218	0.0218
cps	623.04 622.07]	623.53	624.51	626.46 625.00]	625.48	626.46
ppm	6.953 6.942]	6.959	6.969	6.992 6.975]	6.980	6.991

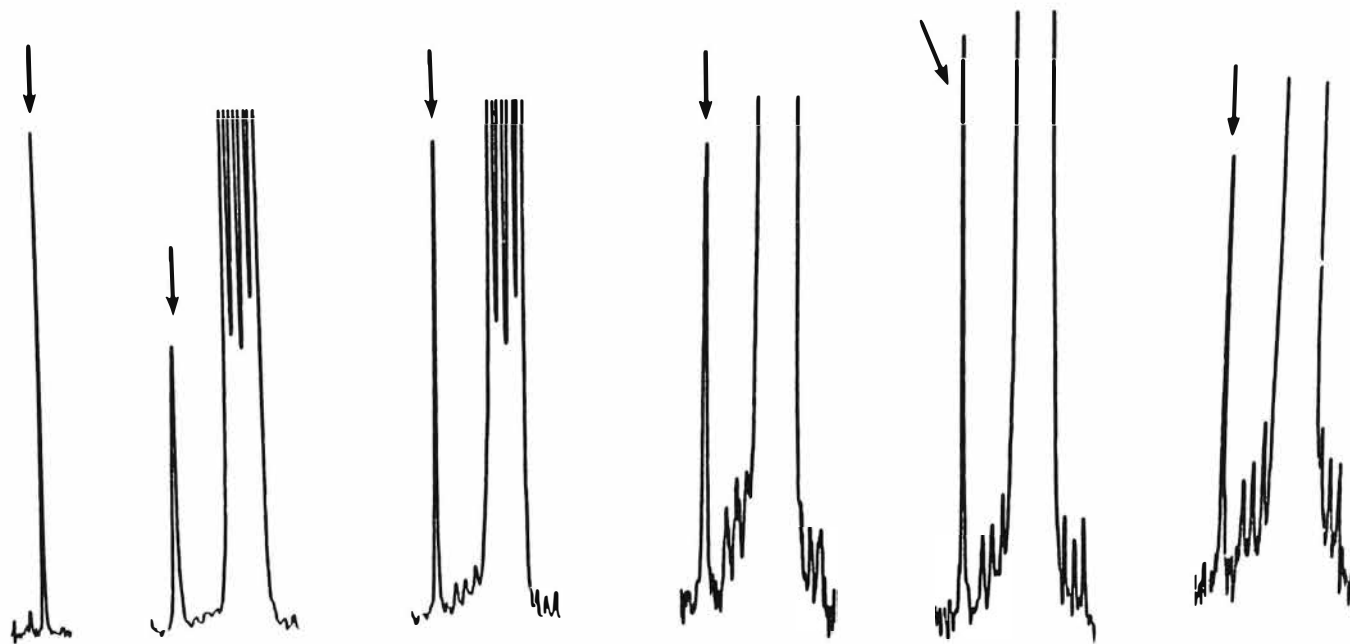


Figure 33.  $^1\text{H}$  NMR Chemical Shifts of Olefinic Protons of Maleic Anhydride (MA) with Several Concentrations of 2-Chloroethyl Vinyl Ether (CEVE) (in  $\text{CCl}_4$  at  $32.3^\circ\text{C}$ ).



Table XXVI

<sup>1</sup>H NMR DATA FOR ATTEMPTED DETERMINATION OF EQUILIBRIUM CONSTANT OF COMPLEXATION  
OF THE MALEIC ANHYDRIDE-2-CHLOROETHYL VINYL ETHER SYSTEM (in CCl<sub>4</sub> at 33°C)

[MA] mol.L <sup>-1</sup>	[CEVE] mol.L <sup>-1</sup>	$\delta^A_{\text{obsd}}$ cps	$\Delta^A_{\text{obsd}}$ cps	1/[CEVE] L.mol <sup>-1</sup>	1/ $\Delta^A_{\text{obsd}}$ cps <sup>-1</sup>
0.0218	-	623.04 622.07 $\delta^O_A$	-	-	-
0.0218	0.7993	623.53	0.49 1.46	1.2511	2.04 0.68
0.0218	1.5986	624.51	1.47 2.44	0.6255	0.68 0.41
0.0218	2.3980	626.46 625.00	3.42 2.93	0.4170	0.29 0.34
0.0218	3.1973	625.48	2.44 3.41	0.3128	0.41 0.29
0.0218	3.9966	626.46	3.42 4.39	0.2502	0.29 0.23

downfield peak - correlation coefficient = 0.9865; slope = 1.7389; intercept = -0.2068

upfield peak - correlation coefficient = 0.9956; slope = 0.4343; intercept = 0.1433

Table XXVII

$^1\text{H}$  NMR Data For Attempted Determination of Equilibrium Constant  
of Complexation (K) of the Maleic Anhydride-Vinyl Ether System (in  $\text{CCl}_4$  at  $33^\circ\text{C}$ )

[MA] $\text{mol.L}^{-1}$	[CEVE] $\text{mol.L}^{-1}$	$\delta_{\text{obsd}}^{\text{A(a)}}$ cps	$\Delta^{\text{A}_{\text{obsd}}}$ cps	$1/[\text{CEVE}]$ $\text{L.mol}^{-1}$	$1/\Delta^{\text{A}_{\text{obsd}}}$ $\text{cps}^{-1}$
0.0218	-	$622.56 = \delta_0^{\text{A}}$	-	-	-
0.0218	0.7993	623.53	0.97	1.2511	1.03
0.0218	1.5986	624.51	1.95	0.6255	0.51
0.0218	2.3980	625.73	3.17	0.4170	0.316
0.0218	3.1973	625.48	2.92	0.3128	0.343
0.0218	3.9966	626.46	3.91	0.2502	0.256

a) mean value of chemical shifts of MA doublet has been used.  
correlation coefficient = 0.9918; slope = 0.7722; intercept = 0.0500.

Table XXVIII

Attempted Determination of Equilibrium Constants of Complexation (K)  
Based on  $^1\text{H}$  NMR Data in  $\text{CCl}_4$

System	Temperature ( $^{\circ}\text{C}$ )	K ( $\text{L}\cdot\text{mol}^{-1}$ )	Relative Standard Deviation of K (%)	Limits of K at 90% Confidence
MA-CEVE	32	$0.06 \pm 0.05$	83	0.01 - 0.11
M1-CEVE	33	$0.5 \pm 0.4$	80	0.0 - 1.0
NCEHI-CEVE	32	a	-	-
NEMI-CEVE	32.1	b	-	-

a) negative intercept.

b) non-linear relationship between  $1/[\text{CEVE}]$  and  $1/\Delta_{\text{obs}}$ .

for K of MI-CEVE cast doubt on the validity of these formation constants. Figures 33-36 and Tables XXVI, XXVII, XXIX -XXXI indicate the data of the CEVE complex studies. Neither an electron-withdrawing group on maleimide (as in NCEMI) nor an electron-donating group (as in NEMI) seemed to enhance complexation of maleimide with CEVE. Olson reported (56) that the olefinic protons of NPMI exhibit very small shifts upon mixing with CEVE in  $\text{CDCl}_3$  or  $\text{CD}_2\text{Cl}_2$ . Similar small shifts have been observed for MA-CEVE solutions by Iwatsuki and Itoh (85). These authors reported that the MA-CEVE complexes are highly reactive leading to the formation of an alternating copolymer and attributed the small  $^1\text{H}$  NMR shifts to the low concentration of the complex in the solution. Such an explanation may also apply to the CEVE complexes in  $\text{CCl}_4$ . It may also be possible that the complex geometry is such that the chemical shifts of the olefinic protons are not affected by complexation.

The effect of solvent on  $^1\text{H}$  NMR shifts of electron acceptors was investigated with MA-furan and NCMI-furan complexation experiments in  $\text{CDCl}_3$  and in 1,4-dioxane at  $30.0^\circ$  C. As Figures 37 and 38 indicate, in 1,4-dioxane there was a regular change in olefinic proton shift of the acceptors with changing furan concentrations, the same as in  $\text{CDCl}_3$ . However, the chemical shift changes in  $\text{CDCl}_3$ , the more polar solvent, were greater for both MA and NCMI (Figures 26, 27, Tables XVIII, XIV). The data of the studies in 1,4-dioxane of MA-furan and NCMI-furan are given in Tables XXXII and

[CEVE] mol/L	0.0	0.8001	1.6002	2.4002	3.2003	4.0004
[NCEMI]	0.0221	0.0221	0.0221	0.0221	0.0221	0.0221
cps	602.53	603.02	604.00	604.49	604.49	604.98
ppm	6.724	6.730	6.741	6.746	6.746	6.752

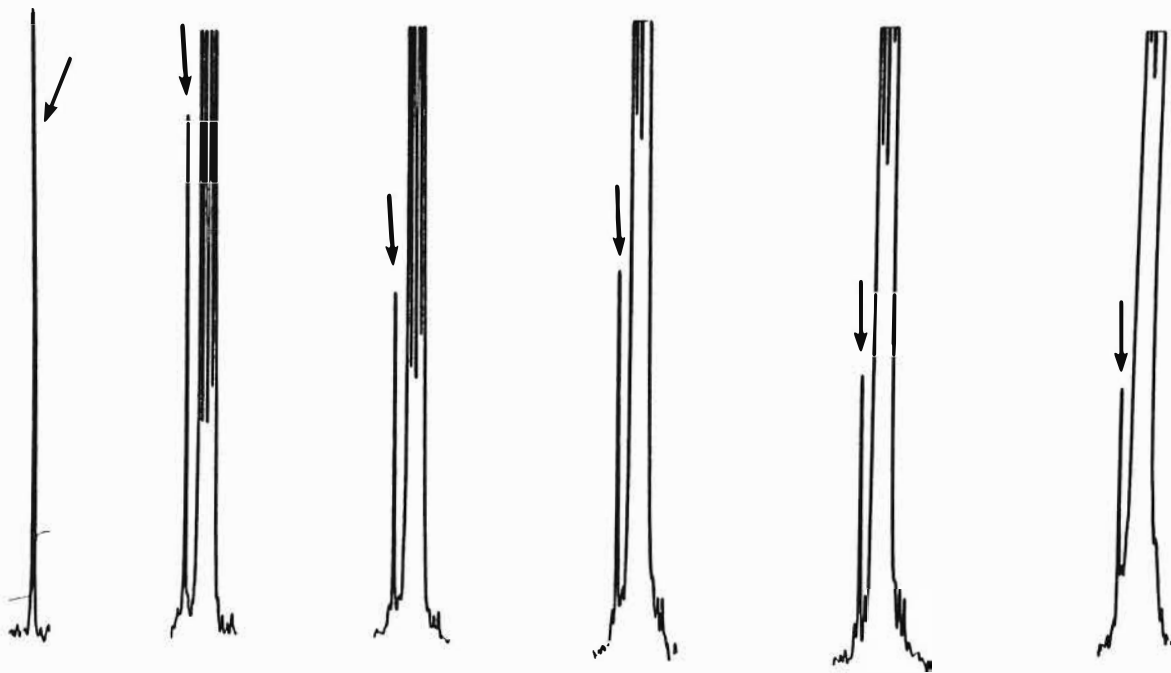


Figure 34 .  $^1\text{H}$  NMR Chemical Shifts of Olefinic Protons of N-carbethoxymaleimide (NCEMI) with Several Concentrations of 2-Chloroethyl vinyl ether (CEVE) in  $\text{CCl}_4$  at  $32.0^\circ\text{C}$ ).

Table XXIX

$^1\text{H}$  NMR DATA FOR ATTEMPTED DETERMINATION OF EQUILIBRIUM CONSTANT OF COMPLEXATION OF THE N-CARBETHOXYMALEIMIDE-2-CHLOROETHYL VINYL ETHER SYSTEM (in  $\text{CCl}_4$  at  $32^\circ\text{C}$ )

[NCEMI] $\text{mol}\cdot\text{L}^{-1}$	[CEVE] $\text{mol}\cdot\text{L}^{-1}$	$\delta^A_{\text{obsd}}$ cps	$\Delta^A_{\text{obsd}}$ cps	$1/[\text{CEVE}]$ $\text{L}\cdot\text{mol}^{-1}$	$1/\Delta^A_{\text{obsd}}$ $\text{cps}^{-1}$
0.0221	-	$602.53 = \delta^A_0$	-	-	-
0.0221	0.8001	603.02	0.49	1.2498	2.04
0.0221	1.6002	604.00	1.47	0.6249	0.68
0.0221	2.4002	604.49	1.96	0.4166	0.51
0.0221	3.2003	604.49	1.96	0.3125	0.51
0.0221	4.0004	604.98	2.45	0.2500	0.41

correlation coefficient = 0.9748; slope = 1.6432; intercept = -0.1078

[CEVE]: mol/L	0.0	0.8001	1.6002	2.4002	3.2003	4.0004
[MI]:	0.0158	0.0158	0.0158	0.0158	0.0158	0.0158
Hz	594.23	593.26	592.77	592.28	592.28	peak
ppm	6.632	6.621	6.615	6.610	6.610	hidden

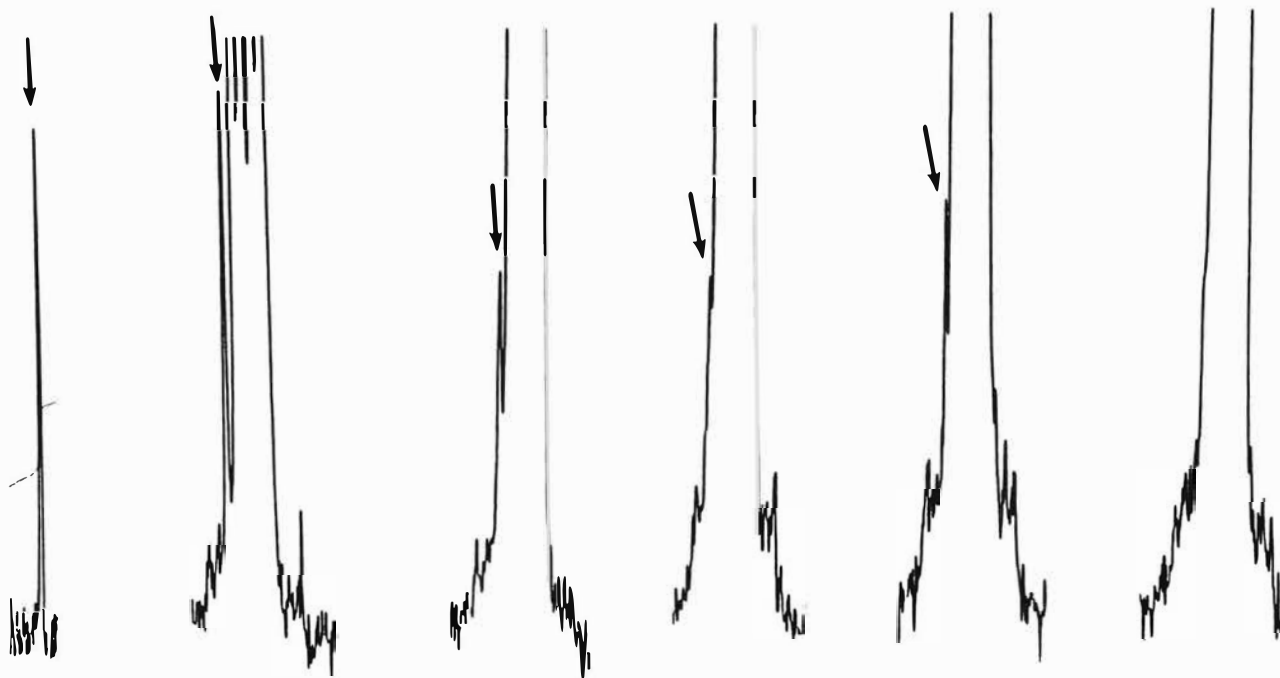


Figure 35.  $^1\text{H}$  NMR Chemical Shifts of Olefinic Protons of Maleimide (MI) with Several Concentrations of 2-Chloroethyl vinyl ether (CEVE) (in  $\text{CCl}_4$  at  $32^\circ\text{C}$ ).

Table XXX

$^1\text{H}$  NMR DATA FOR ATTEMPTED DETERMINATION OF EQUILIBRIUM CONSTANT OF COMPLEXATION  
OF THE MALEIMIDE-2-CHLOROETHYL VINYL ETHER SYSTEM (in  $\text{CCl}_4$  at  $32^\circ\text{C}$ )

$[\text{MI}]$ $\text{mol}\cdot\text{L}^{-1}$	$[\text{CEVE}]$ $\text{mol}\cdot\text{L}^{-1}$	$A$ $\delta_{\text{obsd}}$ cps	$A$ $\Delta_{\text{obsd}}$ cps	$1/[\text{CEVE}]$ $\text{L}\cdot\text{mol}^{-1}$	$1/\Delta_{\text{obsd}}$ $\text{cps}^{-1}$
0.0158	-	$594.23 = \delta_{\text{A}_0}$	-	-	-
0.0158	0.8001	593.26	0.97	1.2498	1.03
0.0158	1.6002	592.77	1.46	0.6249	0.68
0.0158	2.4002	592.28	1.95	0.4166	0.51
0.0158	3.2003	592.28	1.95	0.3125	0.51
0.0158	4.0004	a	a	0.2500	a

a) MI peak was hidden behind a CEVE peak.

correlation coefficient = 0.9943, slope = 0.5805; intercept = 0.3046



[CEVE]	0.0	0.8002	1.6004	2.4006	3.2008	4.0011
mol/L						
[NEMI]	0.0500	0.0500	0.0500	0.0500	0.0500	0.0500
Hz	592.04	592.52	592.52	592.77	593.01	592.77
ppm	6.607	6.612	6.612	6.615	6.618	6.615

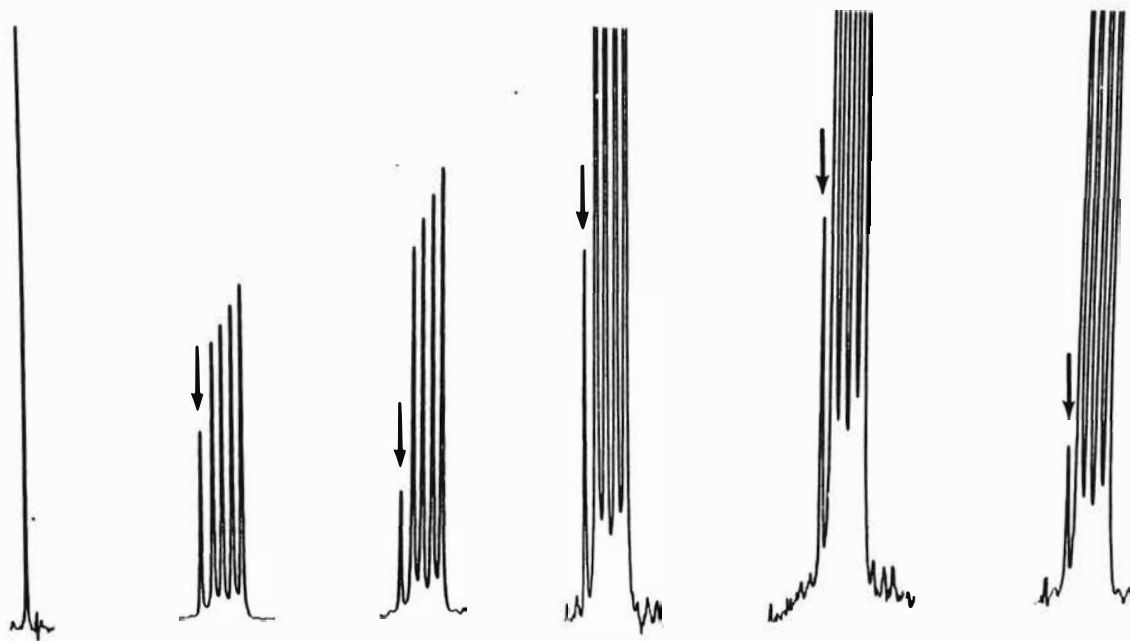


Figure 36.  $^1\text{H}$  NMR Chemical Shifts of Olefinic Protons of N-ethylmaleimide (NEMI) with Several Concentrations of 2-Chloroethyl vinyl ether (CEVE) (in  $\text{CCl}_4$  at  $32.1^\circ\text{C}$ ).

Table XXXI

<sup>1</sup>H NMR DATA FOR ATTEMPTED DETERMINATION OF EQUILIBRIUM CONSTANT OF COMPLEXATION  
OF THE N-ETHYLMALEIMIDE-2-CHLOROETHYL VINYL ETHER SYSTEM (in CCl<sub>4</sub> at 32.1°C)

[NEMI] mol.L <sup>-1</sup>	[CEVE] mol.L <sup>-1</sup>	$\delta^A_{\text{obsd}}$ cps	$\Delta^A_{\text{obsd}}$ cps	1/[CEVE] L.mol <sup>-1</sup>	1/ $\Delta^A_{\text{obsd}}$ cps <sup>-1</sup>
0.0500	-	592.04= $\delta^A_0$	-	-	-
0.0500	0.8002	592.52	0.48	1.2497	2.08
0.0500	1.6004	592.52	0.48	0.6248	2.08
0.0500	2.4006	592.77	0.73	0.4166	1.37
0.0500	3.2008	593.01	0.97	0.3124	1.03
0.0500	4.0011	592.77	0.73	0.2499	1.37

correlation coefficient = 0.7951; slope = 0.9255; intercept = 1.0579

[Furan] mol/L	0.0	1.0000	2.0000	3.0000	4.0000	6.0000
[MA]	0.0500	0.0500	0.0500	0.0500	0.0500	0.0500
Hz	632.32	629.39	625.97	622.07	618.16	608.40
ppm	7.057	7.024	6.986	6.942	6.899	6.790

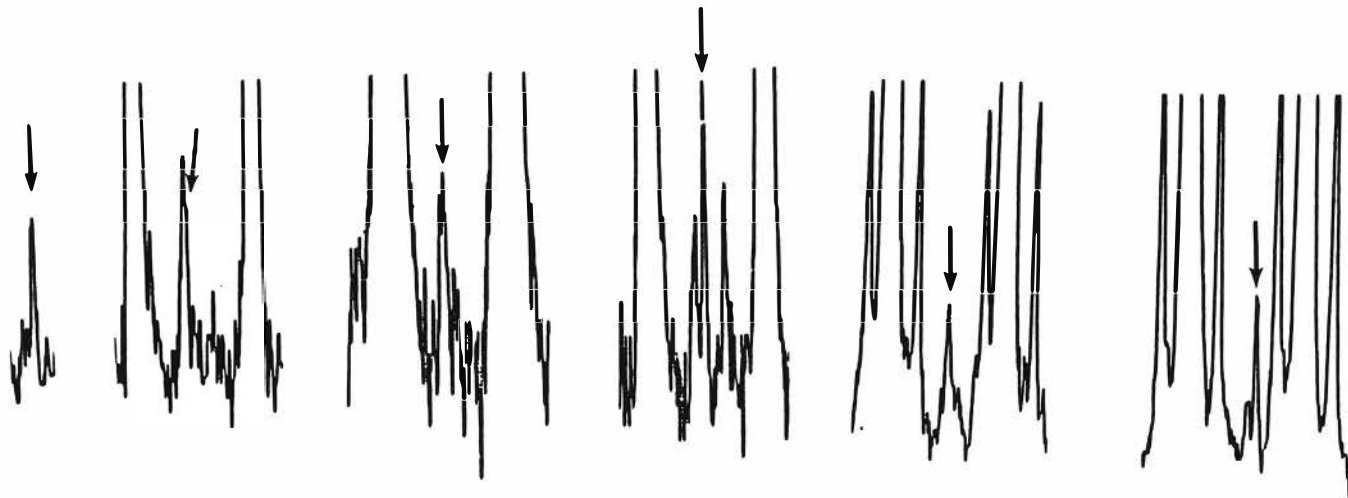


Figure 37.  $^1\text{H}$  NMR Chemical Shifts of Maleic Anhydride with Several Concentrations of Furan (in 1,4-dioxane at 30.0°C).

Table XXXII

$^1\text{H}$  NMR DATA FOR THE DETERMINATION OF EQUILIBRIUM CONSTANT OF COMPLEXATION  
OF THE MALEIC ANHYDRIDE-FURAN SYSTEM (in 1,4-dioxane at 30.0°C)

[MA] mol.L <sup>-1</sup>	[Furan] mol.L <sup>-1</sup>	$\delta_{\text{obsd}}^{\text{A}}$ cps	$\Delta_{\text{obsd}}^{\text{A}}$ cps	1/[Furan] L.mol <sup>-1</sup>	1/ $\Delta_{\text{obsd}}^{\text{A}}$ cps <sup>-1</sup>
0.0500	-	632.32 = $\delta_0^{\text{A}}$	-	-	-
0.0500	1.0000	629.39	2.93	1.0000	0.341
0.0500	2.0000	625.97	6.35	0.5000	0.157
0.0500	3.0000	622.07	10.25	0.3333	0.0976
0.0500	4.0000	618.16	14.16	0.2500	0.0706
0.0500	6.0000	608.40	23.92	0.1667	0.0418

correlation coefficient = 0.9998; slope = 0.3601; intercept = -0.0205

[Furan]	0.0	2.0000	3.0000	4.0000	5.0000	6.0000
mol/L						
[NCMI]	0.0500	0.0500	0.0500	0.0500	0.0500	0.0500
cps	610.83	606.45	602.53	599.60	595.21	591.30
ppm	6.817	6.768	6.724	6.691	6.642	6.599

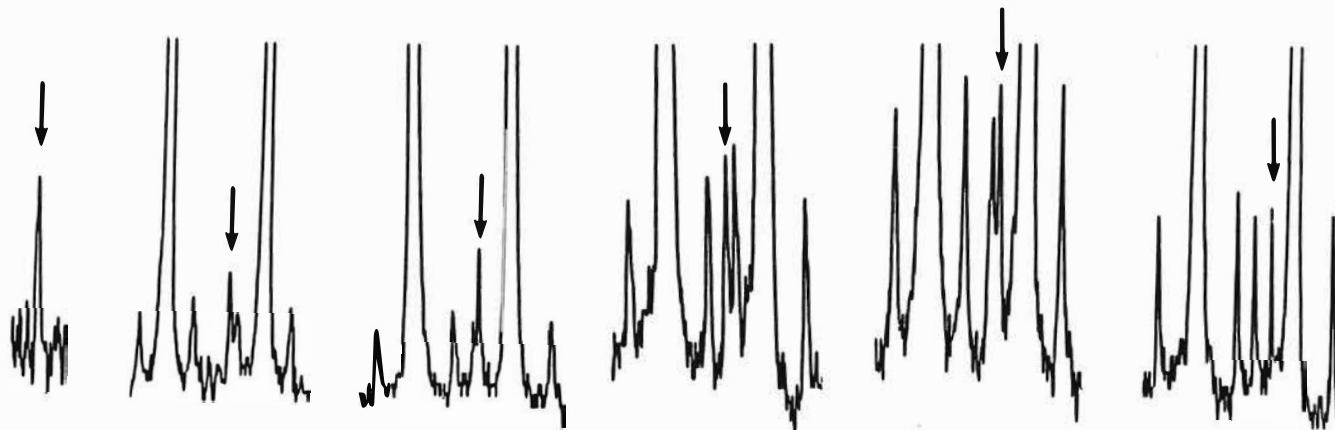


Figure 38.  $^1\text{H}$  NMR Chemical Shifts of Olefinic Protons of N-carbamylmaleimide (NCMI) with Several Concentrations of Furan (in 1,4-dioxane at  $30.0^\circ\text{C}$ ).

Table XXXIII

$^1\text{H}$  NMR DATA FOR THE DETERMINATION OF EQUILIBRIUM CONSTANT OF COMPLEXATION  
OF THE N-CARBAMYLMALEIMIDE-FURAN SYSTEM (in 1,4-dioxane at 30.0°C)

[NCMI] mol.L <sup>-1</sup>	[Furan] mol.L <sup>-1</sup>	$\delta_{\text{obsd}}^A$ cps	$\Delta_{\text{obsd}}^A$ cps	1/[Furan] L.mol <sup>-1</sup>	1/ $\Delta_{\text{obsd}}^A$ cps <sup>-1</sup>
0.0500	-	610.83 = $\delta_0^A$	-	-	-
0.0500	2.0000	606.45	4.38	0.5000	0.2283
0.0500	3.0000	602.53	8.30	0.3333	0.120
0.0500	4.0000	599.60	11.23	0.2500	0.0890
0.0500	5.0000	595.20	15.63	0.2000	0.0640
0.0500	6.0000	591.30	19.53	0.1667	0.0512

correlation coefficient = 0.9935; slope = 0.5292; intercept = -0.0430

XXXIII, respectively. Negative values for the intercepts of plots of  $1/[\text{furan}]$  versus  $1/\Delta_{\text{Obs}}$  for both MA-furan and NCMI-furan (Figures 39 and 40) indicated that no complex formation was taking place in dioxane. It may be possible that the lone pairs of electrons on the oxygen atoms of dioxane influence it to behave as a weak electron-donor and thus compete with furan for complexation with the electron-acceptor.

The chemical shift of MA and NCMI olefinic protons show a solvent dependence. When an electron-donor is present, an increase in the donor concentration usually affects the chemical shift of the olefinic protons of the acceptor to a greater extent than the solvent chemical shift. These effects for MA and NCMI are shown in Tables XXXIV and XXXV, respectively. Polar solvents appear to deshield the olefinic protons more than less polar solvents and induce a downfield shift. The differences in formation constants of charge-transfer complexes in different solvents indicate the importance of polarity of the solvent and whether it is "inactive" or can act as a weak electron-donor or acceptor.

On the basis of the above mentioned UV studies and  $^1\text{H}$  NMR studies, it can be inferred that: (1) styrene and furan form a stronger charge-transfer complex with MA than with MI; (2) in the case of styrene, electron-withdrawing N-substituents on MI appear to increase CT complexation; (3) in the case of furan, electron-withdrawing groups may or may not have an effect on the complexation of maleimide; (4) the

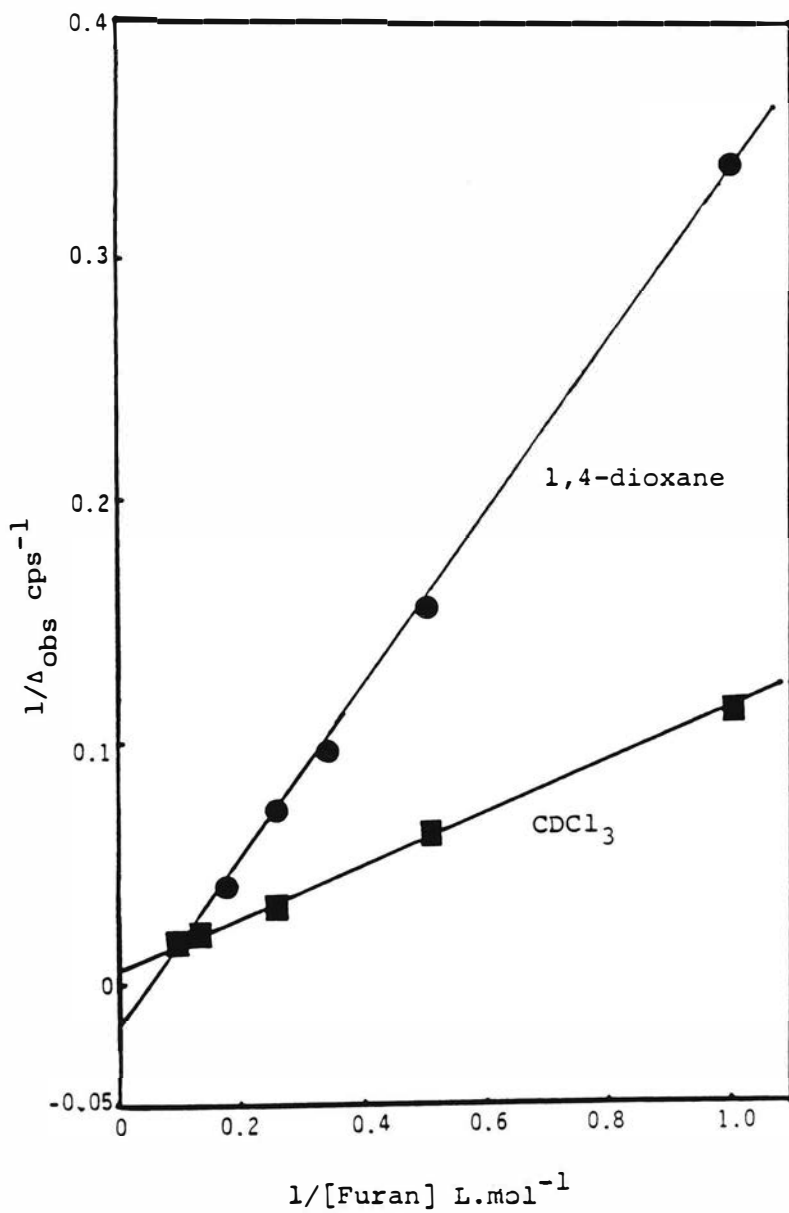


Fig.39. Solvent effect in the NMR determination of the equilibrium constant of complexation between maleic anhydride and furan at 30.0°C



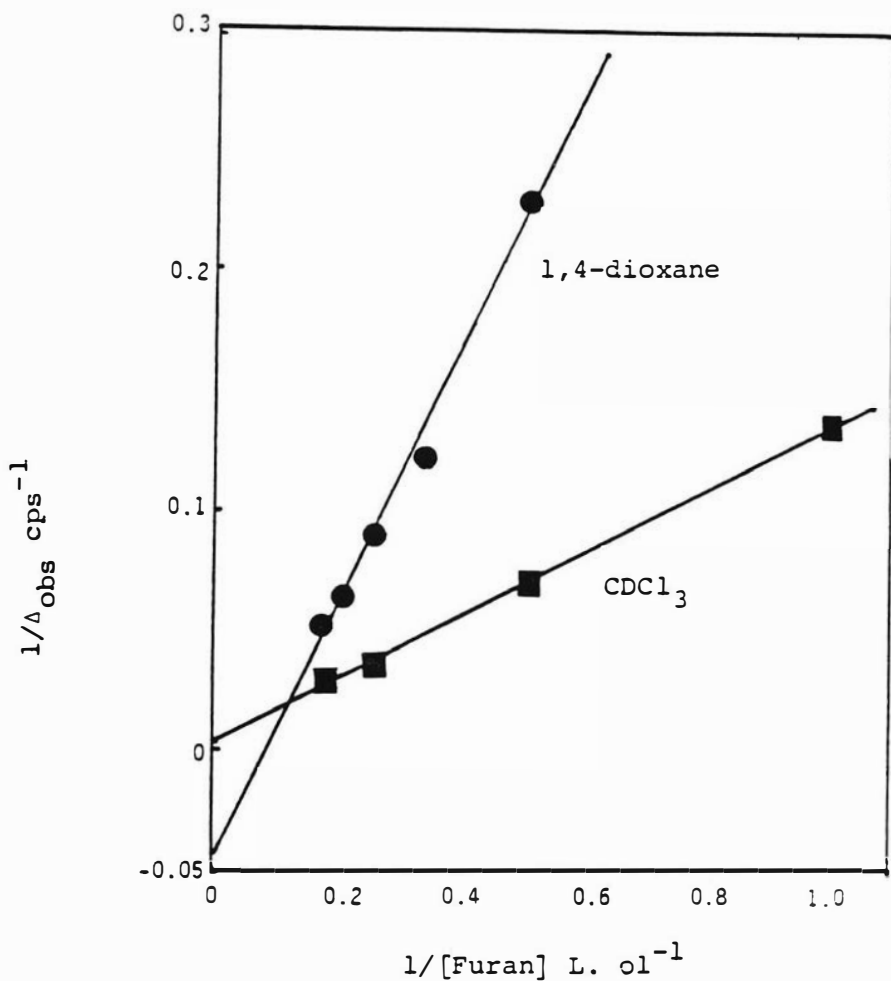


Fig.40. Solvent effect on the NMR determination of the equilibrium constant of complexation between N-carbamylmaleimide and Furan at 30.0°C

Table XXXIV

EFFECT OF SOLVENT ON THE CHEMICAL SHIFT OF MALEIC ANHYDRIDE OLEFINIC PROTONS AND  
EFFECT OF CONCENTRATION OF ELECTRON-DONOR SPECIES ON SOLVENT CHEMICAL  
SHIFTS (89.56 MHz,  $\delta$ , ppm from TMS)

Solvent	Dielectric Constant at 20°C	MA mol.L <sup>-1</sup>	Electron-donor		$\delta_{MA}$	$\delta_{solvent}$
			[Furan] mol.L <sup>-1</sup>	[CEVE]		
1,4-Dioxane	2.209 <sup>a</sup>	0.0500	0.0	0.0	7.057	3.558
1,4-Dioxane	2.209 <sup>a</sup>	0.0500	6.0000	0.0	6.790	3.553
CDCl <sub>3</sub>	4.806	0.0100	0.0	0.0	7.010	7.253
CDCl <sub>3</sub>	4.806	0.0100	6.0000	0.0	6.553	7.046
CCl <sub>4</sub>	2.238	0.0218	0.0	0.0	6.953	-
CCl <sub>4</sub>	2.238	0.0218	0.0	3.9966	6.991	-
CDCl <sub>3</sub>	4.806	0.0475	0.0	0.0	7.024	7.351
CDCl <sub>3</sub>	4.806	0.0475	0.0	3.7288	7.024	7.329
DMSO-d <sub>6</sub> <sup>b</sup>	48.9	~0.760	0.0	0.0	7.37	2.50

a) 25°C

b) 60 MHz

Table XXXV

EFFECT OF SOLVENT ON THE CHEMICAL SHIFT OF N-CARBAMYLMALEIMIDE OLEFINIC PROTONS AND  
EFFECT OF CONCENTRATION OF FURAN ON SOLVENT CHEMICAL SHIFTS (89.56 Hz,  $\delta$ , ppm from TMS)

Solvent	Dielectric Constant (temp., °C)	[NCMI] <sub>1</sub> mol.L <sup>-1</sup>	[Furan] mol.L <sup>-1</sup>	$\delta_{\text{NCMI}}$	$\delta_{\text{solvent}}$
1,4-Dioxane	2.209 <sup>a</sup>	0.0500	0.0	6.817	3.569
1,4-Dioxane	2.209 <sup>a</sup>	0.0500	4.0000	6.691	3.563
CDCl <sub>3</sub>	4.806	0.0100	0.0	6.855	7.247
CDCl <sub>3</sub>	4.806	0.0100	4.0000	6.555	7.111
DMSO-d <sub>6</sub> <sup>b</sup>	48.9	0.720	0.0	6.88	2.53

a) 25°C

b) 60 MHz

type of complexation that aromatic styrene engages in with electron-acceptors may be dissimilar from the complexing mechanism of furan.

The stoichiometry of complexation for all the CT absorptions observed by UV was 1:1. However, higher order complexes for these systems cannot be ruled out. The low concentrations of the monomers would not favor termolecular or higher order complexes. Foster (68) has reported that successive molecular interactions are often competitive and appear to reduce the probability of further association, so that the concentrations of these higher order complexes are smaller than would be if a cooperative effect occurred.

#### Copolymerizations and Homopolymerizations of N-Substituted Maleimides

When NCMI was copolymerized with styrene it was observed that the conversion percent increased to a maximum at a 50:50 feed ratio as the data in Table XXXVI indicate. Some homopolymerization of NCMI appeared to occur with a feed ratio greater than 50% of NCMI. Due to the color difference between the white copolymer and pink polyNCMI, contamination of the copolymer by the homopolymer could be easily observed. At the concentration used, NCMI or styrene had little tendency to homopolymerize (Table XXXVI). The relationship between the mole fraction of NCMI in the monomer feed and the rate of conversion to copolymer is shown in Figure 41. The maximum rate occurring at the mole fraction of 0.5 indicates that copolymerization is preferred

Table XXXVI

Data for NCMI-Styrene Copolymerization (in 1, 4-Dioxane, 60°C,  $[M]_T=0.2M$ )

Mole Fraction of NCMI in Feed	Color of Polymer	Decomposition Point (°C)	Conversion % By Total Monomer Weight	Rate of Conversion (% yield/h)
0.0	White	140 - 150	0.98	0.06
0.1	White	300	15.8	0.97
0.3	White	297	64.5	3.91
0.5	White	300	100.0	7.02
0.7	Very light pink	289	67.7	4.10
0.9	Light pink	285	33.0	2.06
1.0	Pink	290	14.0	0.88

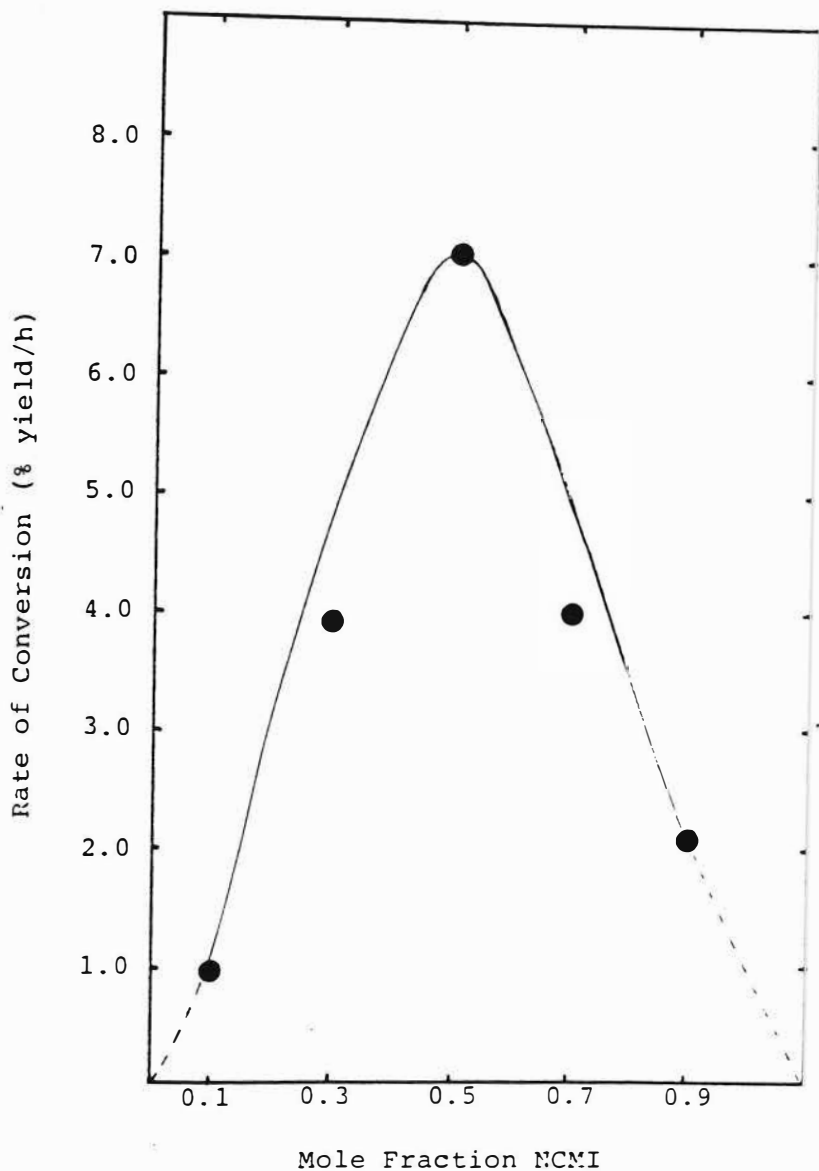


Figure 41. Relationship between Mole Fraction of NCMI in Feed and Rate of Conversion of the Copolymerization of NCMI with Styrene.

over homopolymerization. If a charge-transfer complex forms, it should have the highest concentration at a molar feed ratio of 0.5. This type of rate maximum has been used as supportive evidence for charge-transfer interactions among comonomers (86). To investigate whether solvent could affect the copolymerization of NCMI and styrene and the homopolymerization of NCMI, dimethylsulfoxide (DMSO) was used as the solvent. As the data in Table XXXVII indicate, the rates of polymerization for the homopolymer as well as the copolymer were drastically reduced in DMSO when compared to the rates in dioxane. Copolymerizations in which charge-transfer interactions occur would be expected to be inhibited in polar solvents such as DMSO. However, since the homopolymerization of NCMI too was affected, a charge-transfer mechanism cannot be postulated solely on the basis of this solvent effect. DMSO is used as a solvent for the polymerization of acrylonitrile and other monomers (87) such as methyl methacrylate (88) and styrene (89). It is known to have a low incidence of transfer from the growing chain thus leading to high molecular weight polymers (87). The reason for its inhibitory action in the polymerization of NCMI and NCMI-styrene is not evident.

Effect of Electron-Withdrawing Groups on Maleimide  
Reactivity

Maleimide has a much greater tendency to homopolymerize than maleic anhydride. If electron-withdrawing substituents have the effect of making maleimide more similar to maleic

Table XXXVII

Effect of Solvent on Rate of Conversion to Polymer for Homopolymerization of N-carbamylmaleimide (NCMI) and Copolymerization of NCMI with Styrene (Sty)

Polymer	Solvent	[Monomer] (mol.L <sup>-1</sup> )	% Monomer (w/v)	[AIBN] (mol.L <sup>-1</sup> )	Time (h)	% Yield of Polymer
<u>Homopolymer</u>						
Poly NCMI	1,4-Dioxane	0.2000	2.8020	0.0040	16.0	14.0
Poly NCMI	Dimethylsulfoxide	0.3600	5.0436	0.0040	51.3	4.0
Poly NCMI	Dimethylsulfoxide	1.7800	25.0000	0.0178	25.0	18.4
<u>Copolymer<sup>a</sup></u>						
Poly(NCMI-Sty)	1,4-Dioxane	0.2000	2.4424	0.0040	16.0	100.0
Poly(NCMI-Sty)	Dimethylsulfoxide	3.5600	43.5784	0.0350	24.0	63.6

a) feed ratio of NCMI:Sty was 1:1



anhydride in polymerization behavior, then the homopolymerization rate of maleimide should be inhibited in NCMI and NCEMI. As Table XXXVIII indicates, a significant drop in the conversion rate (as compared to MI) was observed for NCMI and NCEMI. The conversion rate study for copolymerization with styrene was less conclusive since MA has a percent yield similar to that of MI. However, the % yield value given for the MI-styrene copolymer may include some MI homopolymer as well which, if taken into account would give a lower value for the MI-styrene conversion rate. It is apparent that the electron-withdrawing groups have increased the reactivity of maleimide with styrene.

#### Copolymers of Maleic Anhydride with N-Substituted Maleimides

Due to the biological activity of carboxylate polymers with succinimide rings, there was a practical interest in investigating whether copolymers could be formed between MA, an electron acceptor that does not readily homopolymerize and electron acceptor N-substituted maleimides, which do homopolymerize. NPMI and NEMI were selected for this purpose, and, since both comonomers are electron-acceptors, no charge-transfer complexation and no alternating copolymer was expected. NPMI homopolymer precipitated in acetone whereas the NPMI-MA copolymer and NEMI-MA copolymer remained in solution in acetone. As indicated in Table XXXIX, the MA/NPMI feed ratio was changed progressively from 50:50 to 95:05. Equimolar feed ratios gave copolymers composed of 40% MA and 60% NPMI. The use of a large excess of MA in the

Table XXXVIII

Comparison of Rates of Conversion (in 1,4-dioxane, 60.0°C)

Polymer	[Monomer] (mol/L)	[AIBN] (mol/L)	% yield	Rate of conversion (% yield/h)
Homopolymers:				
Polystyrene	$2.0 \times 10^{-1}$	$4.0 \times 10^{-3}$	0.98	0.06
Poly MI	$2.0 \times 10^{-1}$	$4.0 \times 10^{-3}$	41.33	2.58
Poly NCMI	$2.0 \times 10^1$	$4.0 \times 10^{-3}$	13.99	0.88
Poly NCEMI	$2.0 \times 10^{-1}$	$8.0 \times 10^{-3}$	2.40	0.15
Copolymers:				
Poly MI-Sty	$2.0 \times 10^{-1}$	$4.0 \times 10^{-3}$	78.40	4.90
Poly NCEMI-Sty	$2.0 \times 10^{-1}$	$4.0 \times 10^{-3}$	92.55	5.78
Poly NCMI-Sty	$2.0 \times 10^{-1}$	$4.0 \times 10^{-3}$	100.00	7.02
Poly MA-Sty	$2.0 \times 10^{-1}$	$4.0 \times 10^{-3}$	77.17	4.82

Table XXXIX

Data for the copolymerization of Maleic Anhydride (MA) and  
N-Phenylmaleimide (NPMI) in Acetone at 65°C

Designation	Feed Ratio MA:NPMI	Percent Conversion By Total Monomer Weight	Percent Nitrogen	Copolymer Composition	
				based on %N MA:NPMI	based on <sup>1</sup> H NMR
Poly (NPMI-co-MA-1)	50:50	70.6	5.93	39:61	39:61
Poly (NPMI-co-MA-2)	50:50	74.9	-	-	-
Poly (NPMI-co-MA-3)	50:50	11.5	-	-	33:67
Poly (NPMI-co-MA-4)	50:50	19.7	6.95	22:78	-
Poly (NPMI-co-MA-5)	50:50	84.2	6.28	34:66	-
Poly (NPMI-co-MA-6)	50:50	92.1	-	-	-
Poly (NPMI-co-MA-11)	80:20	48.9	-	-	53:47
Poly (NPMI-co-MA-12)	80:20	60.2	-	-	63:37
Poly (NPMI-co-MA-9)	90:10	43.4	4.05	64:36	70:30
Poly (NPMI-co-MA-10)	90:10	42.6	-	-	65:35
Poly (NPMI-co-MA 7)	95:05	29.7	-	-	70:30
Poly (NPMI-co-MA 8)	95:05	28.0	-	-	73:27

monomer feed yielded polymers with a greater amount of the MA component. This was interesting in light of the fact that MA is generally not known to homopolymerize under these conditions. Copolymer composition analysis, done by  $^1\text{H}$  NMR (Figure 42) and elemental N analysis (Table XXXIX) indicated that polymers which did not show a good correlation between these two methods had very large aromatic proton: non-aromatic proton ratios ( $>2.5$ ) which were not in agreement with a copolymer structure. This may be due to some block polymerization of NPMI. The percent conversion increased or decreased relative to the N-substituted maleimide in the monomer feed (Tables XXXIX and XL). This was indicative of the larger reactivity ratios of NPMI and NEMI monomers. The NMR spectra of NEMI-MA copolymers (Figure 43) indicated that an aromatic group was part of the polymeric structure. It appears that the phenyl moiety of benzoyl peroxide is in significant proportion in the polymer chain. This would occur if the chain length of the macromolecule was relatively short. The large initiator concentration used (10% W/W of monomers) would enhance the formation of low molecular weight, short chain length polymers (90). The unaccountably large aromatic integrations which had been obtained for several NPMI-MA copolymers may have been the result of a significant proportion of the initiator being in the polymer chain.

Viscosity data of the NPMI-MA copolymers indicated that the molecular weights of the polymer chains remained fairly

Table XL

Data for the copolymerization of Maleic Anhydride (MA) with  
N-Ethylmaleimide (NEMI) in Acetone at 65°C. MA = M<sub>1</sub>; NEMI = M<sub>2</sub>

Copolymer Designation	MA in monomer mixture (g)	NEMI in monomer mixture (g)	Feed Ratio MA:NEMI	Percent Conversion
Poly (NEMI-co-MA-1)	9.806	0.3766	97:03	10.3
Poly (NEMI-co-MA-2)	9.806	0.3766	97:03	6.8
Poly (NEMI-co-MA-3)	7.8448	0.3879	96:04	4.3
Poly (NEMI-co-MA-4)	7.8448	0.3879	96:04	7.9
Poly (NEMI-co-MA-7)	7.8400	1.1100	90:10	35.2
Poly (NEMI-co-MA-8)	7.8400	1.1100	90:10	
Poly (NEMI-co-MA-5)	2.1600	2.75	50:50	47.9
Poly (NEMI-co-MA-6)	2.1600	2.75	50:50	56.0

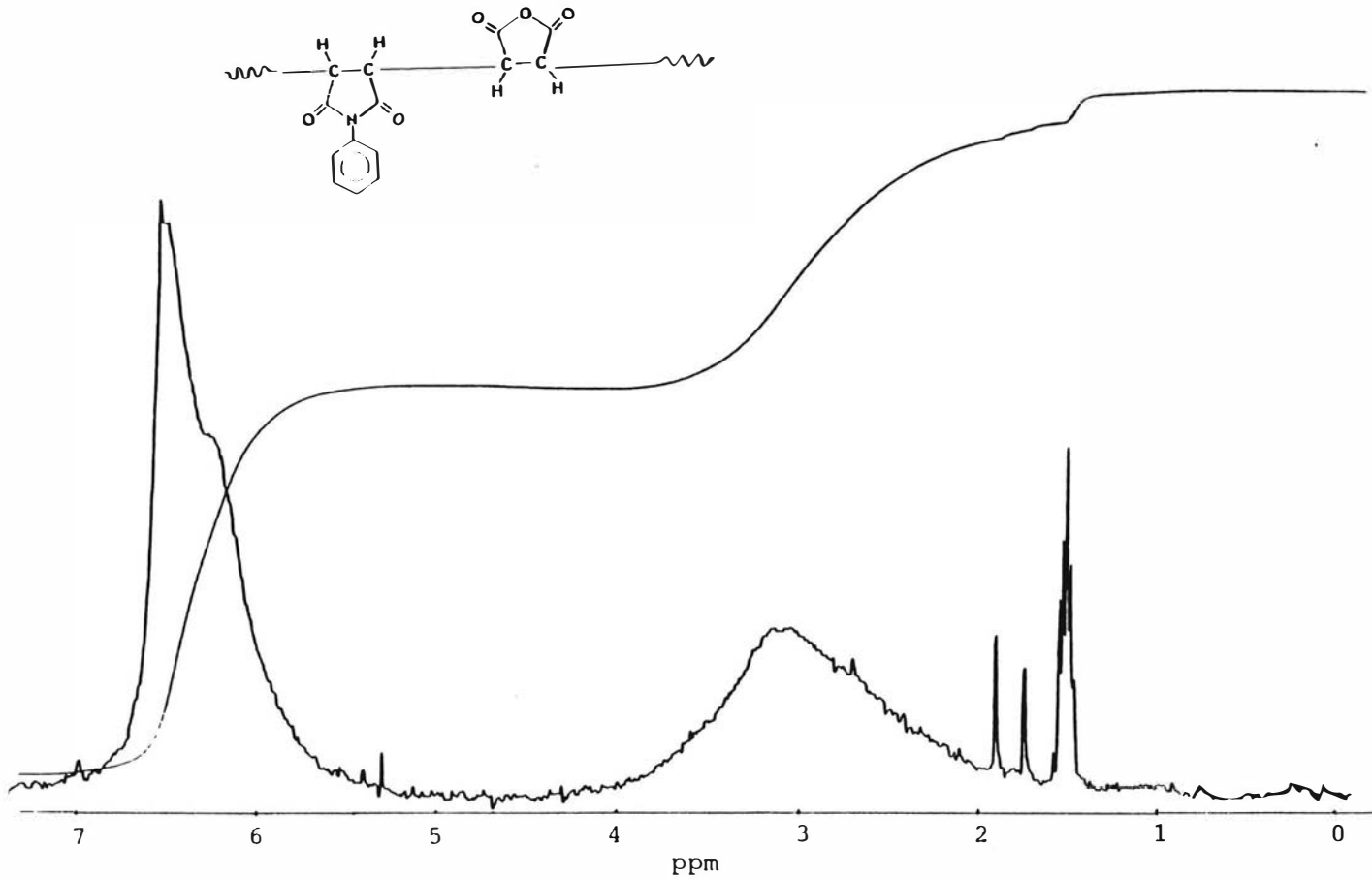


Figure 42. 90 MHz  $^1\text{H}$  NMR Spectrum of Poly(N-phenylmaleimide-co-maleic anhydride-13).

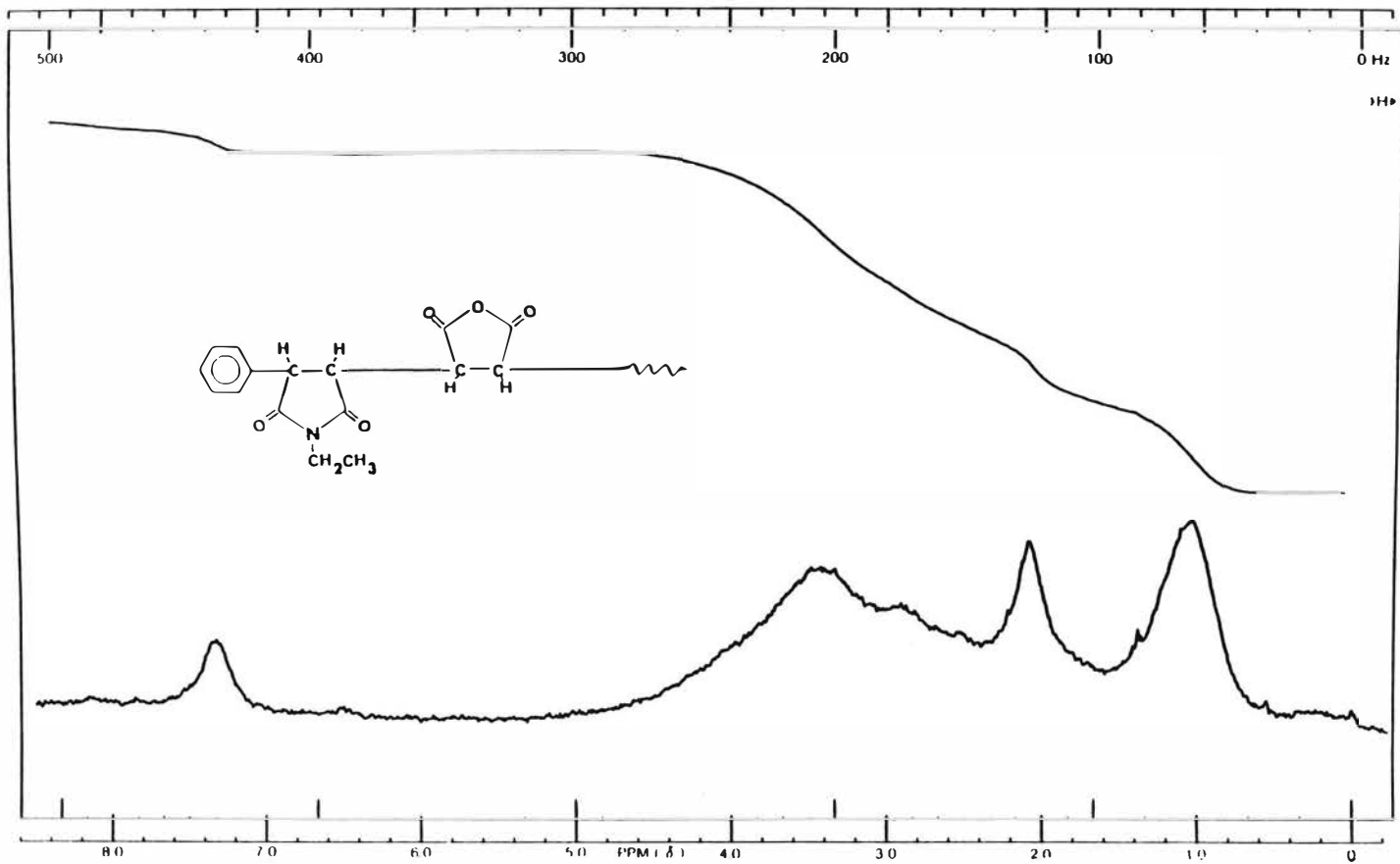


Figure 43. 60 MHz NMR Spectrum of Poly(N-ethylmaleimide-co-maleic anhydride).

consistent with a variation in copolymer composition Table XLI). Characteristically higher viscosities were obtained for polymers prepared with low initiator concentrations.

The copolymer composition data indicate that N-substituted maleimides copolymerize with maleic anhydride in a random manner. Plots of percent monomer in the feed versus percent monomer in the copolymer (Figure 44) indicate that in order to produce a 1:1 copolymer under these experimental conditions, a MA/NPMI feed ratio of 65:35 is required.

### $^{13}\text{C}$ NMR Spectroscopy of Polymers

Since the appearance of commercial  $^{13}\text{C}$  NMR spectrometers in the early 1970s, the technique has been widely used for the structural elucidation of organic molecules. It has proven to be particularly useful in polymer chemistry because of the extreme structural and stereochemical complexity of many polymers.

Carbon-13 NMR has been used extensively for copolymer characterization (92,93,94). Several papers have appeared that discuss the  $^{13}\text{C}$  NMR spectra of maleic anhydride copolymers (95,96,97). With the aid of shift calculations and numerous model compounds, the complete structure of each polymer has been defined, including end groups, sequencing, and tacticity.

The structures of polyimides have been probed by this technique (98,99) which, in conjunction with other spectroscopic techniques, are of great value for determining



TABLE XLI

Viscosities of N-Phenylmaleimide-Maleic  
Anhydride Copolymers

---

Polymer Designation	Solvent: Tetrahydrofuran		Polymer Composition MA:NPMI
	$n_{red}$ (dl/g)	$[\eta]$	
Poly (NPMI-co-MA-1)	0.102 <sup>a</sup>	0.095	39:61
Poly (NPMI-co-MA-4)	0.135	0.121	34:66
Poly (NPMI-co-MA-10)	0.118 <sup>b</sup>		64:36

---

a) Polymers 1 to 4 were run with 50:50 MA/NPMI feed

b) Polymer 10 was run with 90:10 MA/NPMI feed

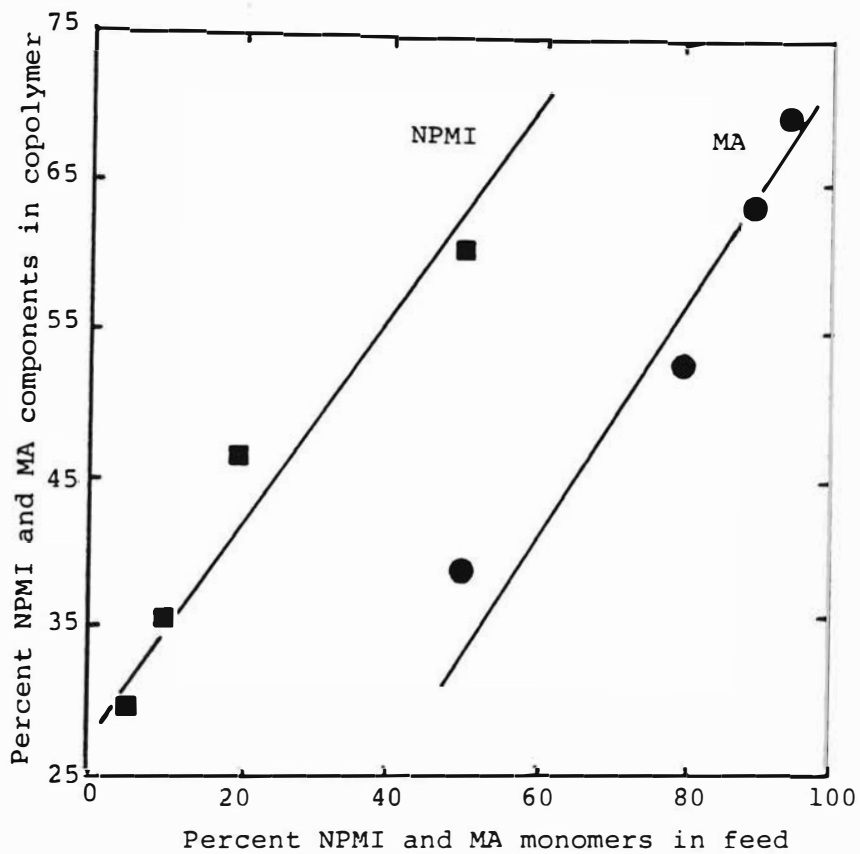


Fig.44 . Relationship between monomer feed and copolymer composition for NPMI and MA

composition of hygroscopic copolymers which can crosslink or form strong intramolecular hydrogen bands, often precluding further characterization.

### NMR Spectra

#### N-Carbamylmaleimide-styrene Copolymers

The  $^1\text{H}$  NMR spectrum and off-resonance  $^{13}\text{C}$  NMR spectrum of NCMI-styrene copolymer are shown in Figures 45 and 46 respectively.

The  $^1\text{H}$  NMR spectrum shows a broad peak at 1-4 ppm due to resonance of the methine and methylene protons of the polymer backbone. Centered at 7 ppm is the aromatic resonance of styrene. Farthest downfield at 11 ppm is a prominent peak which is at a chemical shift region acceptable for hydrogen bonded N-H protons. A coiled polymer chain affords an ideal environment for intermolecular hydrogen bonding. The amide function of NCMI could also easily intramolecularly hydrogen bond, forming a six-membered ring.

General  $^{13}\text{C}$  assignments can be made by comparison with the considerable amount of  $^{13}\text{C}$  shift data available in the literature (91,100). The completely decoupled  $^{13}\text{C}$  spectrum showed two peaks at 179 and 178 ppm, which could be confidently assigned to carbonyl carbons. Peaks appearing at 138, 129, and 128 ppm are due to aromatic carbon resonances. The resonances due to the methine and methylene carbons in the polymer backbone appear as broad resonances

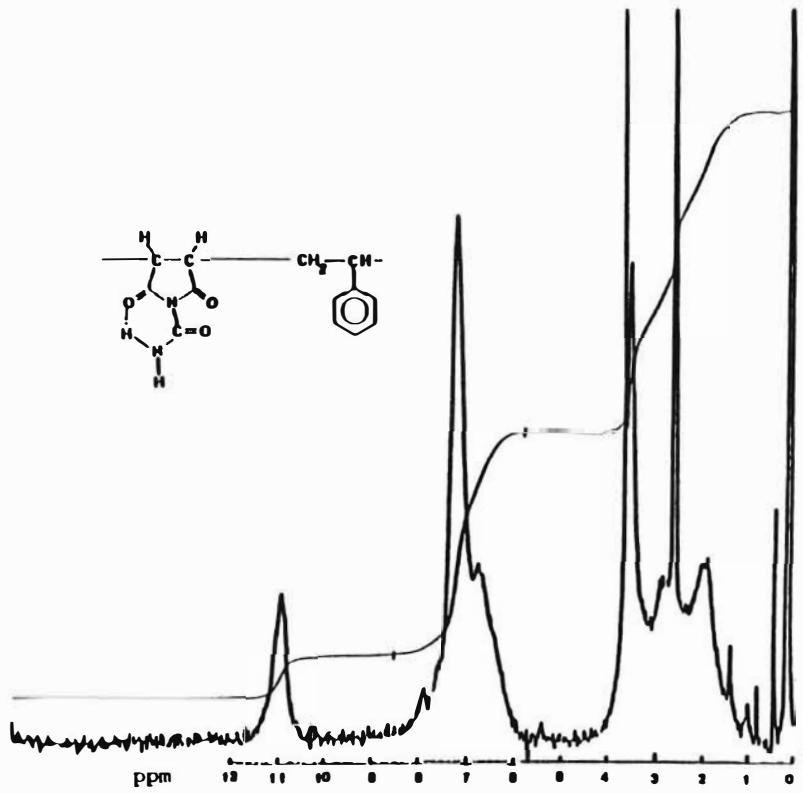


Figure 45. 90MHz <sup>1</sup>H-NMR Spectrum of Poly(N-carbamylmaleimide-co-styrene).

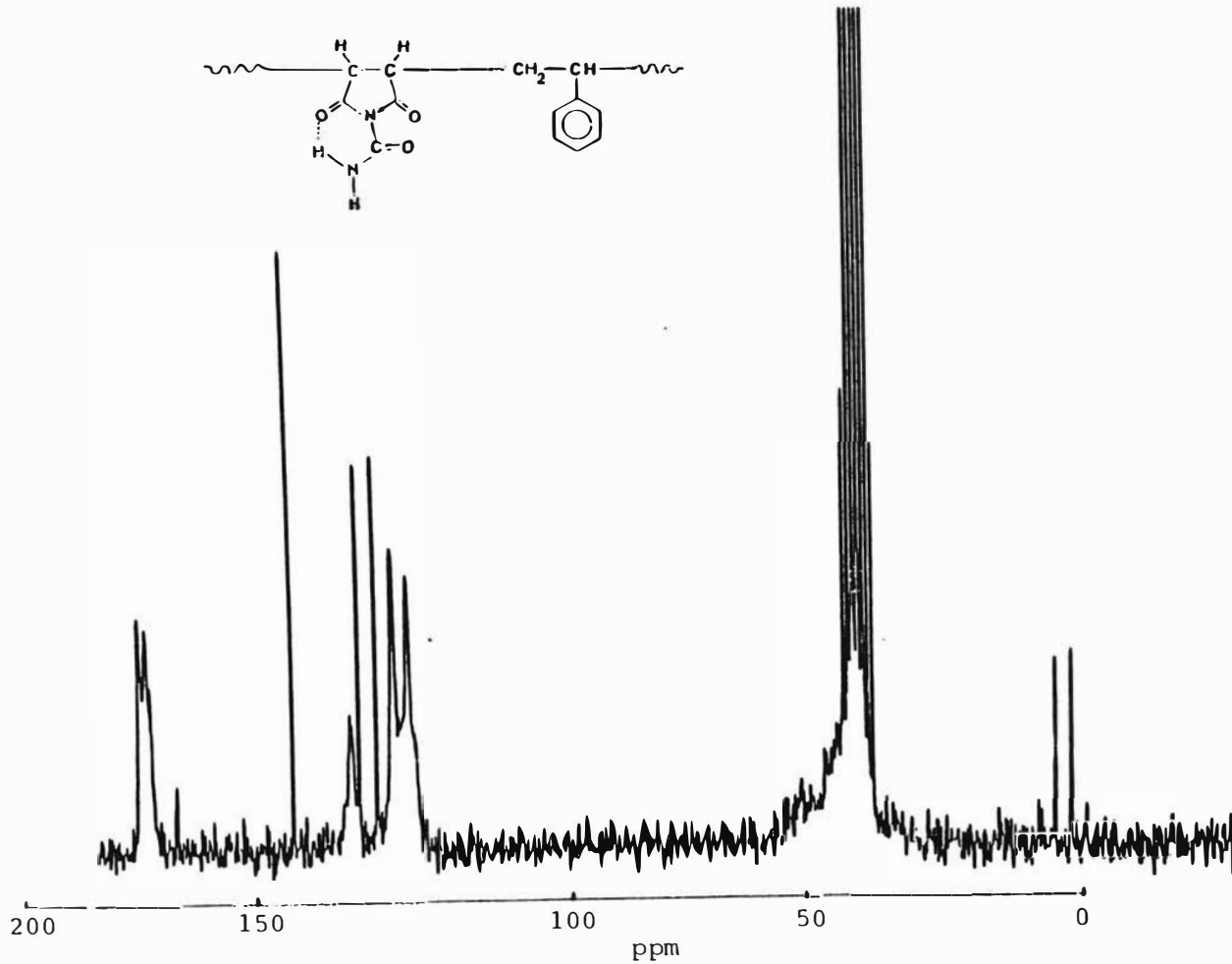


Figure 46 . Off-resonance  $^{13}\text{C}$  NMR Spectrum of Poly(N-carbamylmaleimide-co-styrene).

which are covered by the DMSO-d<sub>6</sub> proton resonance at 36-40 ppm.

In the off-resonance decoupled spectrum (Figure 46), the peaks appearing at 179, 178, and 138 ppm remained as singlets indicating that the carbons in resonance at these positions have no directly bonded protons. This is consistent with the assignment of the carbonyl carbons. The resonance appearing at 138 ppm was assigned to the quaternary aromatic carbon on the basis of this result. The other aromatic carbon peaks are split into doublets on off-resonance decoupling and thus are assigned to the ortho, meta, and para carbons of the phenyl ring. Sometimes, the para carbon resonance, due to its lower intensity, can be distinguished from the ortho and meta carbons resonances. The methine and methylene carbon resonances are further broadened by off-resonance decoupling but again are covered by the DMSO-d<sub>6</sub> resonances.

#### N-Carbethoxymaleimide-styrene Copolymers

The <sup>1</sup>H NMR spectrum of the NCEMI-styrene copolymer (Figure 47), which elemental analysis has shown to be 1:1 in comonomer composition (Table XLIV), shows some readily distinguishable features. The aromatic resonance and the backbone resonance are seen centered at 7 ppm and 2.5 ppm. The methylene protons to oxygen appear in the expected downfield location of 4.5 ppm and the methyl protons appear at 1.5 ppm. Integration confirms the assignments.

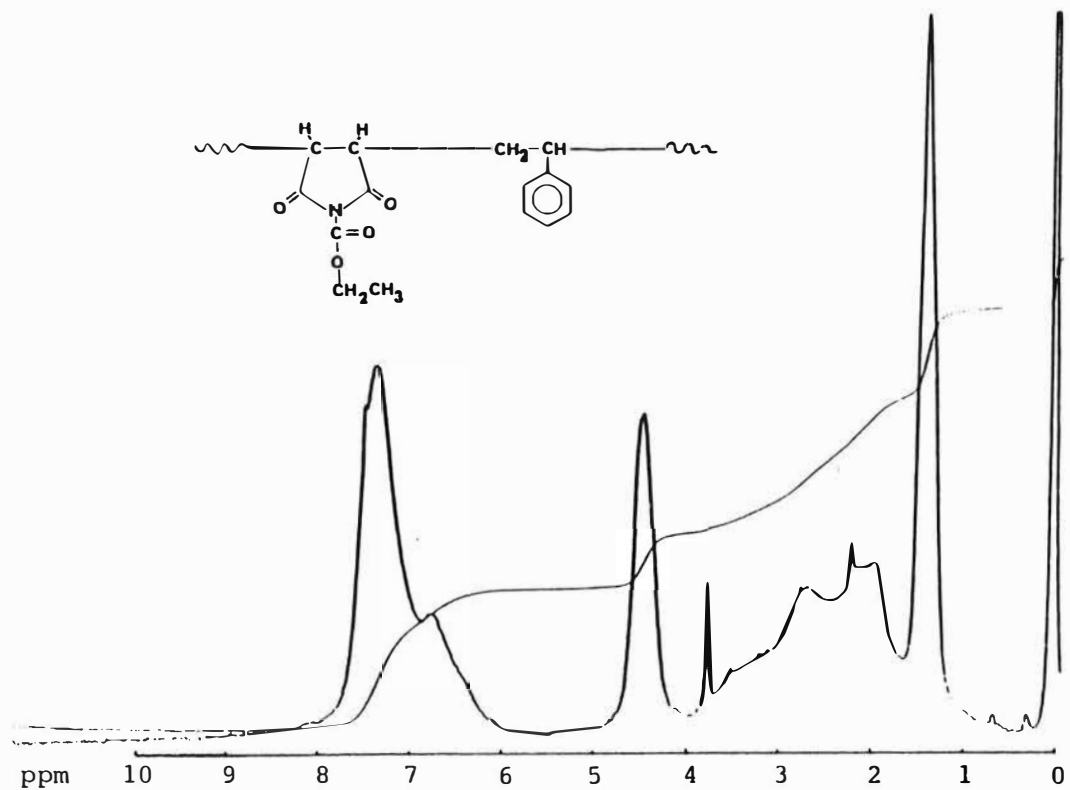


Figure 47. 90 MHz <sup>1</sup>H NMR Spectrum of Poly(N-carbethoxymaleimide-co-styrene).

Comparisons of the completely decoupled and off-resonance decoupled spectra of NCEMI-styrene copolymer (Figures 48 and 49) show very clearly the splitting of the methylene carbon signal ( $\alpha$  to oxygen) into a triplet and the methyl carbon signal into a quartet. The methyl carbon and methylene carbon of the carbethoxy group are located several bonds away from the copolymer backbone, and therefore are not expected to be split or broadened by the different magnetic environments produced by varying backbone stereochemistry.

NMR spectra of other copolymers of N-substituted maleimides and homopolymers are in the appendix.

#### Alternation in Copolymer Structure

A primary interest in this research project was to determine if maleimide could be influenced to form alternating copolymers with electron-donor monomers in a manner similar to maleic anhydride. Our complexation studies indicated that electron-withdrawing N-substituents increased the complexation of maleimide with styrene (Table XVII). Hence, it was of interest to note whether NCMI-styrene and NCEMI-styrene copolymer systems were alternating.

Two essential criteria for an alternating copolymer system are that the copolymer composition is equimolar in comonomers (1:1 copolymer) and that such a 1:1 copolymer is formed regardless of the monomer feed ratio.



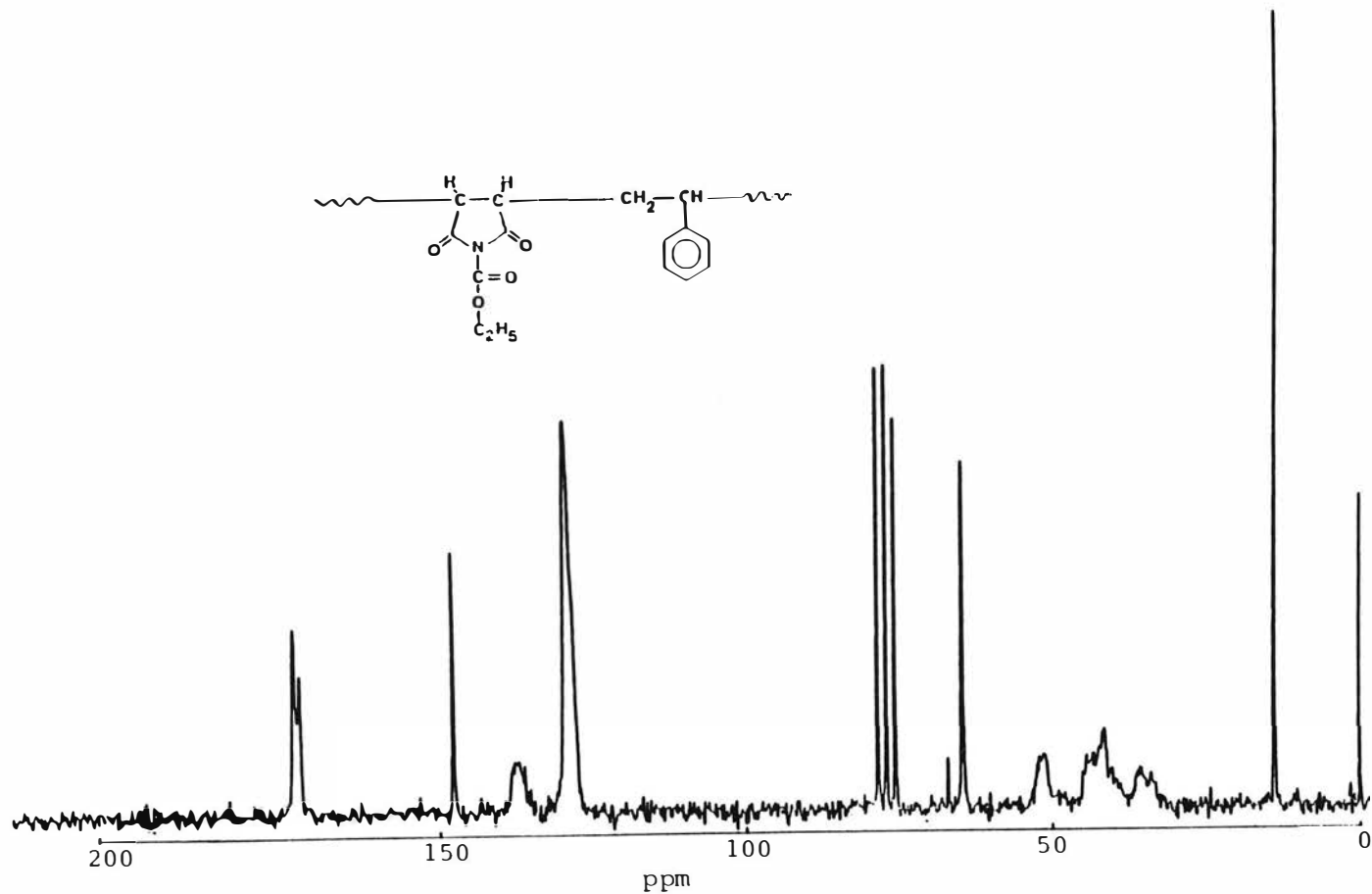


Figure 48 .  $^{13}\text{C}$  NMR Spectrum of Poly(N-carbethoxymaleimide-co-styrene).

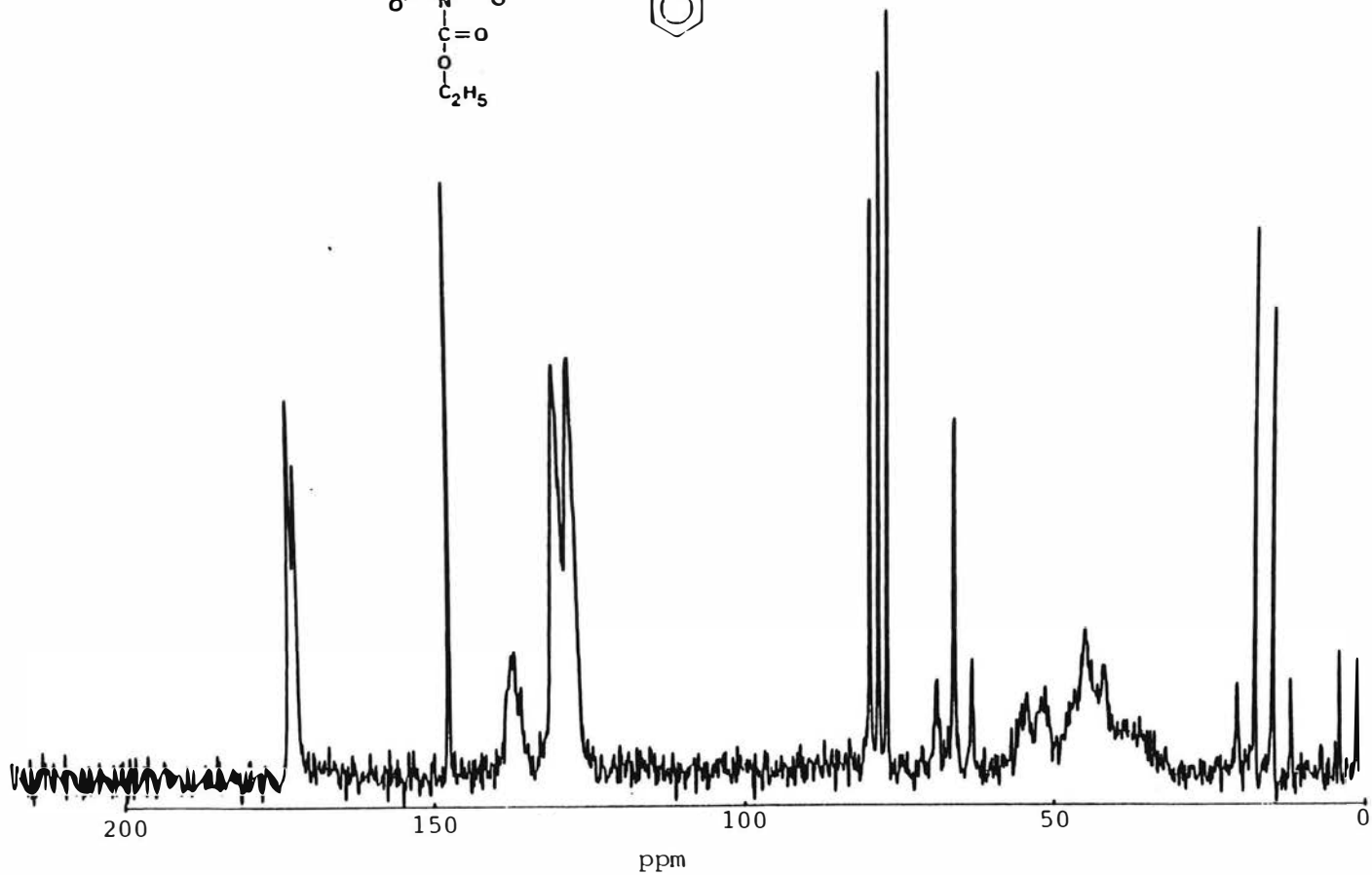
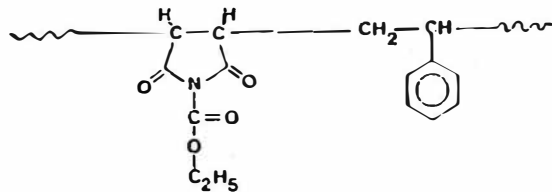


Figure 49 . Off-resonance <sup>13</sup>C NMR Spectrum of Poly(N-carbethoxymaleimide-co-styrene).

1:1 copolymer structure can be verified by several means. One method (101) which is easy to utilize when conditions are suitable is the analysis of integration ratios in  $^1\text{H}$  NMR spectra of the copolymer. For example, the  $^1\text{H}$  NMR spectrum of a 1:1 NCMI-styrene copolymer (Figure 44) should have similar integration values for the aromatic region (6-8 ppm) and the aliphatic region (1-4 ppm). If any impurities, such as the dioxane spike at 3.6 ppm are present, the integration ratios will be subject to error. Another requirement for this method is that the peaks under consideration should not overlap, as is the case for NCMI-styrene, NCEMI-styrene, and NPMI-MA copolymers. As Table XLII indicates, integration ratios of the aromatic protons ( $\text{H}_a$ ) and aliphatic protons ( $\text{H}_o$ ) of NCMI-styrene copolymers varied slightly with a change in the monomer feed ratio. NCEMI-styrene copolymers gave similar  $\text{H}_a/\text{H}_o$  ratios for 50:50 and 80:20 NCEMI:styrene feed ratios but showed a higher styrene content in the copolymer for a 20:80 NCEMI:styrene copolymer. It is unlikely that a significant amount of polystyrene (styrene homopolymer) is mixed with the copolymer because styrene has a very low tendency to homopolymerize in dioxane with the experimental conditions used (Table XXXVI).

$^{13}\text{C}$  NMR has been utilized to determine the sequence of monomers in a polymer chain (102). Lindeman and Adams (103) and Grant and Paul (104) have developed equations for calculation of theoretical  $^{13}\text{C}$  NMR chemical shifts for

carbon atoms on the polymer backbone. A good correlation between observed values for  $^{13}\text{C}$  chemical shifts and theoretical values for an alternating copolymer is supporting evidence for alternation in a copolymer.

Since the NCMI-styrene copolymers were insoluble in most common deuterated solvents,  $\text{DMSO-d}_6$  was the solvent used to prepare the copolymer sample for NMR analysis. Unfortunately the  $^{13}\text{C}$  resonance of the aliphatic carbons of the copolymer were obscured by the  $^{13}\text{C}$  resonance of  $\text{DMSO-d}_6$  carbons (Figure 45) making the above mentioned method unsuitable for analysis of NCMI-styrene copolymers. NCEMI-styrene copolymers, however, are soluble in  $\text{CDCl}_3$ . The four possible triads for the copolymer are shown in Figure 50 with the calculated chemical shifts based on published incremental  $^{13}\text{C}$  chemical shift values for substituents (100,105). Since the incremental chemical shift value due to a  $\text{CONH}_2$  group beta to the carbon of interest has not been determined, these calculations assigned an incremental substituent effect of 0 ppm to such a group and thus may have introduced a significant error into the calculated result. The  $^{13}\text{C}$  NMR spectrum of the NCEMI-styrene copolymer prepared with an equimolar feed (Figure 47) showed three broad resonances centered at 35.9, 41.6 and 51.6 ppm. Neither the alternating structures (I and III in Figure 50) nor the random structures (II and IV in Figure 50) had calculated values which correlated with all three of the observed values.

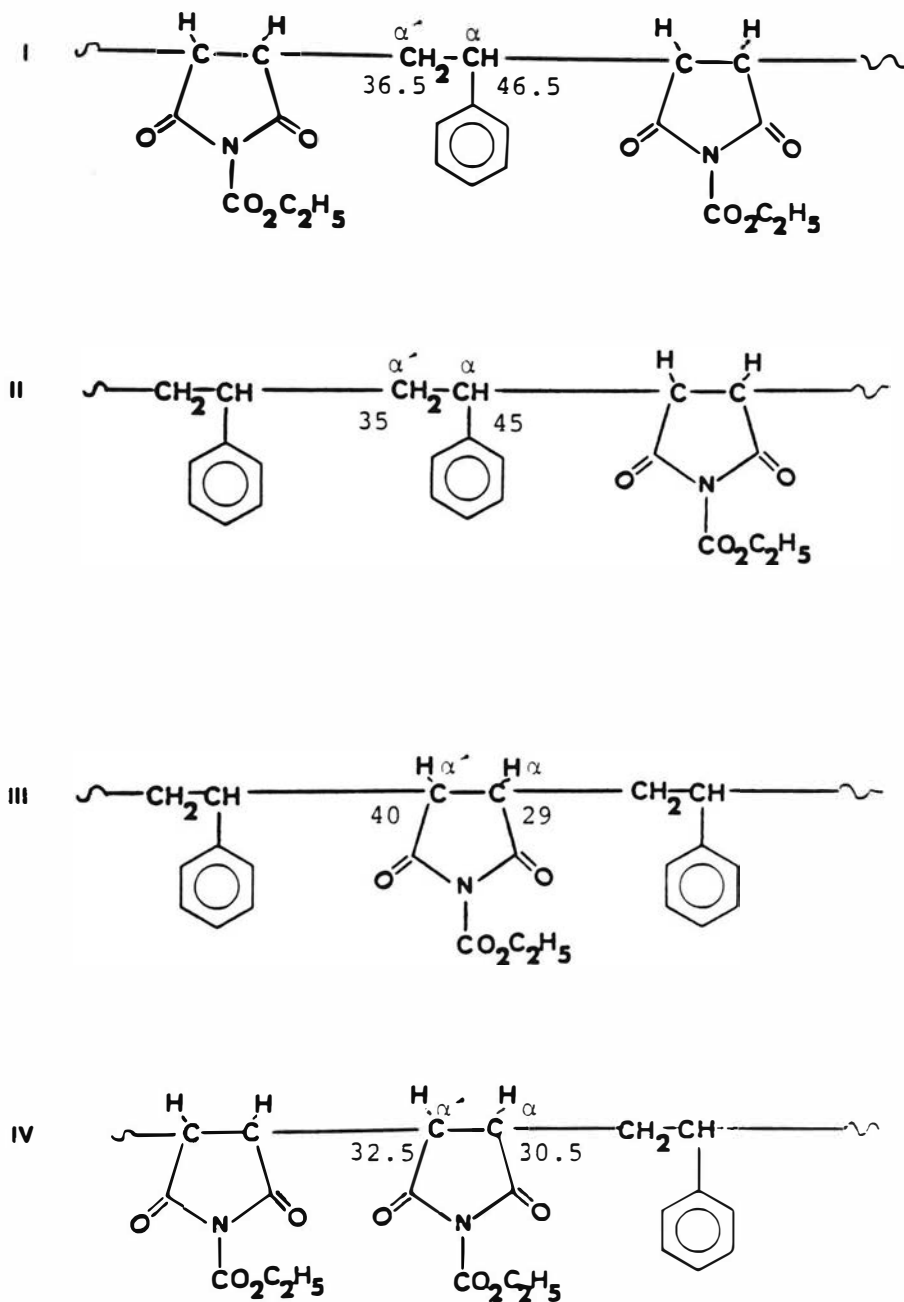


Figure 50. Calculated Chemical Shift Values (ppm) for Internal Carbons of Possible Triads for NCEMI-Styrene Copolymer

The lack of incremental chemical shift data for imide and amide structures greatly limited use of  $^{13}\text{C}$  NMR chemical shift calculations for the determination of polymer sequence. Thus, the  $^{13}\text{C}$  NMR chemical shift calculations for NCEMI-styrene copolymers were inconclusive.

The classic method utilized for determining the reactivity ratio ( $r$ ) of a monomer in a copolymerization system relates the monomer feed ratio to the composition of the copolymer (47,105). Copolymer composition is ascertained by elemental analysis. The yield of the copolymer is confined to 10% or less because if the two monomers have different reactivities, their ratio in the feed will gradually change with reaction time so that the copolymer composition at the later stages of reaction will not have a valid proportionality with the initial monomer feed. The exception to this is an alternating copolymer system, where both comonomers will have the same  $r$  values of zero or one of them will have an  $r$  value of zero while the others'  $r$  value will be close to zero. The monomer feed ratio will not significantly change during the course of the reaction which will always yield a copolymer with an alternating sequence of monomer units. Therefore, consistent formation of a copolymer with a 1:1 composition of comonomer units regardless of monomer feed ratio and reaction time is strong evidence of an alternating copolymer system. As mentioned earlier, maleic anhydride shows this

feature with a wide variety of electron-donating monomers whereas maleimide does not.

Since earlier experiments on complexes indicated that electron-withdrawing N-substituents increased the complex formation between maleimide and styrene, it was of interest to determine whether NCMI and NCEMI would form alternating copolymers with styrene. Therefore, NCMI-styrene and NCEMI-styrene copolymerization reactions were run at varied monomer feed ratios to high conversion rates and the compositions of the resulting copolymers were analyzed by elemental analysis (Table XLIII) and  $^1\text{H}$  NMR spectroscopy (Table XLII). The results (Table XLIV) indicated that equimolar monomer feeds produced copolymers that were 1:1 in monomeric units. A large decrease of NCMI in the feed decreases its incorporation in the copolymer. Although  $^1\text{H}$  NMR and nitrogen analysis gave conflicting information about the copolymer composition from a 70/30 NCMI:styrene feed ratio, it is clear that a 1:1 NCMI-styrene copolymer does not form at varying feed ratios under these experimental conditions.

Interestingly, NCEMI-styrene copolymer remained almost equimolar in monomeric units at a high NCEMI feed ratio (80:20) but a large excess of styrene in the monomer feed increased the styrene units in the copolymer.

The results indicate that under these reaction conditions, NCMI-styrene and NCEMI-styrene are not alternating systems. The fact that large variations of

TABLE XLII

<sup>1</sup>H NMR Integration Ratios of Aromatic Protons (H<sub>a</sub>)  
to Aliphatic Protons (H<sub>o</sub>) for NCMI-Styrene and NCEMI-Styrene Copolymers

Feed Ratio <sup>a</sup>	Feed Ratio <sup>a</sup>	H <sub>a</sub> /H <sub>o</sub>	H <sub>a</sub> /H <sub>o</sub>
NCMI : Styrene	NCEMI : Styrene	NCMI-Styrene	NCEMI-Styrene
30 : 70	---	0.98	---
50 : 50	---	0.83	---
70 : 30	---	0.71	---
---	20 : 80	---	0.73
---	50 : 50	---	0.49
---	80 : 20	---	0.50

<sup>a</sup>) [M]<sub>T</sub> = 0.2 M; solvent: 1,4-dioxane; time = 16 h



TABLE XLIII

Elemental analysis Data for NCMI-Styrene  
and NCEMI-Styrene Copolymers

Feed Ratio <sup>a</sup> NCMI : Styrene	Feed Ratio <sup>a</sup> NCEMI : Styrene	% Yield	C %	H%	N%
0.30 : 0.70	---	64.5	69.02 <sup>b</sup>	5.72 <sup>b</sup>	7.92 <sup>b</sup>
0.50 : 0.50	---	100.0	63.67 <sup>c</sup>	5.14 <sup>c</sup>	11.05 <sup>c</sup>
0.70 : 0.30	---	67.7	64.32 <sup>c</sup>	5.19 <sup>c</sup>	9.27 <sup>c</sup>
---	0.20 : 0.80	49.8	70.23 <sup>b</sup>	5.99 <sup>b</sup>	4.39 <sup>b</sup>
---	0.50 : 0.50	92.6	65.92 <sup>b</sup>	5.54 <sup>b</sup>	5.09 <sup>b</sup>
---	0.80 : 0.20	84.9	64.46 <sup>b</sup>	5.50 <sup>b</sup>	5.53 <sup>b</sup>

a)  $[M]_T = 0.2 \text{ M}$ ; Solvent: 1,4-dioxane; time = 16 h

b) Elemental analysis done by Atlantic Microlabs, Inc., Atlanta, Georgia

c) Elemental analysis done by A.H. Robbins Co., Richmond, Virginia

Table XLIV

Copolymer Compositions of NCMI ( $M_1$ )-Styrene( $M_2$ ) and NCEMI( $M_1$ )-Styrene( $M_2$ )

Copolymer System	Feed Ratio $M_1 : M_2$	Composition Based on $^1\text{H}$ NMR $M_1 : M_2$	Composition Based on N% $M_1 : M_2$
NCMI-Styrene	30 : 70	0.51 : 0.49	0.33 : 0.67
NCMI-Styrene	50 : 50	0.60 : 0.40	0.50 : 0.50
NCMI-Styrene	70 : 30	0.67 : 0.33	0.40 : 0.60
NCEMI-Styrene	20 : 80	0.35 : 0.65	0.41 : 0.59
NCEMI-Styrene	50 : 50	0.51 : 0.49	0.50 : 0.50
NCEMI-Styrene	80 : 20	0.50 : 0.50	0.55 : 0.45

experimental conditions are listed in Table XLIII

monomer feed in NCEMI-styrene cause only small deviations from a 1:1 copolymer structure indicate that there is a significant 1:1 intermolecular interaction between NCEMI and styrene.

The copolymerizations were performed at a total monomer concentration of 0.2 mol/L which corresponds to a 2.4% (W/V) solution for an equimolar NCMI-styrene feed and a 2.7% (W/V) solution for an equimolar NCEMI-styrene feed. It should be noted that most copolymerization reactions are performed at 10-20% (W/V) concentrations. The reason that the relatively very low concentrations of monomers were used was because NCMI did not dissolve in most common organic solvents and its saturation point in the copolymerization solvent, 1,4-dioxane, was at about 0.2 moles/L concentration. The NCEMI-styrene total monomer concentration was kept similar to that of the NCMI-styrene concentration in order to compare the copolymerization behavior of the two systems.

The  $^1\text{H}$  NMR experiments indicated that NCMI and NCEMI do form charge-transfer complexes with styrene (Table XVII). However, the formation constants of these complexes are very small, meaning that large monomer concentrations are necessary if a charge-transfer complex concentration that is significant enough to affect the mechanism of copolymerization is to form. In order to fully evaluate a charge-transfer complex effect in the NCMI-styrene and NCEMI-styrene copolymers, solutions with larger concentrations of the comonomers are necessary.

### High Pressure Liquid Chromatography

Kinetics of solution copolymerizations have traditionally been followed by analysis of copolymer concentrations formed per unit time (86). This usually involves the precipitation of copolymer by addition of the reaction solution into a non-solvent for the copolymer (a precipitating agent) followed by use of a gravimetric technique to determine the mass of copolymer formed for the specific reaction time. The assumption is made that all of the copolymer precipitates in the non-solvent. Usually there are unreacted monomers and solvent trapped in the copolymer coils which make it necessary for purification of the copolymer by one or more redissolving and reprecipitating steps which contribute to the experimental error in the analysis of the weight of the copolymer formed.

Analysis of monomer concentrations in the evaluation of copolymerization kinetics has been reported sporadically in the literature. Harwood et al (106) and Buckley et al (107) reported the successful use of liquid chromatography for evaluation of change in monomer concentrations. However, gas chromatography, UV spectroscopy, and NMR spectroscopy have not been found to be applicable in the analysis of monomer concentrations of an N-phenylmaleimide - 2-chloroethyl vinyl ether copolymer system (56).

Reversed phase high pressure liquid chromatography (HPLC) was investigated to determine whether it was a suitable technique for evaluation of the kinetics of

copolymerization in the NCMI-styrene system. This system was considered suitable for analysis by HPLC for the following reasons:

- (1) When evaluating changes in monomer concentration with time, the assumption is made that any reduction in the monomer concentration is due to that monomer being incorporated in a polymer chain. If the reaction follows a step-growth polymerization mechanism, the monomer may become a component of a trimer or tetramer or oligomer which eventually leads to the formation of a long-chain polymer (108). In such a step-growth polymerization reaction, the solubility of these very short chain oligomers may not be significantly different from that of the polymer and therefore, when the polymer or copolymer is removed from solution, a significant amount of oligomers may remain in solution and lead to analysis problems such as chemically interacting with monomer molecules and thus changing the elution profile and retention time of the pure monomer. It could also cause problems by adversely affecting the packing material of the column. None of these problems should arise in the NCMI-styrene system since the reaction is a free radically induced chain reaction polymerization. In such polymerizations the polymer or copolymer form instantaneously and there is no intermediate oligomer in solution (108). Hence the loss in monomer concentration during a reaction time

peak height versus log concentration gave a slope of 0.9946 for styrene indicating that the styrene concentration has a linear relationship with the absorption signal of the HPLC. Such linearity was also observed for NCMI. The log of the total of the two peak heights as well as the log of each individual peak height when plotted against log concentration had slope values close to 1.0. The calibration curve for the NCMI solution is given in Figure 51. When a mixture of NCMI and styrene was used, the water/MeOH solvent program had to be adjusted such that suitable elution profiles could be obtained for NCMI and styrene ("WM3"). The retention times for the NCMI "doublet" were 3.2 and 3.6 minutes. The styrene retention time was 17.2 minutes. In all solvent programs, the solvent, dioxane, was the first component to elute. The absorptions were linear with concentration as indicated by the calculated slopes for the log peak height versus log concentration for the NCMI-styrene mixture:

styrene	:	1.0198
NCMI (1st peak height)	:	0.9300
NCMI (2nd peak height)	:	0.9643
NCMI (total of peak heights)	:	0.9472

The calibration curve for NCMI in the NCMI-styrene mixed solution is shown in Figure 52.

It has been demonstrated that NCMI and styrene have linear absorption in the HPLC system and calibration curves have been established. It appears that HPLC is a suitable

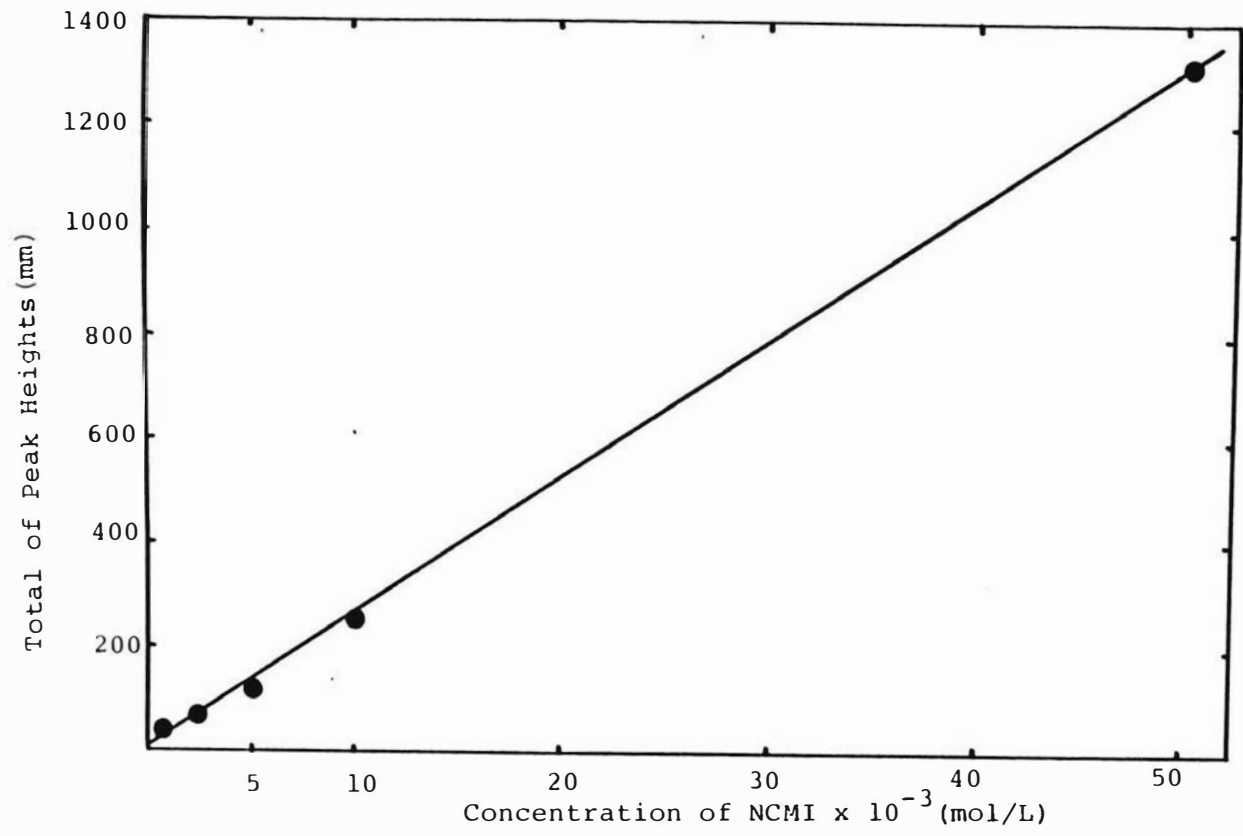


Figure 51. Calibration curve for NCMI/Dioxane solutions at concentrations of  $1.0 \times 10^{-3}$  to  $5.0 \times 10^{-2}$  M

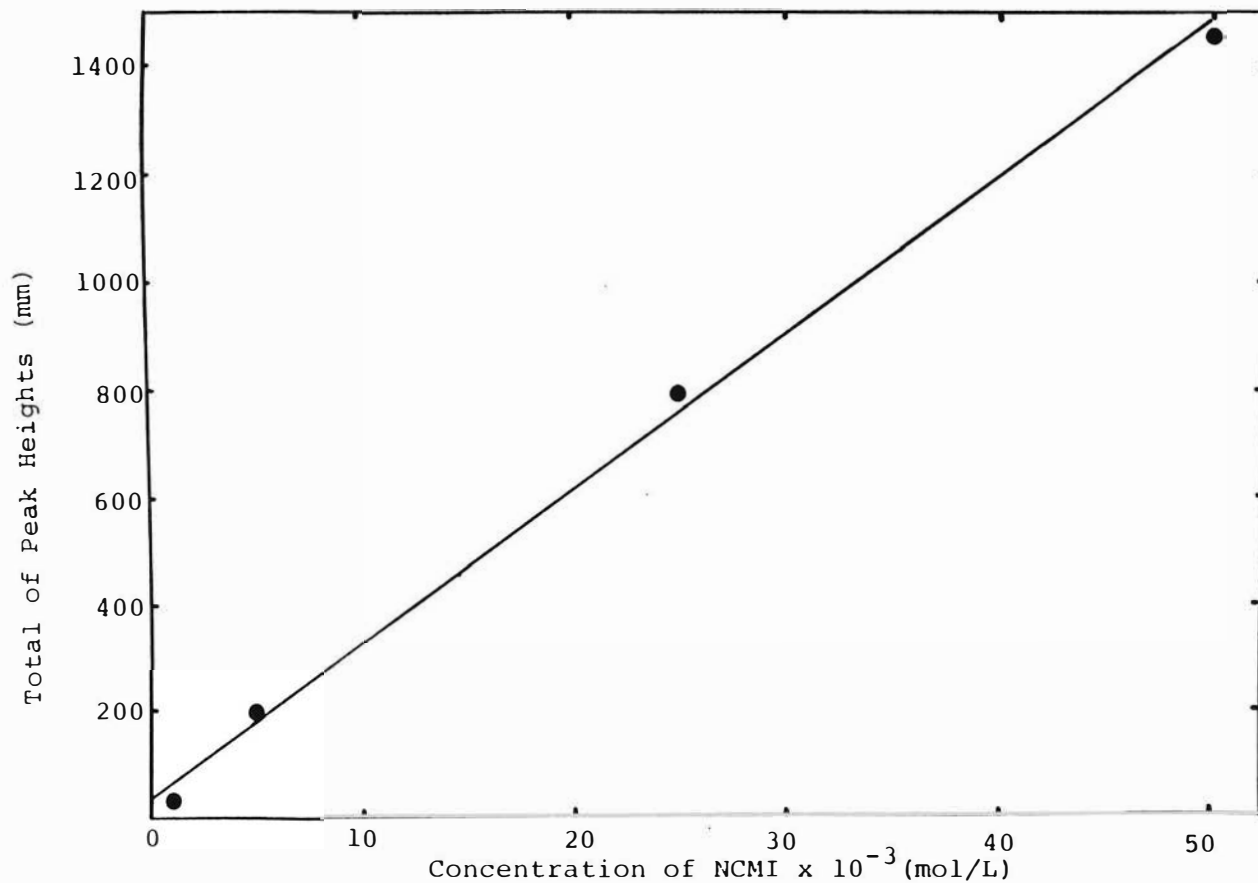


Figure 52. Calibration curve for NCMi in NCMi/Styrene/Dioxane at NCMi concentration of  $1.0 \times 10^{-3}$  to  $5.0 \times 10^{-2}$  M



technique for following the change in monomer concentration of a NCMI-styrene copolymerization in 1,4-dioxane. An experimental procedure would involve extracting samples from the NCMI-styrene reaction solutions at different times during the reaction and immediately cooling each sample to quench the polymerization reaction. Then an aliquot from each sample would be withdrawn with a filter syringe, diluted in a volumetric flask with dioxane (since the monomer concentration may be greater than the upper limit of detection for the components) and injected into the HPLC.

The determination of copolymerization kinetics would give valuable information about the reactivities of the comonomers.

## EXPERIMENTAL

### General

Melting points were obtained on a Thomas-Hoover melting point apparatus and are uncorrected. Proton nuclear magnetic resonance spectra ( $^1\text{H}$  NMR) were obtained at 60 MHz on a Varian T-60 spectrometer and at 90 MHz on a JEOL FX 90 Q spectrometer at 89.56 MHz.  $^{13}\text{C}$  NMR spectra were obtained on a JEOL FX 90 Q spectrometer at 22.5 MHz. The solvents used for the NMR spectra were  $\text{CDCl}_3$  (99.8%, Aldrich),  $(\text{CD}_3)_2\text{SO}$  (99.5% D, Wilmad Glass Co., Inc.),  $(\text{CD}_3)_2\text{SO}$  (99.9% D, Aldrich),  $(\text{CD}_3)_2\text{SO}$  (99.5% D, MSD Isotopes, Montreal, Canada), and Unisol (99.8% D, composed of  $(\text{CD}_3)_2\text{SO}$ ,  $\text{CDCl}_3$ ,  $\text{CD}_2\text{Cl}_2$ , Norell, Inc.). Chemical shifts are reported in parts per million (ppm,  $\delta$ ) downfield from the internal standard, tetramethylsilane. Splitting patterns are designated as follows: s, singlet; d, doublet; t, triplet; q, quartet; m, multiplet; b, broad. Infrared spectra (IR) were recorded on a Perkin Elmer model 283 spectrometer. IR signals are designated as follows: w, weak; m, medium; s, strong; v, very strong. Ultraviolet (UV) spectra were run on a Beckman ACTA M VII spectrophotometer (Beckman Instruments, Irvine, CA) using 1 cm quartz cells or 1 mm silica cells. High Pressure Liquid Chromatograms (HPLC) were obtained on a Gilson Model #41 High Performance Liquid Chromatograph (Gilson Medical Electronics, Inc., Middleton, WI) which was interfaced with

a Hewlett Packard #3385 A Automation System (Hewlett Packard, Inc., Avondale, PA) for integration and a Kipp & Zonen #BD 41 recorder (Kipp & Zonen, Holland). Viscosities were determined in an Ubbelohde Cannon 50 A968 viscometer. Elemental analyses were performed by A.H. Robins Company, Richmond, Virginia and by Atlantic Microlabs, Inc., Atlanta, Georgia.

#### Purification of Materials

Maleic anhydride (Aldrich) was purified by vacuum distillation or by recrystallizing twice from toluene or chloroform followed by vacuum drying. Purified maleic anhydride, mp 51-53°C, was stored in a dessicator until needed. Aniline was vacuum distilled prior to use. Benzoyl peroxide (Aldrich) was purified by dissolving in cold chloroform and adding methanol to the point of saturation (109). 2,2'-Azobisisobutyronitrile (Aldrich) was recrystallized from methanol (m.p. 102-104°C). Acetone was distilled and collected at 55-57°C, dried over anhydrous  $\text{CaSO}_4$ , decanted, redistilled and stored over molecular sieves 3A (110). Cyclohexane was washed several times with concentrated sulfuric acid, then with water, dried over anhydrous  $\text{CaCl}_2$ , decanted and distilled (110). Tetrahydrofuran (Curtis Matheson and Aldrich) was purified by drying over sodium metal-ribbon and distilled from  $\text{LiAlH}_4$ . Methylene chloride was washed sequentially with

concentrated sulfuric acid, 5% aqueous  $\text{Na}_2\text{CO}_3$  and water, dried over anhydrous  $\text{CaCl}_2$  and distilled from  $\text{P}_2\text{O}_5$  (111). Benzene was dried over anhydrous  $\text{CaCl}_2$  and distilled (110). Purification of dioxane was accomplished (112) by refluxing 1,4-dioxane (99 + %, Aldrich) over sodium hydroxide pellets for 48 h, distilling this refluxed dioxane and redistilling the middle portion of the distillate (bp 101-102°C) over sodium metal strips. Dimethylsulfoxide (grade 1, Sigma Chemical Co.) was purified (111) by drying over sodium hydroxide pellets for 24 h followed by distillation. Anhydrous ether (Curtis Matheson), petroleum ether, and ethyl acetate were used with no additional purification.

### Monomer Syntheses

The maleimides used in this study were prepared using previously reported laboratory procedures. N-ethylmaleimide (5) was obtained from Aldrich Chemical Company and was purified by recrystallization from benzene followed by sublimation.

### N-Phenylmaleimide (1)

N-Phenylmaleimide (NPMI, 1) was prepared by following the method outlined in U.S. patent 2,444,536 (113) and reported by Cava et. al. (114). 1 was synthesized by first preparing maleanilic acid (2).

### A. Maleanilic Acid (2)

A 2-L three-necked round bottomed flask, fitted with a paddle-type stirrer, a reflux condenser, and an addition-funnel was charged with 78.5 g (0.8 mol) of maleic anhydride (3) and 1 L of anhydrous ethyl ether. When all of 3 had dissolved, 72.8 mL (0.8 moles) of aniline (4) were added dropwise from the addition funnel. When the first drops of aniline were introduced into the solution of 3, a deep yellow color appeared which dissipated with stirring, immediately followed by the appearance of the cream colored product, 2. As more aniline was added, the mixture became more viscous and stirring became difficult. The mixture was stirred at room temperature for 80 minutes and then cooled to 15-20°C in an ice bath. The product 2 was collected by filtration and dried overnight under vacuum. The yield was 147.5 g (96.5%), mp 198.5-199° (lit (114) mp 201-202°C) IR (KBr, 1%) 3290 (1 N-H, w), 3050-3150 (Ar-H, alkene C-H, carboxylic -OH, m), 1705 (C=C, s), 1635 (C=C, m), 1585, 1550, 1495, 1455 (ring C=C, s), 855 (O-H, s), 760  $\text{cm}^{-1}$  (N-H wag, w);  $^1\text{H}$  NMR ( $\text{CD}_3$ )<sub>2</sub>SO  $\delta$  6.40 (q, 2H,  $-\underline{\text{C}}\underline{\text{H}}=\underline{\text{C}}\underline{\text{H}}-$ ), 7.45 (m, 5H, Ar-H), 10.40 (s, 1H,  $-\text{CONH}\underline{\text{H}}$ ), 12.90 (1H,  $-\text{COOH}$ ).

### B. N-Phenylmaleimide (1)

A 1-L flask was charged with 300 mL of acetic anhydride (reagent, A.C.S.) and 29 g of anhydrous sodium acetate (certified, A.C.S.). To this, 140 g (0.732 mol) of

2 were added. The mixture was swirled and heated over a steam bath until most of the solid material was dissolved. The resultant dark red solution contained some undissolved sodium acetate which settled to the bottom. The reaction mixture was cooled to room temperature and then poured into 575 mL of ice-water. The precipitated product was recovered by filtration, washed three times with 50 mL portions of ice-cold water and once with a 50 mL portion of petroleum ether (bp 30-60°C) and dried under vacuum. This material was then recrystallized three times from cyclohexane giving canary-yellow needle-like crystals of 1, 44.7 g (35.2%), mp 87-88°C (lit mp 89-89.8°C (2)). IR (KBr, 2%): 3100 (Ar-H, m), 1720 (-C=C, v), 1600 (m), 1510 (s), 1460 (m) (ring C=C), 1390 (C-N, s), 1150, 1160 (-C-N, s), 830, 700  $\text{cm}^{-1}$  (C=C-H, s).  $^1\text{H}$  NMR ( $\text{CDCl}_3$ ) ppm 6.8 (s, 2H-CH-), 7.4 (s, 5H, Ar-H).

#### N-Carbamylmaleimide (5)

The procedure reported by Tawney et al (115) was followed for the preparation of 5 via the preparation of its intermediate, N-carbamylmaleamic acid (6).

#### A. N-Carbamylmaleamic Acid (6)

A stoppered flask containing 570 mL of glacial acetic acid, 294.2g (3.0 mol) of maleic anhydride and 180.2 g (3.0 mol) of urea was heated at 50°C for 12 h and then stirred overnight at room temperature. The white crystalline

product, washed with 100 ml glacial acetic acid and dried at 50°C, weighed 229.1 g (48% yield; lit (115) 56% yield), mp 157.5°-159°C, mp lit (115) 161-162°C. The mother liquor and washings were recharged with 196.1 g (2 mol) of maleic anhydride and 120.1 g (2 mol) of urea and heated at 56°C for only 5 h. After stirring overnight at room temperature 247.3 g of 6 was obtained [78% yield; lit (1) 77%], mp 158-160°C; lit (115) 159-160°C. Another repetition of this process produced 260.5 g [82.4% yield; lit (115) 83.8%], mp 153.5-154.5°C, lit (115) mp 156-159°C. The average yield was 72%. IR (KBr, 1%) 3400, 3250 (NH<sub>2</sub>, NH, carboxylic OH, m), 1725, 1705, 1680 (carboxylic C=O, amide C=O, s), 1650 (NH<sub>2</sub>, C=C, m), 1430 cm<sup>-1</sup> (C-N, m). <sup>1</sup>H NMR (DMSO-d<sub>6</sub>) ppm 10.4 (b, 1H, N-H), 7.6, 7.3 (b, 2H, NH<sub>2</sub>), 6.4 (s, 2H, C=C-H).

#### B. N-Carbamylmaleimide (5)

Continuing the procedure of Tawney (115) et al, 6 (200g, 1.26 mol) was added to 600 mL of acetic anhydride which had been heated to 90-95°C. The suspension was stirred (by a mechanical stirrer) very vigorously at 90-97°C for 1 h at which time it was a brown colored mixture. After a hot filtration the filtrate was cooled to room temperature, and the precipitated solid was filtered off, washed with 30 mL of acetone and vacuum dried. The crystalline product weighed 77.7 g (44% yield, lit (115) 76.7%); mp 154-157°C, lit (115) mp 157-158°C. IR (KBr, 1%) 3560, 3480, 3430, 3400 (free N-H, s), 3300, 3240,

(associated N-H,m), 3100, (associated N-H, C=C,m), 1817, 1795, 1745 (imide C=O,s), 1697 (amide C=O,s), 1600 (N-H,s).  $^1\text{H}$  NMR (DMSO- $d_6$ )  $\delta$  7.3 (b,2H,amide), 7.1 (3,2H,C=C-H),  $^{13}\text{C}$  NMR (DMSO- $d_6$ )  $\delta$  168.5 (s,C=O,imide), 147.8 (s,C=C-H).

### Maleimide (7)

Tawney et als procedure (115) was modified for the preparation of 7. A 2-L flask, fitted with a stirrer and thermometer was charged with 510 mL of N,N-dimethyl formamide (DMF) and heated to 90-95°C by means of an oil bath. Heating was stopped and 240g (1.7 mol) of 5 was added with stirring. Heat was applied to maintain the temperature at 95-100°C for a total reaction time of 1h. The mixture was cooled to room temperature and stirred overnight. Precipitated cyanuric acid was filtered off and DMF was removed by rotoevaporation under vacuum until a slurry was obtained. The DMF remaining in the brown slurry was removed by triturating with benzene and the resulting brown solid was recrystallized from hot benzene to yield white, crystalline maleimide, 7, 50 g (36%), mp 92-93.5°C lit (115) mp 92-94°C, IR (KBr,1%), 3200, 3100 (associated N-H,m), 3070 (C=C-H,w), 1750, 1710 (imide C=O,w,s), 1350  $\text{cm}^{-1}$  (C-N,m).  $^1\text{H}$  NMR (DMSO- $d_6$ ) ppm 10.9 (b,1H,N-H), 6.9 (d,2H,C=C-H);  $^{13}\text{C}$  NMR (DMSO- $d_6$ ) ppm 172.6 (s,C=O), 135.1 (s,C=C-H).



N-Carbethoxymaleimide (8)

The procedure of Butler and Zampini (116) which was a modified procedure of Keller and Rudinger (117) was utilized for the preparation of 8. A solution of 10 g (0.103 mol) of maleimide (7) in 500 mL of anhydrous ethyl ether was charged with 10.4 g (0.103 mol) of triethylamine by dropwise addition at room temperature and stirred for 30 min. To this, 11.2g (0.103 mol) of ethylchloroformate dissolved in an equal volume of anhydrous ethyl ether was added dropwise. Upon addition of ethylchloroformate, immediate formation of a white solid was observed. The mixture was allowed to stir overnight at room temperature. After filtering off the triethylamine hydrochloride salt, ethyl ether was removed from the filtrate by rotoevaporation at room temperature. Crude 8 was a quantitative yield and the triethylamine hydrochloride salt was 14.2g (87.4% yield). 8 was purified by vacuum distillation (bp 104-111°C/0.24-0.15 torr) and sublimation; mp 58-60°C (lit mp (116) 58-59°C). IR (KBr, 0.25%), 3100 (C=C-H, m), 1800, 1770 (C=O, s), 1270 (C-C(=O)-O, s), 1370 (CH<sub>2</sub>, m), 1400 cm<sup>-1</sup> (CH<sub>3</sub>, m); <sup>1</sup>H NMR (DMSO-d<sub>6</sub>) ppm 6.9 (s, 2H, C=C-H), 4.5 (q, 2H, -CH<sub>2</sub>), 1.4 (t, 3H, -CH<sub>3</sub>); <sup>13</sup>C NMR (DMSO-d<sub>6</sub>) ppm 165.7 (s, C=O), 135.1 (s, C=C-H), 63.8 (s, -CH<sub>2</sub>), 14.0 (s, -CH<sub>3</sub>).

## Copolymer Syntheses

### Copolymerizations of Electron-donor Monomers with Electron-acceptor Monomers

Copolymerization between the electron accepting monomers (maleic anhydride, maleimide, and N-substituted Maleimides) and the electron donating monomers (styrene and furan) were carried out in the same manner. Azobisisobutyronitrile (AIBN, Aldrich) was used as the initiator in all the above mentioned copolymerizations. The solvent used was 1,4-dioxane. The initiator, solvent, and monomers were purified as mentioned previously.

Typically, solutions of the desired concentrations were made by weighing appropriate amounts of the maleimide, styrene and AIBN into a volumetric flask and diluting to the mark with solvent. This solution was then transferred to a pressure bottle and the solution was flushed with nitrogen gas which had been deoxygenated by passage through a column of oxisorb (Messer Griesheim, West Germany). The pressure bottle was then sealed and placed in an oil bath (Blue M, Blue Island, Illinois) thermostated at  $60.0^{\circ}\text{C} \pm 0.1^{\circ}\text{C}$  for the desired amount of time. At the end of this time, the pressure bottles were removed from the bath and the reaction was terminated by immersing the bottles in a dry ice-isopropanol bath or ice-water bath. Reaction time was measured as the time interval between placing the pressure bottle in the oil bath and immersing it in the dry ice-isopropanol bath or ice-water bath. Since

N-carbamylmaleimide was insoluble in most common organic solvents, being appreciably soluble only in dimethylsulfoxide, dimethylformamide or, to a limited extent, in 1,4-dioxane, the solvent that was used for these polymerizations was 1,4 dioxane. Due to the limited solubility of N-carbamylmaleimide in 1,4-dioxane, the total monomer feed concentrations for all systems was kept at a relatively low concentration of 0.2 mol/L. The AIBN concentration was 0.004 mol/L.

The NCMI-Styrene copolymers required appreciable purification. They were purified by stirring the polymer in 1,4-dioxane overnight and drying in a heat pistol under vacuum at 138°C for 48 h. When the NCMI-styrene copolymer was contaminated with the NCMI homopolymer (poly NCMI), the copolymer was purified by repeated washings in acetone:methanol(1:1) which selectively dissolved poly NCMI.

#### Copolymerizations of N-Substituted Maleimides with Maleic Anhydride

N-phenylmaleimide (NPMI) and N-ethylmaleimide (NEMI) were copolymerized with maleic anhydride (MA). All copolymerization reactions were done in duplicate.

Typically, solutions of the desired concentrations were made by weighing appropriate amounts of the maleimide, maleic anhydride, and initiator into a pressure bottle and adding the appropriate amount of solvent. The initiator used was benzylperoxide (BPO) and the solvent was acetone.

All materials were purified as described previously. The total monomer concentration was maintained at 10% (W/V) and the BPO concentration was 10% (W/W) of monomers in most cases. The polymerization reactions were carried out under a nitrogen atmosphere in a thermostated oil bath at  $65.0 \pm 0.1^\circ\text{C}$ . NPMI-MA copolymerizations were generally run for 54.25 h and NEMI-MA copolymerizations were run for 48 h. Data of the polymerizations are given in Tables XXXIX and XL.

NPMI-MA copolymers formed a red colored solution in acetone and were precipitated in anhydrous ethyl ether or cyclohexane or petroleum ether. Anhydrous ethyl ether was the preferred precipitating agent because the monomers were soluble in it (whereas the copolymer was not) and it was available in pure form. NEMI-MA copolymers were precipitated from solution using anhydrous ether or  $\text{MeCl}_2$ :cyclohexane(1:2) or chloroform as the non-solvent. The NPMI-MA copolymers and NEMI-MA copolymers were purified by redissolving them in acetone or tetrahydrofuran followed by reprecipitation in anhydrous ethyl ether.

#### Homopolymer Syntheses

Homopolymers of maleimide, N-carbanylmaleimide, N-carbathoxymaleimide and styrene were prepared in 1,4-dioxane with monomer concentrations of 0.2 mol/L using AIBN as the initiator at a concentration of 0.004 mol/L and

reaction temperature of  $60^{\circ}\text{C} \pm 0.1$ . Reaction time was generally 16 h.

Poly(N-carbamylmaleimide) precipitated in 1,4-dioxane as a cream colored solid which, when filtered and dried under vacuum, was a pink colored powder. Both poly-maleimide and poly(N-carbethoxymaleimide) remained in solution in 1,4-dioxane. Polymaleimide was precipitated as a white powder in methanol and poly(N-carbethoxymaleimide) was precipitated as a white powder in hexane. A large portion of NCEMI did not polymerize and oiled out of the hexane to later crystallize. Data for these polymerizations are given in Table XXXVIII.

Poly(N-phenylmaleimide) was prepared under the same conditions as used for its copolymerization with maleic anhydride except that reaction time was 24 h. The solvent was acetone, the initiator was BPO (10% W/W of NPMI). NPMI concentration was 10% (W/V). Poly(N-phenylmaleimide) precipitated from acetone as a light green colored powder to give a 52.8% yield.

## Polymer Characterization

The copolymers and homopolymers were characterized by  $^1\text{H}$  NMR,  $^{13}\text{C}$  NMR and IR spectral analyses. Copolymer compositions were ascertained by elemental analyses and, where possible by  $^1\text{H}$  NMR and  $^{13}\text{C}$  NMR. Viscosity determinations were performed on certain NPMI-MA copolymers (Table XLI) and melting points were ascertained using a capillary melting point apparatus (Table XLV).

The  $^1\text{H}$  NMR spectra of these polymers generally appeared as a series of broad peaks due to their structural and stereochemical complexity.  $^{13}\text{C}$  NMR analysis of the polymers proved to be much superior to the  $^1\text{H}$  NMR spectra because of greater spectral simplicity resulting from the lack of coupling and the increased spectral width (usually 200 ppm for  $^{13}\text{C}$  and 10 ppm for  $^1\text{H}$ ). Like the  $^1\text{H}$  NMR spectra, the IR spectra of the polymers showed broader bands than their respective monomers. The IR spectra of the copolymers did not differ significantly with varying monomer feed ratios. The  $^1\text{H}$  NMR spectra differed significantly for varying monomer feeds only in the area under the resonance signals but not in chemical shift positions. For each copolymer system, the information obtainable regarding the sequence of monomers in the polymer chain from backbone carbon resonance in  $^{13}\text{C}$  NMR was limited because the  $\text{DMSO-d}_6$  solvent had resonance in the same region. Due to these reasons, only one set of spectra is shown below for each copolymer.

Copolymers

NCMI-styrene: IR (KBr, 1%), 3450-3100 (N-H, b), 3070 (C=C-H, w), 1800, 1755 (imide C=O, m, s), 1715 (amide C=O, s), 1600 (N-H, C=C-H, w), 1345 (C-N, m), 700  $\text{cm}^{-1}$  (C=C-H), w);  $^1\text{H}$  NMR (DMSO- $d_6$ ) ppm 12.0-11.0 (b, associated N-H), 8.0-6.0 (b, Ar-H), 4.0-1.0 (b, H,  $\text{CH}_2$ );  $^{13}\text{C}$  NMR (DMSO- $d_6$ ) ppm 179.8, 179.6, 178.1, 177.5, 176.7, 172.5, 161.2 (b,m, C=O), 140.0, 139.7, 139.2, 183.5, 137.8, 135.1, 130.4, 128.6, 126.6 (bm, ring C=C), 73.6, 67.1, 60.0, 52.4, 51.3, 50.4, 49.4, 48.4, 47.9, 47.4, 46.7, 45.4, 42.9, 42.3, 41.4, 40.4 (bm, -CH, - $\text{CH}_2$ ). Elemental analysis data is listed in Table XLIII.

NCEMI-Styrene: IR (KBr, 1%), 3080, 3022 (C=C-H, w), 2980 (-C-H, w), 1810, 1770 (imide C=O, s), 1725 (ester C=O, s), 1325 (C-N, s), 1280 (C-O, s), 700  $\text{cm}^{-1}$  (C=C-H, m);  $^1\text{H}$  NMR ( $\text{CDCl}_3$ ) ppm 8.0-6.0 (b, Ar-H) 4.8-4.0 (b, O- $\text{CH}_2$ -), 4.0-1.7 (b, -CH, - $\text{CH}_2$ ), 1.7-1.0 (b, - $\text{CH}_3$ );  $^{13}\text{C}$  NMR ( $\text{CDCl}_3$ ) ppm 173.7, 172.9 (bd, imide, C=O), 147.7 (s, - $\text{CO}_2\text{R}$ ), 129.1 (b, - $\text{C}=\text{C}$ ), 64.7 (s, O $\text{CH}_2$ -), 52.5, 51.6, 45.1-40.6 (b, -CH, - $\text{CH}_2$ ), 13.9 (s, -O $\text{CH}_2\text{CH}_3$ ). Elemental analysis data is listed in Table XLIII.

MI-Styrene: IR (KBr, 1%) 3500-3200 (N-H, b), 3080 (C=C-H, w), 1775, 1710 (C=O, w, s), 1350 (C-N, m), 700  $\text{cm}^{-1}$  (C=C-H, w);  $^1\text{H}$  NMR (DMSO- $d_6$ ) ppm 11.7-10.8 (b, associated N-H), 8.0-6.0 (b, Ar-H), 4.0-1.8 (b, -CH).

NCMI-Furan:  $^1\text{H}$  NMR (DMSO- $d_6$ ) ppm 11.2 (b, associated N-H), 7.9 (b, -C=C-H), 6.0, 5.3 (bm, -OCH-C=C-), 4.0-2.0 (bm, -CH);  $^{13}\text{C}$  NMR (DMSO- $d_6$ ) ppm 177.7, 176.5 (bm, C=O), 129.6, 128.4 (bm, C=C-H), 85.7, 82.9, 81.6, 80.0 (bm, -OCH-C=C-), 52.0, 50.6, 48.3, 48.0, 46.5 (m, -CH).

NPMI-MA: IR (KBr, 1%) 3080 (Ar-H, w), 2930 (C-H, w), 1851, 1781 (anhydride C=O, w, m), 1710 (imide C=O, s), 1500 (ring C=C, m), 1400 (C-N, s), 695  $\text{cm}^{-1}$  (-C=C-H, w);  $^1\text{H}$  NMR (DMSO- $d_6$ ) ppm 7.8-6.3 (b, Ar-H), 5.0-2.1 (b, -CH);  $^{13}\text{C}$  NMR (DMSO- $d_6$ ) ppm 175.7, 172.7 (b, C=O), 131.8, 130.0, 128.6, 126.4 (b, Ar-C), 45.6-35.7 (b, -CH). Elemental analysis data is listed in Table XXXIX.

NEMI-MA: IR (KBr, 1%) 2947 (C-H, w), 1854, 1775 (anhydride C=O, w, s), 1700 (imide C=O), 1450, 1414  $\text{cm}^{-1}$  ( $\text{CH}_3$ , w, m).

### Homopolymers

Poly MI: IR (KBr, 1%) 3500-3100 (N-H, b), 1775, 1710 (C=O, m, s), 1365 (C-N, m);  $^1\text{H}$  NMR (DMSO- $d_6$ ) ppm 11.9-11.0 (b, associated NH), 4.3-2.0 (b, CH).

Poly NCMI: IR (KBr, 1%) 3500-3100 (NH, b), 1800, 1760, 1720 (C=O, s), 1620, 1590 (NH, m), 1365, 1335 (C-N, m);  $^1\text{H}$  NMR (DMSO- $d_6$ ) ppm 12.3-10.5 (b, associated NH), 4.7-1.6 (b, -CH);  $^{13}\text{C}$  NMR (DMSO- $d_6$ ) ppm 180.2, 178.3, 177.4 (bm, C=O), 44.3, 42.3, 41.3, 40.3 (b, -CH).



Poly NPMI:  $^1\text{H}$  NMR (DMSO- $d_6$ ) ppm 8.0-6.3 (b, Ar- $\underline{\text{H}}$ ), 3.2-3.7 (b,  $-\underline{\text{CH}}$ );  $^{13}\text{C}$  NMR (DMSO- $d_6$ ) ppm 176.5, 175.6, 170.6 (bm, C=O), 131.2, 130.0, 128.7, 126.6 (bm, ring C=C),  $\underline{\text{C}}$ -H covered by DMSO- $d_6$  resonance.

Polystyrene:  $^1\text{H}$  NMR (Benzene- $d_6$ ) ppm 7.0, 6.7 (b, Ar- $\underline{\text{H}}$ ), 2.0 (b,  $-\underline{\text{CH}}$ ), 1.6 (b,  $-\underline{\text{CH}}_2$ );  $^{13}\text{C}$  NMR (Benzene- $d_6$ ) ppm 128.9, 128.2, 127.8, 126.7, 125.9 (m, ring C=C), 48.4-40.0 (b,  $-\underline{\text{CH}}$ ), 41.0 (s,  $-\underline{\text{CH}}$ ).

#### Rates of Conversion of Copolymers

In all cases, the total monomer concentration was kept constant at 0.2 mol/L and the initiator concentration was 0.004 mol/L in most cases. The solvent was 1,4-dioxane and the reaction temperature 60.0°C. Reaction times were taken as the time interval between placing the pressure bottle in the oil bath (when reaction began) and immersing it in the dry ice-isopropanol or ice-water bath (when reaction terminated). All polymerizations were performed under an oxygen free nitrogen atmosphere.

Conversion rate determination involved gravimetric analysis. After the polymerization reaction had been quenched by immersing the pressure bottle in dry ice-isopropanol, the polymer suspension (or solution) was allowed to come to room temperature to ensure that any unreacted monomers that precipitated upon lowering of the temperature went back into solution. If the polymer had

precipitated in dioxane, it was carefully filtered out using a fine porosity filter paper (Whatman number 5, pore size  $2.5 \mu\text{m}$ ) which had been preweighed. After filtration, the filter paper and the polymer were air dried for 30 min and then dried under vacuum at room temperature for 24 h. The filter paper was then reweighed and the weight of the polymer was calculated by difference. If it was suspected that some moisture remained in the polymer, vacuum drying was continued until a constant weight was obtained.

When the copolymer or homopolymer were soluble in dioxane, they were precipitated in methanol, followed by filtration. Occasionally it was necessary to digest the polymer solution in order to increase the particle size and facilitate filtration. This was done (56) by gentle heating ( $\sim 35\text{--}45^\circ\text{C}$ ) of the suspension for about one hour and then allowing it to stand undisturbed at room temperature for several days. In all cases, practically all of the polymer was filtered out of the dioxane in this manner and accounted for in the conversion percent.

Rates of conversion (% yield/h) were determined for several mole fractions of NCMI in the monomer feed when investigating the NCMI-styrene copolymerization (TableXXXVI). Also, the effect of the electron-withdrawing N-substituents (amide and carbethoxy groups) on the homopolymerization rate of maleimide and copolymerization rate of maleimide with styrene was determined and compared with the rate of

copolymerization for the MA-styrene system under the same reaction conditions (Table XXXVIII).

### Complexation Studies

Complexation between the electron-acceptor species (maleic anhydride, maleimide, and N-substituted maleimides) and electron-donor species (styrene, furan and 2-chloroethyl vinyl ether) was investigated using  $^1\text{H}$  NMR spectroscopy and UV spectroscopy. Maleic anhydride (Aldrich) was purified by vacuum distillation or by recrystallization from chloroform. Maleimide and N-ethylmaleimide were recrystallized from benzene. N-carbethoxymaleimide was vacuum distilled and then sublimated. N-carbamylmaleimide was recrystallized from acetic anhydride and N-phenylmaleimide was recrystallized from cyclohexane. Styrene, furan, and CEVE were distilled prior to use.

### Complex Study by $^1\text{H}$ NMR Spectroscopy

$^1\text{H}$  NMR spectroscopy was used to determine the formation constant of complexation for the electron donor - acceptor complexes.  $\text{CDCl}_3$  (99.8 atom% D, Aldrich, 99.8 atom % D, Sigma) was the solvent that was used predominantly for the complex studies involving styrene and furan. Since the MA-CEVE system did not indicate any complexation in  $\text{CDCl}_3$ , non-polar  $\text{CCl}_4$  (certified A.C.S. spectranalyzed, Fisher) was used as the solvent for the CEVE systems.

Solvent effects on the complexation of furan with maleic anhydride and N-carbamylmaleimide was investigated by using 1,4-dioxane as solvent. Dioxane was purified (112) by refluxing over sodium hydroxide pellets for at least 48 h, followed by distillation and then redistilling the middle fraction of the distillate over sodium metal strips.

The  $^1\text{H}$  NMR spectra were obtained on a 90MHz JEOL FX 90 Q spectrometer. When an undeuterated solvent (i.e.  $\text{CCl}_4$  and 1,4-dioxane) was used, an external deuterium lock was employed.

A 0.05M solution of NCEMI in  $\text{CDCl}_3$  shows an olefinic proton resonance at 6.8 ppm. When a solution is prepared in which there is a high concentration of furan relative to the same 0.05M concentration of NCEMI in furan, it is seen that the olefinic proton resonance has moved upfield. A second solution containing even a greater concentration of furan with NCEMI concentration kept constant at 0.05M gives an olefinic  $^1\text{H}$  resonance that is even further upfield. Thus, the experiments involved monitoring the olefinic proton resonance of a constant and low concentration of an electron-acceptor species while varying the concentration of an electron-donor species which had a concentration always significantly greater than that of the electron-acceptor. The difference in chemical shift (cps) of the olefinic protons of the electron acceptor in its free form (no electron-donor present) and in its complexed form (electron

donor present) gave a value,  $\Delta_{\text{Obsd}}$ . When the reciprocal of the donor concentration was plotted against the reciprocal of the corresponding  $\Delta_{\text{Obsd}}$  values using computer linear regression analysis, a correlation coefficient, intercept, and slope were obtained for a straight line. The intercept corresponds to  $1/\Delta_{\text{CT}}$  where  $\Delta_{\text{CT}}$  is the difference in chemical shift between the free olefinic proton resonance of the electron-acceptor and its olefinic proton resonance in the pure-complex form (Figure 19). The slope corresponds to the  $(1/K)(\Delta_{\text{CT}})$  value where  $K$  is the formation constant of the complex. Division of the intercept by the slope yielded a value for  $K$ . Data for these studies are given in tables XI to XXXII.

In most cases each electron-donor-acceptor system was investigated with at least five different electron-donor concentrations. Occasionally the olefinic proton resonance was hidden behind a spinning side band of the electron donor. When this occurred, the spin rate of the probe was changed so that the spinning side band shifted and uncovered the location of the olefinic proton resonance. Sometimes the olefinic proton resonance would be hidden behind a resonance of the electron-donor. Since the concentration of the electron-donor was many times greater (more than 10x) than that of the electron acceptor, the resonances of the electron donor protons were very much stronger and wider than the olefinic proton resonance of the electron acceptor

and hence, even integration of the resonances could not pinpoint the exact chemical shift of the electron-acceptor's olefinic protons.

In a typical procedure, stock solutions of the electron-donor and electron-acceptor were prepared by carefully weighing the appropriate moiety into a volumetric flask and filling to the mark with the solvent. Each electron-donor-acceptor combination was prepared immediately prior to obtaining the  $^1\text{H}$  NMR spectrum. The appropriate volumes of donor and acceptor solutions were transferred to a 2 mL volumetric flask which was then filled to the mark with solvent, shaken for thorough mixing, and then an aliquot was transferred to a clean 5 mm NMR probe for obtaining the  $^1\text{H}$  NMR spectrum. To ensure that the spectra were obtained at a constant temperature, the probe temperature of the NMR instrument was taken immediately before and after the experiment. The calculated K values of the styrene and furan systems are given in tables XVII and XXV. The reliability of the least squares parameters were checked (82-84) to obtain a standard deviation, range and confidence interval for the calculated formation constants.

#### Complex Study by UV Spectroscopy

In this technique, the existence of a charge-transfer complex was deduced from the analysis of some change in the absorption spectrum of a mixture of electron-donor and

electron-acceptor species (the appearance of a new band or the intensification of a previously existing band) when compared to the spectra of the individual components. The electron-acceptors were maleic anhydride, maleimide, and N-substituted maleimides and the electron-donors were styrene, furan and 2-chloroethyl vinyl ether. The solvents used were 1, 4-dioxane (purified as previously described),  $\text{CHCl}_3$  (99+%, spectrophotometric grade, Aldrich) and benzene (reagent, A.C.S., B & A) which was distilled prior to use. The ultraviolet spectra were obtained on a Beckman ACTA M VII spectrophotometer (Beckman Instruments, Irvine, CA) using 1 cm quartz cells or 1 mm silica cells.

If a band attributable to a charge-transfer complex appeared, the stoichiometric composition of the complex was determined by observing the change in the absorbance due to the complex with variation of the mole fraction of one of the components.

In a typical procedure, equimolar stock solutions of electron-acceptor and electron-donor were prepared by careful weighing of the substrates into volumetric flasks followed by filling up to the mark with solvent. Experimental solutions of each species were then prepared by transferring appropriate amounts of the stock solutions to a series of volumetric flasks with glass pipettes, followed by dilution to the mark with solvent. UV spectra of each concentration were then obtained against solvent in

the reference cell. After the UV absorption of each species for specified concentrations were recorded, pipetted aliquots of the electron donor and electron acceptor solutions were mixed together in a series of volumetric flasks. This mixing was carefully done so that the resultant concentration of each species matched a concentration for which the absorption had already been determined. UV absorption spectra for the mixtures were then obtained against the solvent in the reference cell. If no charge-transfer complexation occurred, the observed absorption would be simply the sum of the absorptions of the two components, in accordance with the Beer-Lambert law. In some cases, an increased absorption was observed at certain wavelengths which were attributed to charge-transfer bands. Subtraction of the absorption due to the components gave the absorption due to the charge-transfer band. Peak height was measured and converted to absorbance units. In some cases (MA-Furan, NCMI-Furan) spectra for the donor-acceptor mixtures were obtained with the reference cell containing the component which absorbed the most (the electron-acceptor). While this method automatically subtracted the component absorption to show the charge-transfer absorption, it had a serious limitation in that the large absorption by the component in the reference cell lead to the slit opening wide at a rapid rate and cutting off well before the solvent cut-off point was reached. Total concentrations of the



species were 0.1M in most cases. Typical instrument settings used were: slit width 0.4, span 3, period 1, scan speed 2 nm/sec, and chart speed 50 nm/inch. If absorption was so intense that the recorder went off-scale before being able to scan a significant portion of the UV region, 1 mm silica cells were used instead of 1 cm quartz cells and the chart speed was changed to 10 nm/inch.

It was noticed that repetitive runs on a single sample did not give exactly reproducible absorbance readings. This was corrected for by noting that the ACTA M VII instrument changes slits at 350 nm at which time there is a pause in the scan and a mark is left on the recorder chart paper. When the absorption spectrum was calibrated from the mark attributed to the 350 nm wavelength, highly reproducible absorbance readings were obtained.

In every case where charge-transfer absorption was observed, the complex absorption reached a maximum at a mole fraction of 0.5 for either component (Figures 15-18). The UV studies are summarized in tables IX and X.

#### High Pressure Liquid Chromatography (HPLC)

It was investigated whether reversed phase HPLC was a viable technique to monitor the change in concentration of monomers with reaction time for the NCMI-styrene copolymerization in 1, 4-dioxane. The instrument used was a Gilson Model #41 High Performance Liquid Chromatograph

(Gilson Medical Electronics, Inc., Middleton, WI) which was interfaced with a Hewlett Packard #3385 A Automation System (Hewlett Packard, Inc., Avondale, PA) for integration and a Kipp & Zonen # BD 41 recorder (Kipp & Zonen, Holland). The packing material of the column was Bondapak  $c_{18}$ . Solvent mixtures of nanopure deionized water (Barnstead, Sybron Co., Boston, MA) and chromatographic grade methanol (J. T. Baker Chemical Co., Phillipsburg, N. J.) were used as the mobile phase. The ratios of water:methanol were changed as needed (by computer assisted solvent programming) for the elution of NCMI and styrene at suitable retention times.

First, it was investigated whether solutions of the individual components (NCMI and styrene) in dioxane would show reasonable elution profiles, what their upper and lower limits of detection would be and whether their absorbance had a linear relationship with concentration for each species. When styrene and NCMI showed such linearity in their respective solvent programs, a solution of styrene and NCMI within their upper and lower limits of detection was prepared and run with a third solvent program which accommodated the elution of the less polar styrene and the more polar NCMI.

The instrument settings were: UV detector at 254 nm, 200 mV full scale recorder and a chart speed of 10 mm/min. The range of the instrument was adjusted from 2.0 to 0.2 to change the sensitivity of the recorder for different

concentrations of each component. The peak heights of the elution profiles of each component were taken as proportional to the area under each elution peak and peak heights were normalized to one range (sensitivity) setting of the recorder. Plots of log peak heights versus log of concentration indicated that individual solutions of NCMI and styrene as well as mixtures of NCMI and styrene solutions were linear for their respective concentration ranges and thus calibration curves (figures 51 and 52) were established. The solvent programs used were as follows:  
for styrene/dioxane solution:

"WMI" Solvent Program (water/MeOH)

<u>Time</u> (min)	<u>% MeOH</u>
0	50
6	90
12	90
15	50

for NCMI/dioxane solution:

"WM2" Solvent Program (water/MeOH)

<u>Time</u> (min)	<u>% MeOH</u>
0	20
8	50
12	50
15	20

for NCMI/styrene/dioxane solution:

"WM3" Solvent Program (water/MeOH)

<u>Time</u> (min)	<u>% MeOH</u>
0	25
10	80
12	80
15	25

For a NCMI/styrene solution in dioxane, the linear relationship between concentration of each component and the elution peak height indicated that high pressure liquid chromatography would be a viable technique for monitoring changes in monomer concentration during a NCMI-styrene copolymerization reaction.

### Viscosities

Viscosity measurements were taken with the viscometer in a thermostated bath at  $25 \pm 0.1^\circ\text{C}$  using a Haake Thermostat Model E 52. Viscosities were determined in an Ubbelohde Cannon 50 A968 viscometer using tetrahydrofuran as solvent. The viscometer was cleaned by soaking it in chromic acid for several hours and then metal decontaminated (111) by soaking it in an aqueous solution containing 1% disodium ethylenediaminetetracetate and 2% sodium hydroxide followed by rinsing several times with deionized water. The viscometer was dried with a stream of  $\text{N}_2$  gas and by vacuum aspirator.

Approximately 10 mL of solvent was transferred to the viscometer which was then placed in the constant temperature bath. After 45 minutes for temperature equilibration, flow times were recorded until three consecutive measurements, agreeing within 0.1 sec, were obtained.

A measured volume of a 1% polymer solution (which had been filtered through a sintered glass funnel) was transferred to the viscometer using a glass syringe. Flow times were then recorded. When consistent measurements were obtained, dilution of the solution in the viscometer was achieved by introducing a measured quantity of solvent and mixing it by shaking the viscometer several times and by drawing the solution up the viscometer three times. After 30 minutes for temperature equilibration, flow times of the

new concentration were recorded. Several dilutions were performed in this manner.

Reduced viscosity ( $\eta_{sp}/C$ ) was calculated for each concentration,  $C$ , and a plot of  $\eta_{sp}/c$  vs.  $C$  was made to determine intrinsic viscosity.

## BIBLIOGRAPHY

BIBLIOGRAPHY

1. Donaruma, L. G., Ottenbrite, R. M., and Vogl, O. eds. "Anionic Polymeric Drugs", John Wiley and Sons, New York, 1980.
2. Ottenbrite, R. M., "The Antitumor and Antiviral Effects of Polycarboxylic Acid Polymers", Carraher, Jr., Charles E. and Gebbelein, Charles G., eds., "Biological Activities of Polymers", ACS Symposium Series 186 (1982).
3. Ascoli, F. and Botre, C., Sci., 1962, 17, 214.
4. Regelson, W. and Holland, J. F., Nature (Lond), 1958, 181, 46.
5. Regelson, W., Adv. Chemotherapy, , 3, 304.
6. Breslow, D. S. and Hulse, G. E., J. Am. Chem. Soc., 1954, 76, 6399.
7. Regelson, W. and Holland, J. F., Nature (Lond), 1958, 181, 46.
8. Regelson, W. and Holland, J. F., Clin. Pharmacol. Therap., 1962, 3, 730.
9. Butler, G. B., J. Poly. Sci., 1960, 48, 279.
10. Merigan, T. C., Nature, 1967, 214, 416.
11. Merigan, T. C., New Engl. J. Med., 1967, 277, 1283.
12. Merigan, T. C., Ciba Foundation Symposium on Interferon, Wolstenholme, G. W., O'Conner, M. J. and Churchill, A., eds., London, pp. 50-60, 1967.
13. DeClereq, E., and Merigan, T. C., Arch. Intern. Med., 1970, 126, 949.
14. Mohr, S. J., Chirigos, M. A., Fuhrman, F. S., Pryor, J. W., Cancer Res., 1975, 35, 3750-3654.
15. Morahan, P. S. and Kaplan, A. M., Int. J. Cancer, 1976, 17, 82-89.
16. Regelson, W., Adv. Exp. Med. Biol., 1967, 1, 135.
17. Merigan, T. C., Finklestein, M. S., Virology, 1968, 35, 363.



18. DeClereq, E., Merigan, T. C., J. Gen. Virol., 1969, 5, 359.
19. Regelson, W., Munson, A., Wooles, W., Internat. Symp. on Stand. of Interferon and Interferon Inducers, London, 1969; Symp. Series Immunobiolog. Stand., 14, 227-236, Karger Basel/N.Y. 1970.
20. Pindak, F. F., Infec. Immun., 1970, 1, 271.
21. Givon, D. J., Schmidt, J. P., Ball, R. J., Pindak, F. F., Antimicrob. Agents and Chemother., 1972, 1, 80.
22. Richmond, J. Y., Infec. Immun., 1971, 3, 249; Arch. Ges. Virusforsch., 1972, 36, 232.
23. Schuller, G. B., Morahan, P. S., Snodgrass, M. J., 10th National Meeting of the Reticulo. Soc., 1973, Abstract 28.
24. Campbell, C. H., Richmond, J. Y., Infec. Immun., 1973, 7, 199.
25. Regelson, W., Munson, A. E., Ann. N.Y. Acad. Sci. 1970, 173, 831.
26. Shamash, Y., Alexander, B., Biochim. Biophys. Acta, 1969, 1, 449.
27. Breslow, D. S., Pure Appl. Chem., 1976, 46, 103-113.
28. Kapusta, M. A., and Mendelson, J., Arthritis Rheum., 1969, 12, 463.
29. Baxter, D. W., Rosenthal, M. W., and Lindenbaum, A., Abst. 21st Ann. Meeting Radiation Res. Soc., St. Louis, MO, Apr. 29, 1973; Lindenbaum, A., Rosenthal, M. W., Baxter, D. W., Egan, N. E., Kalesperus, G. S., Moretti, E. S., and Russel, J. J., Ann. Rept., Div. Biol. Med. Res., Argonne National Laboratory, 1972, 121-125.
30. Leavitt, T. J., Merigan, T. C., Freeman, J. M., Am. J. Dis. Child, 1971, 121, 43.
31. Munson, A. E., White Jr., K. L., Klykken, P., "Pharmacology of MVE Polymers", in "Augmenting Agents in Cancer Therapy", Hersch, E. M., Ed., Raven Press, 1981.

32. Regelson, W., Kuhar, S., Tunis, M., Fields, J., Johnson, J., and Gluesenkamp, E., Nature, 1960, 186, 778.
33. Fields, J. E., Asculai, S. S., Johnson, J. H., Monsanto Company, St. Louis, MO., U.S. Patent 4,255,537, March 10, 1981.
34. Fields, J. E., Asculai, S. S., Johnson, J. H., and Johnson, R. K.; J. Med. Chem., 1982, 25, 1060.
35. Falk, R. E., Makowka, L., Nossal, N., Falk, J. A., Fields, J. E. and Aseulia, S. S., Br. J. Surg., 1979, 66, 861-863.
36. Falk, R. E., Makowka, L., Nossal, N. A., Rotstein, L. E., and Falk, J. A., Surgery, 1980, 88, 126.
37. Lang, J. A.; Pavelich, W. A.; Clarey, A. D.; Chem. Eng. News, 1961, Sept. 11, 39, 52; J. Polym. Sci., 1961, 55, 31; J. Polym. Sci., 1963, A1, 1123.
38. Joshi, R. M., Macromol. Chem., 1962, 53, 33.
39. Tawney, P.O., Snyder, R.A., Conger, R.P., Leibrand, K.A., Stiteler, C.H., Williams, A.R., J. Org. Chem., 1961, 26, 15.
40. Van Paesschen, G., Timmerman, D., Macromol. Chem., 1964, 78, 112.
41. Coleman, Jr., L. E., Conrady, J. A., J. Polym. Sci., 1959, 38, 241.
42. Ivanov, V. S., Maentszak, M., Medvedev, Yu V., Levando, L. K., Polym. Sci. USSR, 1965, 7, (2), 207.
43. Ivanov, V. S., Petrukhno, L. A., Kozhevnikov, S. P., Polym. Sci. U.S.S.R., 1968, 10 (10), 2790.
44. Volmert, B., "Polymer Chemistry", Translated from the German by Immergut, E. H., Springer-Verlag, New York, 1973, 104.
45. Barrales-Rienda, J. M., Gonzalez de la Campa, J. I., Gonzalez, Ramos, J. Macromol. Sci. -Chem., 1977, All (2), 267
46. Yamaguchi, H., Minoura, Y., J. Polym. Sci., A-1, 1970, 8, 1467.
47. Yamada, M., Takase, I., Kobunshi Kagaku, 1966, 23, 348.
48. Trivedi, B. C. and Culbertson, B. M., "Maleic Anhydride", Plenum Press, New York, 1982.

49. Alfrey, Jr., T. Price, C. C. J. Polym. Sci., 1947, 2, 101.
50. Elias, Hans-Georg, "Macromolecules-2", Plenum Press, New York, 1977.
51. Shillady, D. S., Private Communication based on Marsh, R. E., Ubell, E., Wilcox, H. E., Acta Cryst., 1962, 15, 35.
52. Shillady, D. S., Private Communication based on Seres, J., Naray-Szabo, G., Simon, K., Daroczi-Cusuka, K., and Szilagyi, I., Tetrahedron, 1981, 37, 1565.
53. Matsuo, T., Can. J. Chem., 1967, 45, 1829.
54. Takase, I., Fukushima, S., Aida, H., Yamada, M., Kobunshi Kagaku, 1973, 30, 632.
55. Yamada, M., Takase, I., Mishima, T., Kobunshi Kagaku, 1967, 24, 326.
56. Olson, K. G., Ph.D. Dissertation, University of Florida, 1981.
57. Olson, K. G. and Butler, G. B., Macromolecules, 1983, 16, 707.
58. Blann, W. G., Fyfe, C. A., Lyerla, J. R., Yannoni, C. S. J. Am. Chem. Soc., 1981, 103, 4030.
59. Nelson, G. L., Williams, E. A. in "Progress in Physical Organic Chemistry", Vol. 12, Taft, R. W., Ed., John Wiley and Sons, New York, 1976.
60. L. J. Bellamy, "The Infra-red Spectra of Complex Molecules", Richard Clay and Company, Ltd., Bungary, Suffolk, 1962.
61. Mulliken, R. S., J. Am. Chem. Soc., 72, 610 (1950).
62. Hanna, Melvin, W., and Lippert, Joseph L., "Theory of the Ground State Structure of Molecular Complexes" in "Molecular Complexes", Vol. 1, Foster, Roy, Ed., The Gresham Press, Old Woking, Surrey, 1973.
63. Prout, C. K., "Crystal Structures of Electron-Donor-Acceptor Complexes" in "Molecular Complexes", Vol. 1, Foster, Roy, Ed., The Gresham Press, Old Woking, Surrey, 1973.

64. Rose, J., "Molecular Complexes", Pergaman Press, New York, 1967.
65. Andrews, L. J., Keefer, R. M., "Molecular Complexes in Organic Chemistry", Holden-Day, Inc., San Francisco, 1964.
66. Kosower, E. M., in "Progress in Physical Organic Chemistry", Vol. 3, Cohen, S. G., Streitweiser, A., Taft, R. W., Ed., Wiley-Interscience, New York, 1965.
67. Mulliken, R. S., Person, W. B., "Molecular Complexes: A Lecture and Reprint Volume", Wiley-Interscience, New York, 1969.
68. Foster, R., Ed., "Molecular Association", Vol. 2, Academic Press, London, 1979.
69. Benesi, H. A., Hildebrand, J. H., J. Am. Chem. Soc., 1949, 71, 2703.
70. Scott, R. L., Rec. Trav. Chim. Pays-Bas, 1956, 75, 787.
71. Scatchard, G., Ann. New York Acad. Sci., 1949, 51, 660.
72. Tsuchida, Eishun, and Tomono, Tsugikazu, Makromol. Chem., 1971, 141, 265.
73. Iwatsuki, S., Iguchi, S., and Yamashita, Y., Kogyo Kagaku Zasshi, 1966, 69, 145.
74. Iwatsuki, S., and Yamashita, Y., Kogyo Kagaku Zasshi, 1964, 67, 1470.
75. Iwatsuki, Siouji, and Takahito, Itoh, Makromol. Chem., 1979, 180, 663.
76. Butler, George B., and Badgett, J. Thomas, 1970, J. Macromol. Sci.-Chem., 1970, A4, 51.
77. Butler, George B., and Campus, Alfred F., J. Poly. Sci. A-1, 1970, 8, 523.
78. Vosberg, W. C., Cooper, G. R., J. Am. Chem. Soc., 1941, 63, 437.
79. Tsuchida, T., Tomono, T., and Sano, H., Makromol. Chem., 1972, 151, 245.
80. Hanna, M. W., and Ashbaugh, A. L., J. Phys. Chem., 1964, 68, 811.

81. McCornell, A. M., J. Chem. Phys., 1958, 28, 430.
82. Harris, Daniel C., "Quantitative Chemical Analysis," Freeman Press, San Francisco, 1982.
83. Peters, Dennis G., Hayes, John M., and Hieftje, Gary M., "Chemical Separations and Measurements", Saunders, Philadelphia, 1974.
84. Day, Jr., R. A. and Underwood, A. L., "Quantitative Analysis", 3rd Ed., Prentice-Hall, Inc., New Jersey, 1974.
85. Iwatsuki, S., Itoh, T., Makromol. Chem., 1979, 180, 663.
86. Ragab, Yousif A., Butler, George, B., J. Poly. Sci. Chem., 1981, 1175-1196.
87. "Dimethyl Sulfoxide (DMSO) Technical Bulletin," Crown Zellerbach, Vancouver, WA.
88. Ouchi, T., Tatsumi, A., Imoto, M., J. Poly. Sci., Poly. Chem. Ed., 1978, 16, 707.
89. Bamford, C. H., Ferrar, A. N., Proc. Roy. Soc., 1971, Ser. A 321, 425.
90. Vollmert, Bruno, "Polymer Chemistry", Translated from the German by Immergut, Edmund H., Springer-Verlog, New York, 1973.
91. Levy, G. E., Lichter, R. L., Nelson, G. L., "Carbon-13 Nuclear Magnetic Resonance Spectroscopy", Second Edition, John Wiley and Sons, New York, 1972.
92. Randall, J. C., "Polymer Sequence Determination, Carbon-13 NMR Method", Academic Press, New York, 1977.
93. Katritzky, A. R., Weiss, D. E., J. Chem. Soc. Perkin II, 1974, 1542.
94. Stothers, J. B., "Carbon-13 NMR Spectroscopy", Academic Press, New York, 1972.
95. Buchok, B. E., Ramey, K. C., J. Poly. Sci.-Polym. Lett. Ed., 1976, 14, 401.
96. Roth, H., Ratzsch, M., Freidrich, H., Roth, H. K., Acta Polymerica, 1980, 31, 582.
97. Koenig, Karl E., Macromolecules, 1983, 16, 99.

98. Seshadri, K. S., Antonoplos, P. A., and Heilman, W. J., J. Poly. Sci., Polym. Chem. Ed., 1980, 18, 2649.
99. McCormick, Charles L., Chen, Gow-Sheng, and Hutchinson, Brewer, H., J. Appl. Poly. Sci., 1982, 27, 3103.
100. Silverstein, R. M., Bassler, G. C., and Morrill, T. C., "Spectrometric Identification of Organic Compounds", Fourth Ed., John Wiley & Sons, New York, 1981.
101. Abayasekara, Dilip R., Ottenbrite Raphael M., Polymer Preprints, 1984, 25(1), 164.
102. Lindeman, L. P., Adams, J. Q., Anal. Chem., 1971, 43, 1245.
103. Grant, D. M., Paul, E. G., J. Am. Chem. Soc., 1964, 86, 2984.
104. Wehrli, F. W., Wirthlin, T., "Interpretation of Carbon-13 NMR Spectra", Heyden, New York, 1976.
105. Mayo, F. R., and Lewis, F. M., J. Am. Chem. Soc., 1944, 66, 1594.
106. Harwood, H., Baikowitz, H., Trommer, H., Polymer Preprints, 1963, 4(1), 133.
107. Buckley, D. A., Augustini, P. P., Brit. Polym. J., 1981, 27, 27.
108. Billmeyer, Jr., F. W., "Textbook of Polymer Science", Second Ed., Wiley-Interscience, New York, 1962.
109. Fieser, L., Fieser, M., "Reagents for Organic Synthesis", John Wiley and Sons, Inc., New York, 1967.
110. Loewenthal, H. J. E., "Guide for the Perplexed Organic Experimentalist", Heyden and Sons Ltd., Philadelphia, 1978.
111. Gordon, A. J., Ford, R. A., "The Chemist's Companion", John Wiley and Sons, Inc., New York, 1967.
112. Marshall, H. P., Grunwald, E., J. Am. Chem. Soc., 1953, 76, 2000.

113. Searle, N. E. (E. I. du Pont de Nemours), U. S. Pat. 2,444,536, 1948, C. A., 1948, 42, 7340c.
114. Cava, M. P., Deana, A. A., Muth, K., Mithcell, M. J., Organic Syntheses 1973, 5, 944.
115. Tawney, P. O., Snyder, R. H., Bryan, C. E., Conger, R. P., Dovell, F. S., Kelly, R. J., Stiteler, C. H., J. Am. Chem. Soc., 1959, 25, 56.
116. Butler, G. B., Zampini, A., J. Macromol. Sci-Chem., 1977, A 11 (3), 491.
117. Keller, O., Rudinger, J., Helv. Chim. Acta, 1975, 58, 531.

## APPENDIX



The Appendix consists of the following:

- Table XLV. Decomposition points of the Homopolymers and Copolymers
- Figure 53. 90 MHz  $^1\text{H}$  NMR Spectrum of Maleimide
- Figure 54.  $^{13}\text{C}$ -NMR Spectrum of Maleimide
- Figure 55. 90MHz  $^1\text{H}$ -NMR Spectrum of N-carbamylmaleimide
- Figure 56.  $^{13}\text{C}$ -NMR Spectrum of N-carbamylmaleimide
- Figure 57. Off-resonance  $^{13}\text{C}$ -NMR Spectrum of N-carbamylmaleimide
- Figure 58. 90MHz  $^1\text{H}$ -NMR Spectrum of N-carbethoxymaleimide
- Figure 59.  $^{13}\text{C}$ -NMR Spectrum of N-carbethoxymaleimide
- Figure 60. Off-resonance  $^{13}\text{C}$ -NMR Spectrum of N-carbethoxymaleimide
- Figure 61. 90 MHz  $^1\text{H}$ -NMR Spectrum of N-ethylmaleimide
- Figure 62.  $^{13}\text{C}$ -NMR Spectrum of N-ethylmaleimide
- Figure 63. 60 MHz  $^1\text{H}$  NMR Spectrum of N-phenylmaleimide
- Figure 64.  $^{13}\text{C}$ -NMR Spectrum of Poly (N-carbamylmaleimide)
- Figure 65. Off-resonance  $^{13}\text{C}$ -NMR Spectrum of Poly (N-phenylmaleimide)
- Figure 66.  $^{13}\text{C}$ -NMR Spectrum of Poly (N-carbamylmaleimide - co-furan)
- Figure 67. Off-resonance  $^{13}\text{C}$ -NMR Spectrum of Poly (N-carbamylmaleimide - co-furan)
- Figure 68.  $^{13}\text{C}$ -NMR Spectrum of Poly(N-phenylmaleimide - co-maleic anhydride - 10)
- Figure 69. IR Spectrum of Polymaleimide
- Figure 70. IR Spectrum of Poly (N-carbamylmaleimide)

## Appendix Continued:

- Figure 71. IR Spectrum of Poly(maleimide -co-styrene)
- Figure 72. IR Spectrum of Poly (N-carbamylmaleimide-co-styrene)
- Figure 73. IR Spectrum of Poly(N-phenylmaleimide-co-maleic anhydride - 12)
- Figure 74. IR Spectrum of Poly (N-ethylmaleimide-co-maleic anhydride - 7)

Table XXXV  
Decomposition Points of Homopolymers and Copolymers

Polymer	Decomposition point (°C)
<b>Homopolymers:</b>	
Polystyrene	140-150
Poly maleimide	300
Poly N-phenyl maleimide	a
Poly N-carbamyl maleimide	300
Poly(maleic anhydride)	300 <sup>b</sup>
<b>Copolymers<sup>c</sup>:</b>	
Poly(N-phenyl maleimide-co-maleic anhydride)	285
Poly(N-ethyl maleimide-co-maleic anhydride)	290
Poly(maleimide-co-styrene)	295
Poly(N-carbamyl maleimide-co-styrene)	300
Poly(N-carbethoxy maleimide-co-styrene)	250-270
Poly(maleic anhydride-co-styrene)	255-300

a) did not melt or decompose up to 345°C

b) reference 37

c) prepared from 1:1 monomer feeds

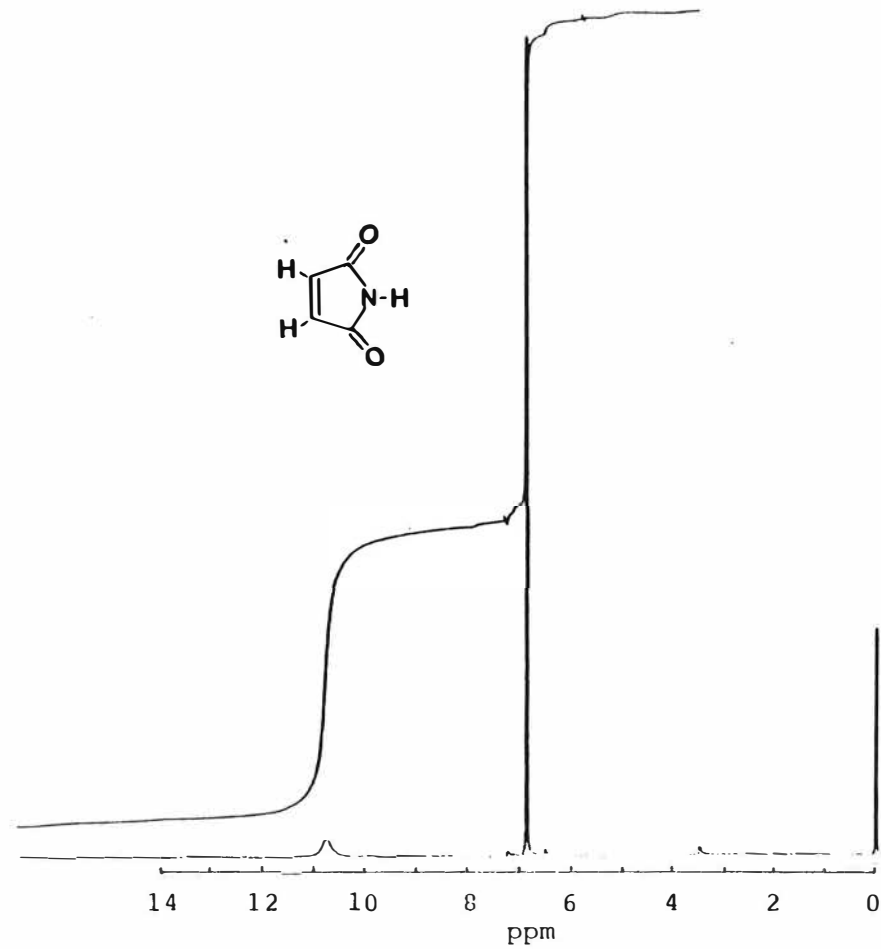


Figure 53 . 90 MHz  $^1\text{H}$  NMR Spectrum of Maleimide.

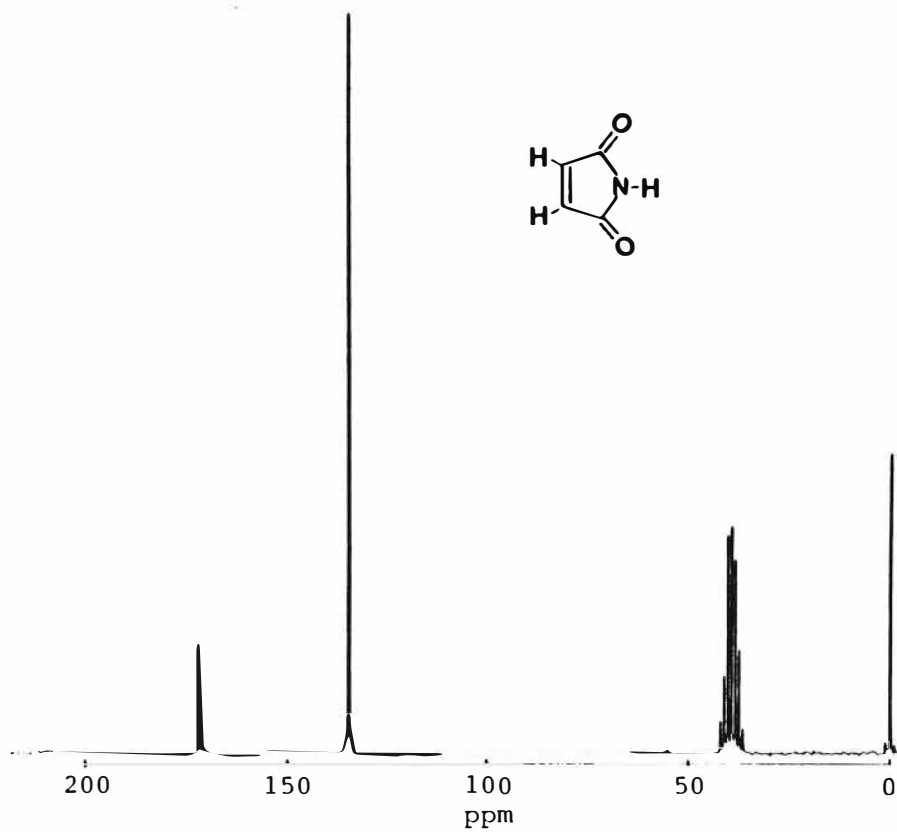


Figure 54.  $^{13}\text{C}$  NMR Spectrum of Maleimide.

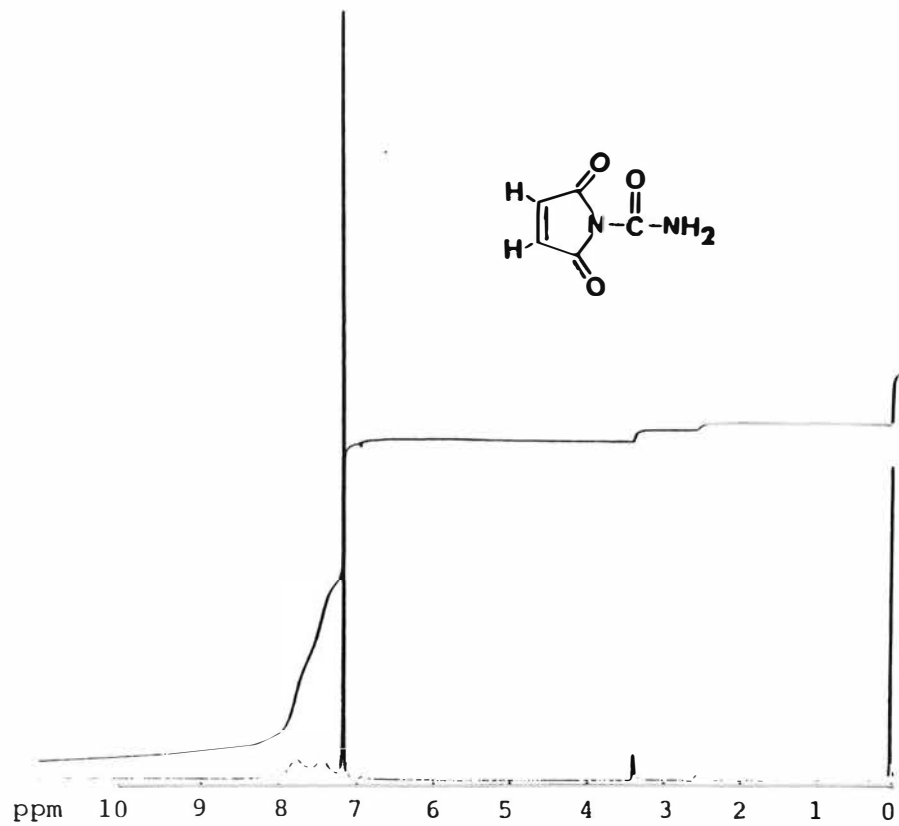


Figure 55. 90 MHz  $^1\text{H}$  NMR Spectrum of N-carbamylmaleimide.

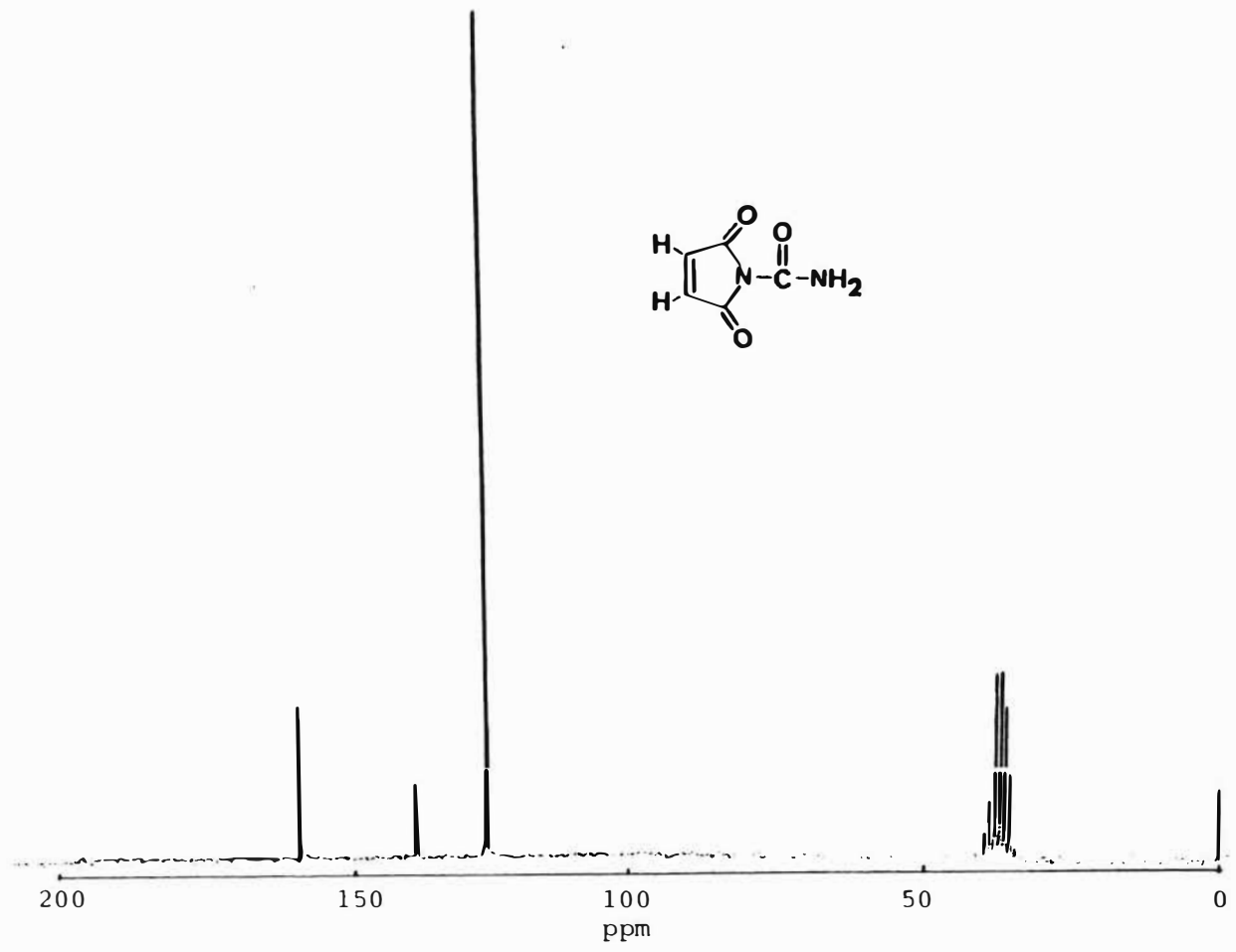


Figure 56.  $^{13}\text{C}$  NMR Spectrum of N-carbamylmaleimide.

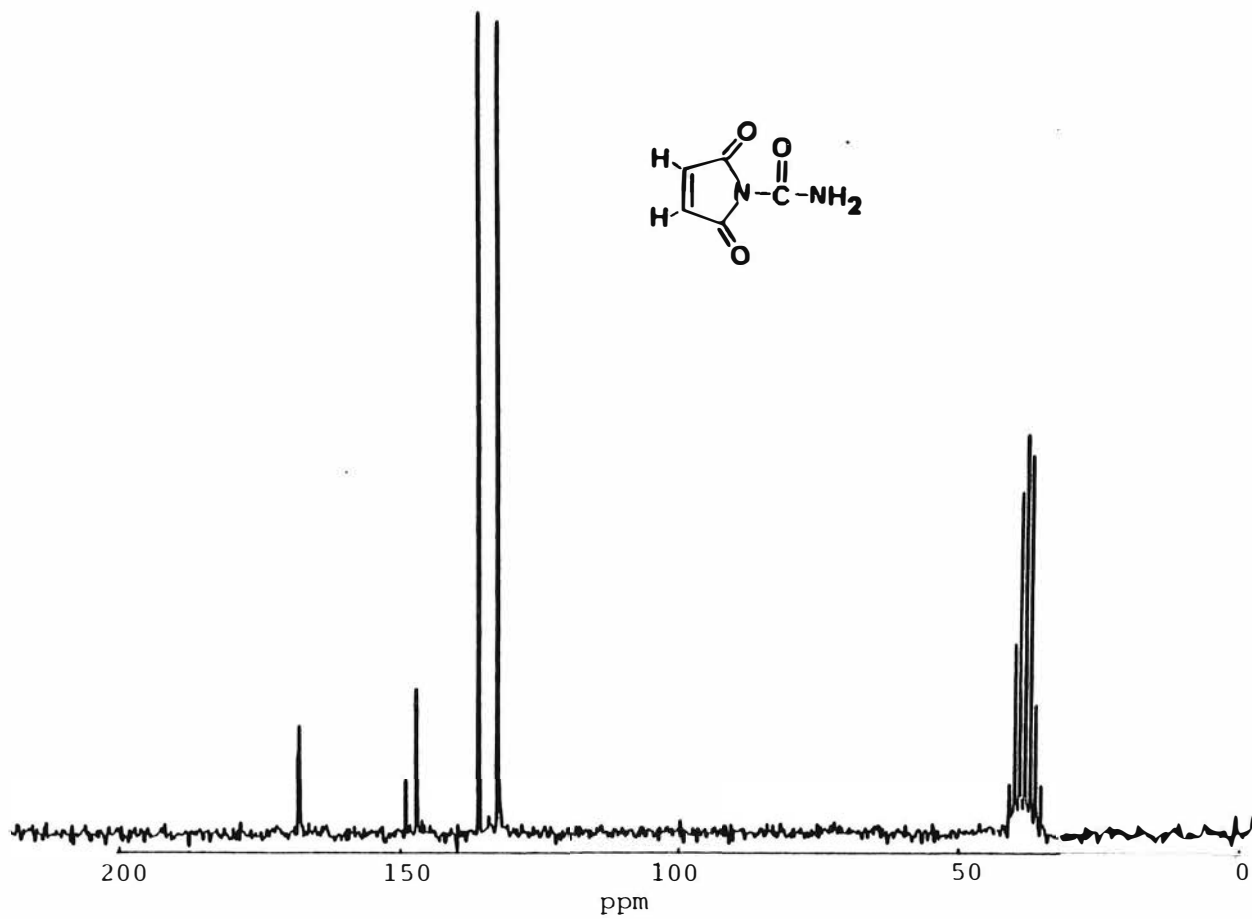


Figure 57. Off-resonance  $^{13}\text{C}$  NMR spectrum of N-carbamylmaleimide.



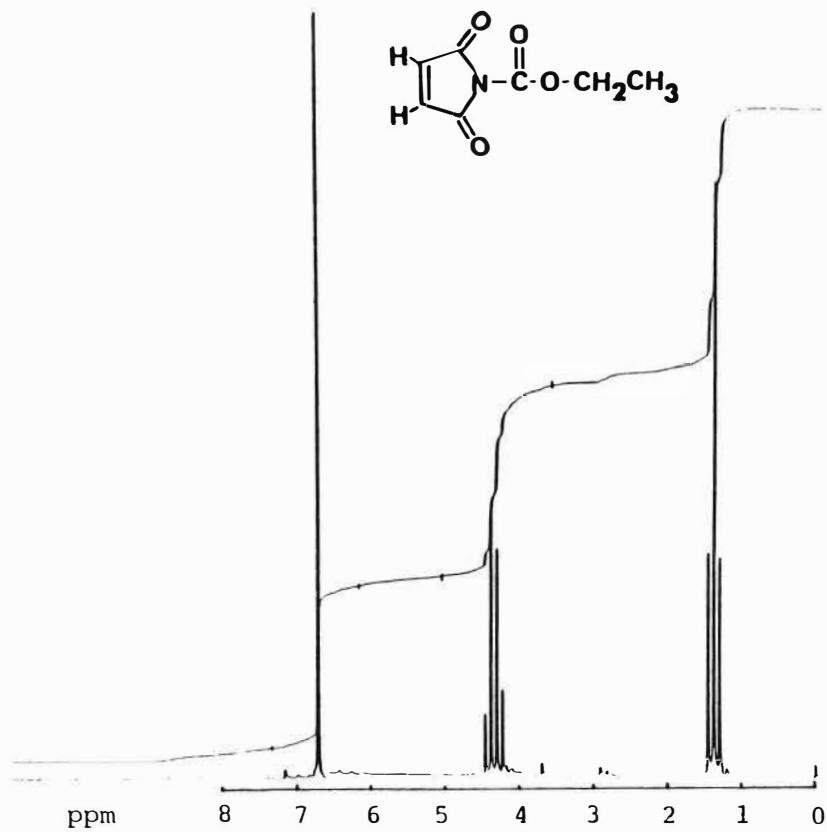


Figure 58 . 90 MHz  $^1\text{H}$  NMR of N-carbethoxymaleimide.

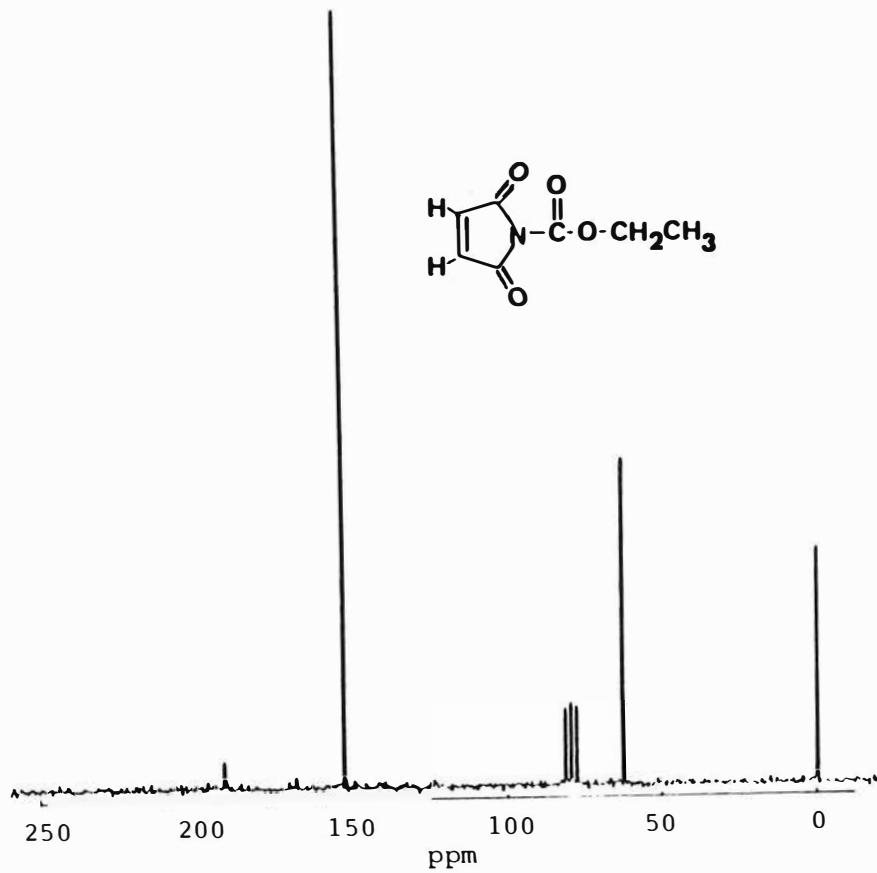


Figure 59 .  $^{13}\text{C}$  NMR Spectrum of N-carbethoxymaleimide.

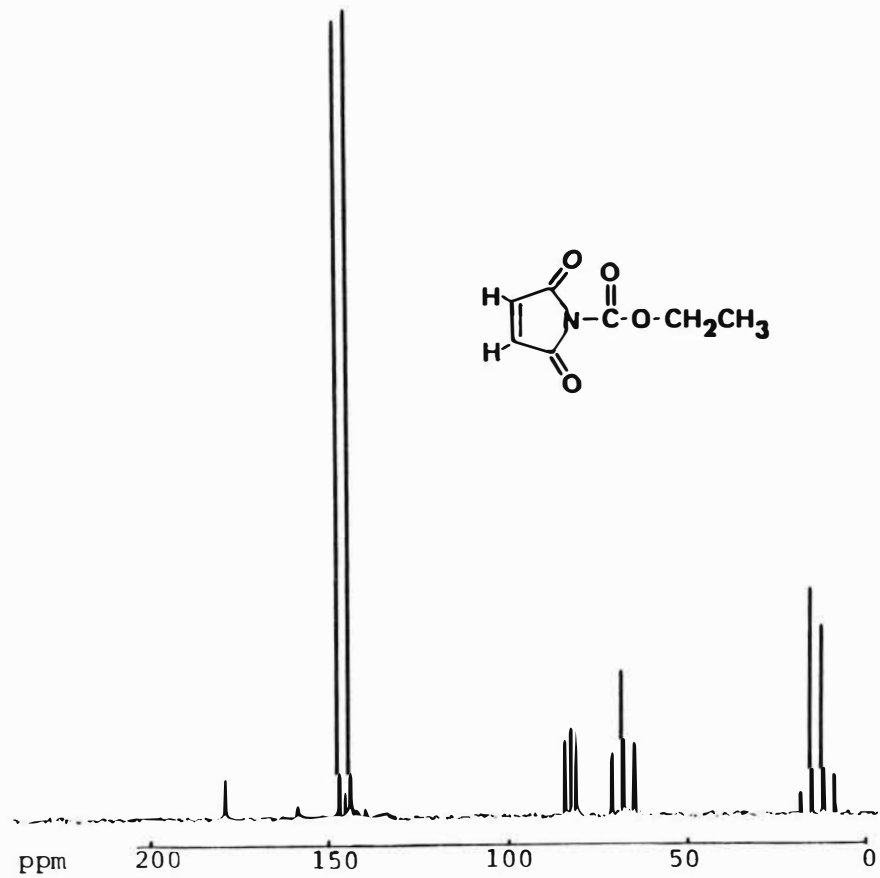


Figure 60. Off-resonance  $^{13}\text{C}$  NMR Spectrum of N-carbethoxymaleimide.

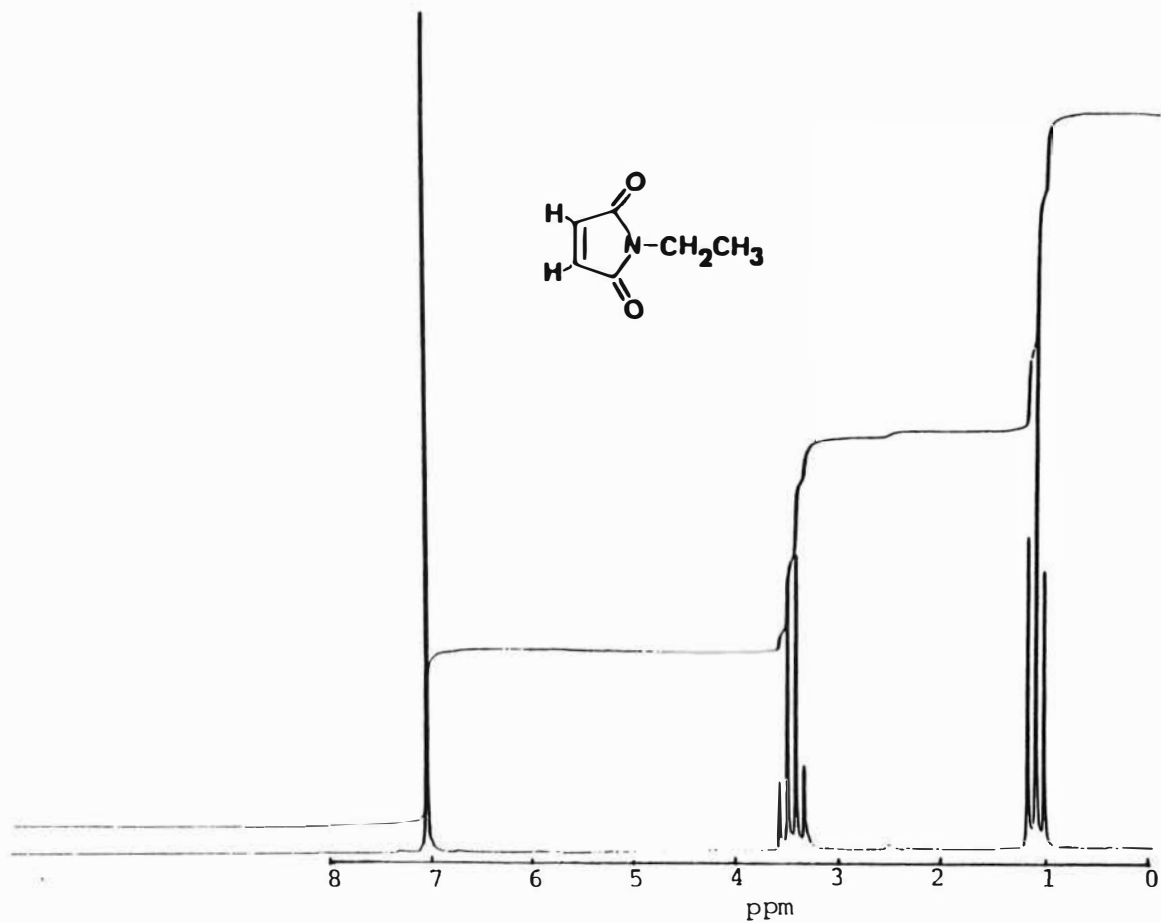


Figure 61. 90 MHz  $^1\text{H}$  NMR Spectrum of N-ethylmaleimide.

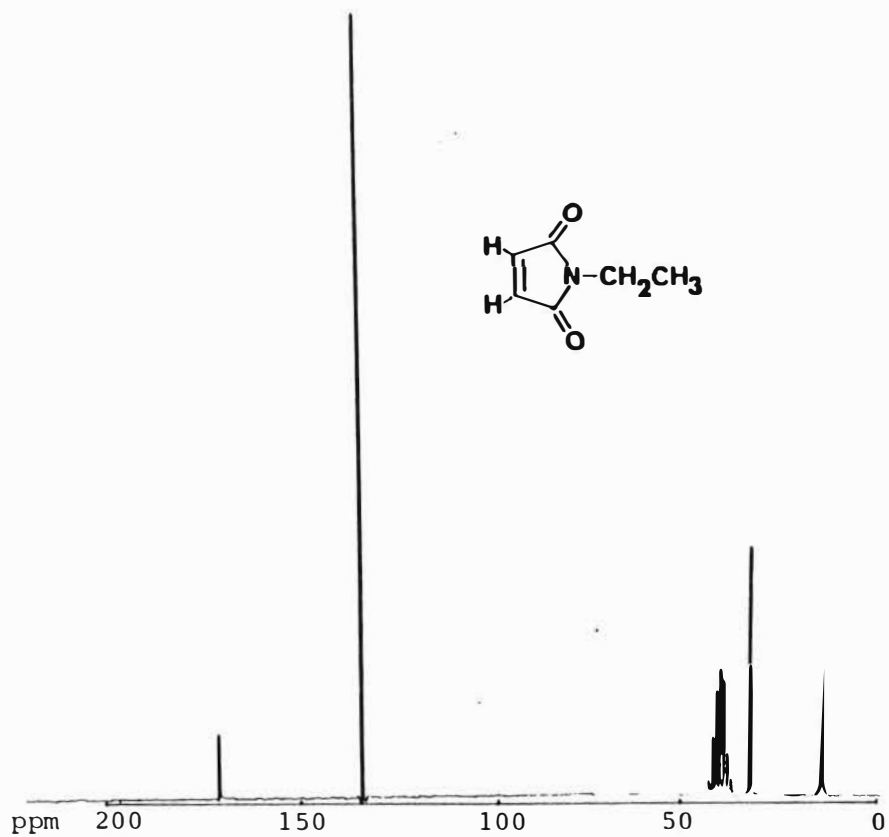


Figure 62 .  $^{13}\text{C}$  NMR Spectrum of N-ethylmaleimide.

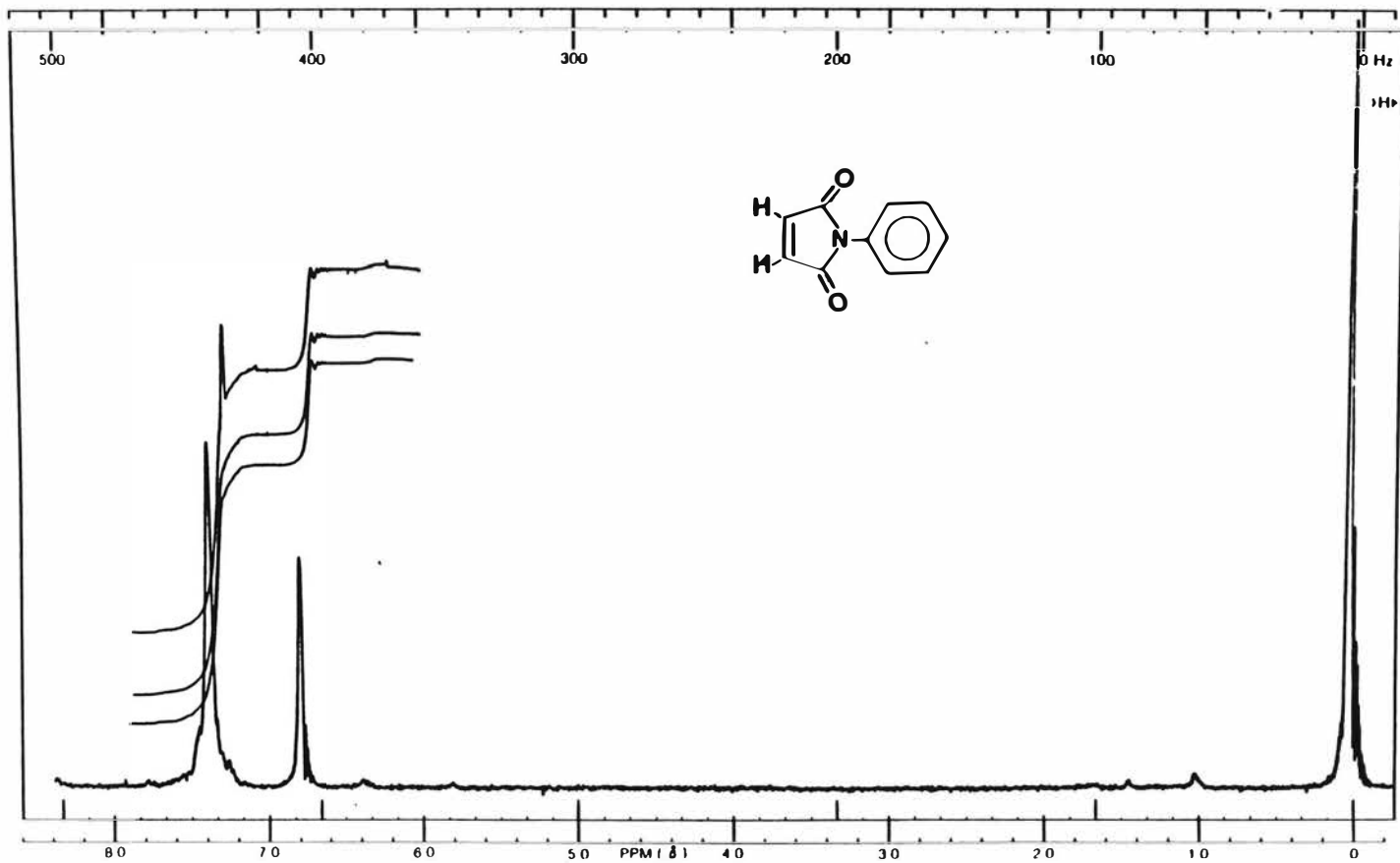


Figure 63 . 60MHz <sup>1</sup>H-NMR Spectrum of N-phenymaleimide.

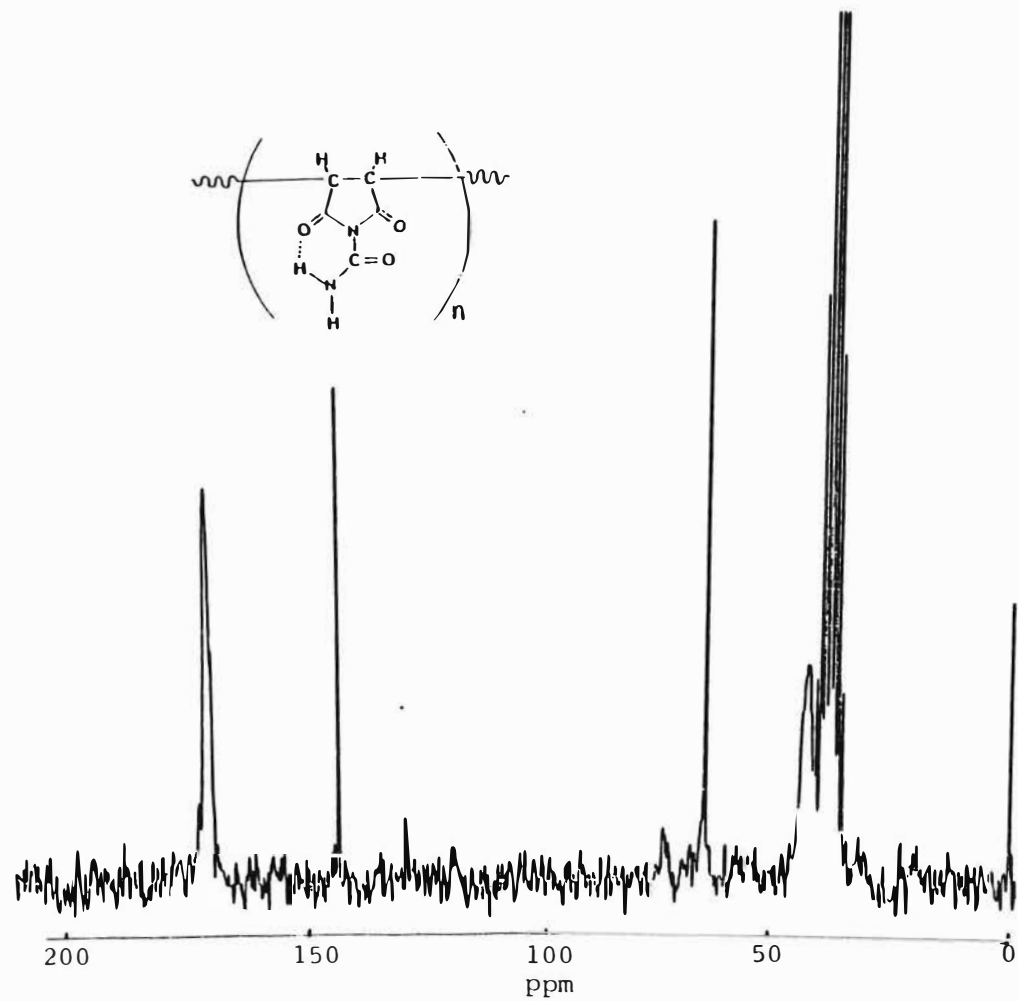


Figure 64 .  $^{13}\text{C}$  NMR Spectrum of Poly(N-carbamylmaleimide).

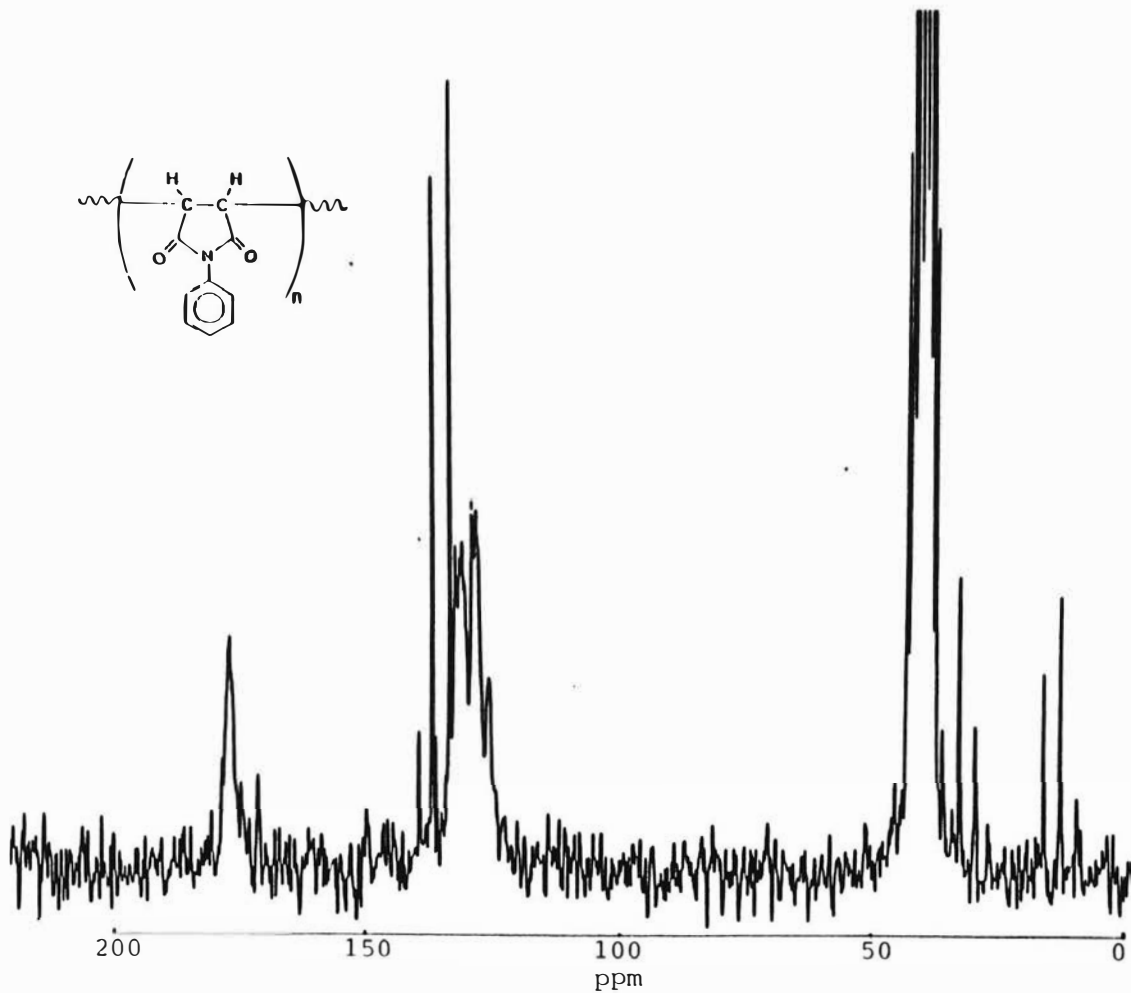


Figure 65 . Off-resonance  $^{13}\text{C}$  NMR Spectrum of Poly(N-phenylmaleimide).



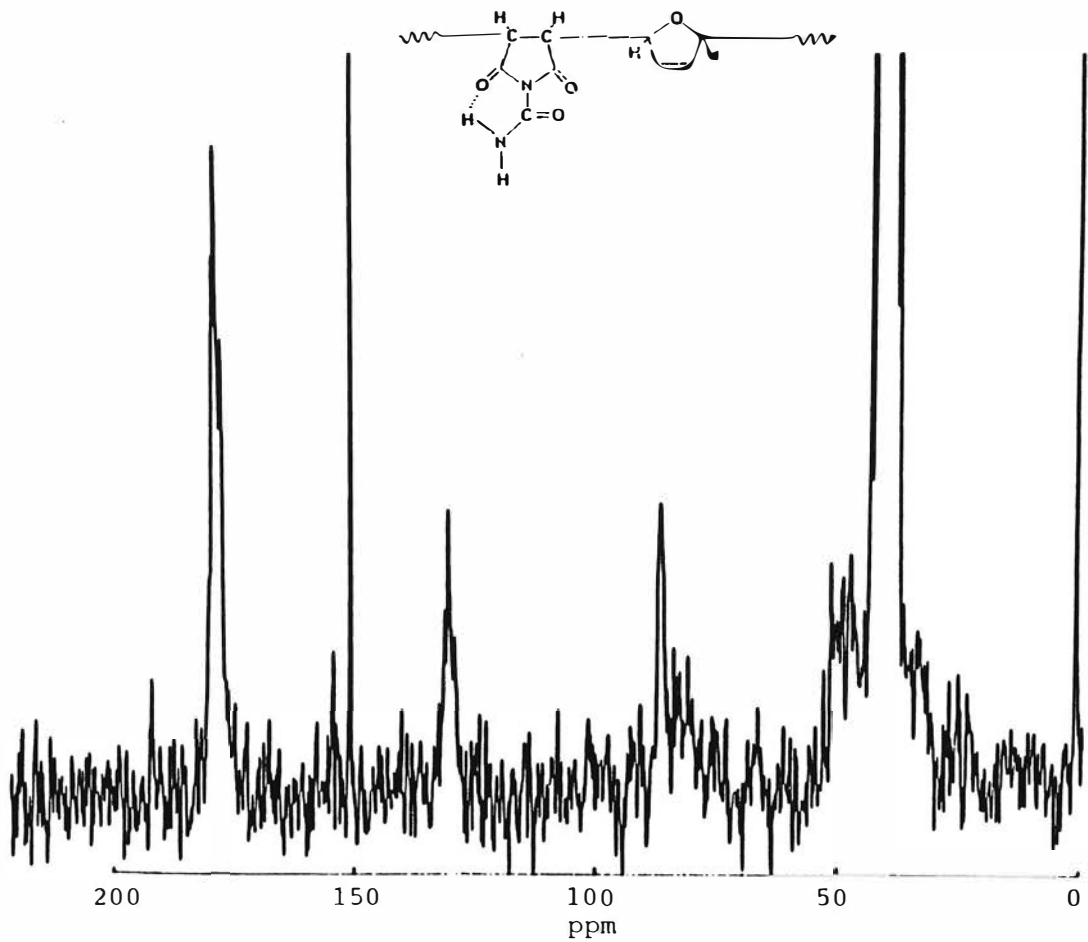


Figure 66 .  $^{13}\text{C}$  NMR Spectrum of Poly(N-carbamylmaleimide-co-Furan).

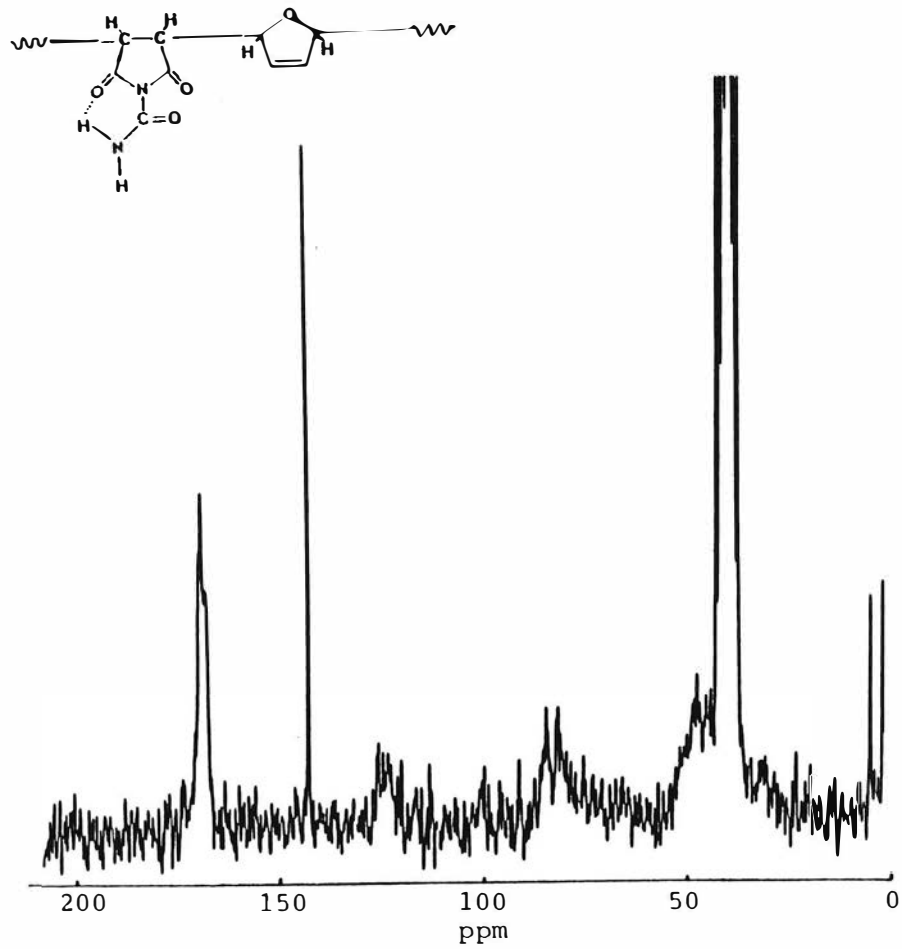


Figure 67. Off-resonance  $^{13}\text{C}$  NMR Spectrum of Poly(N-carbamylmaleimide-co-furan).

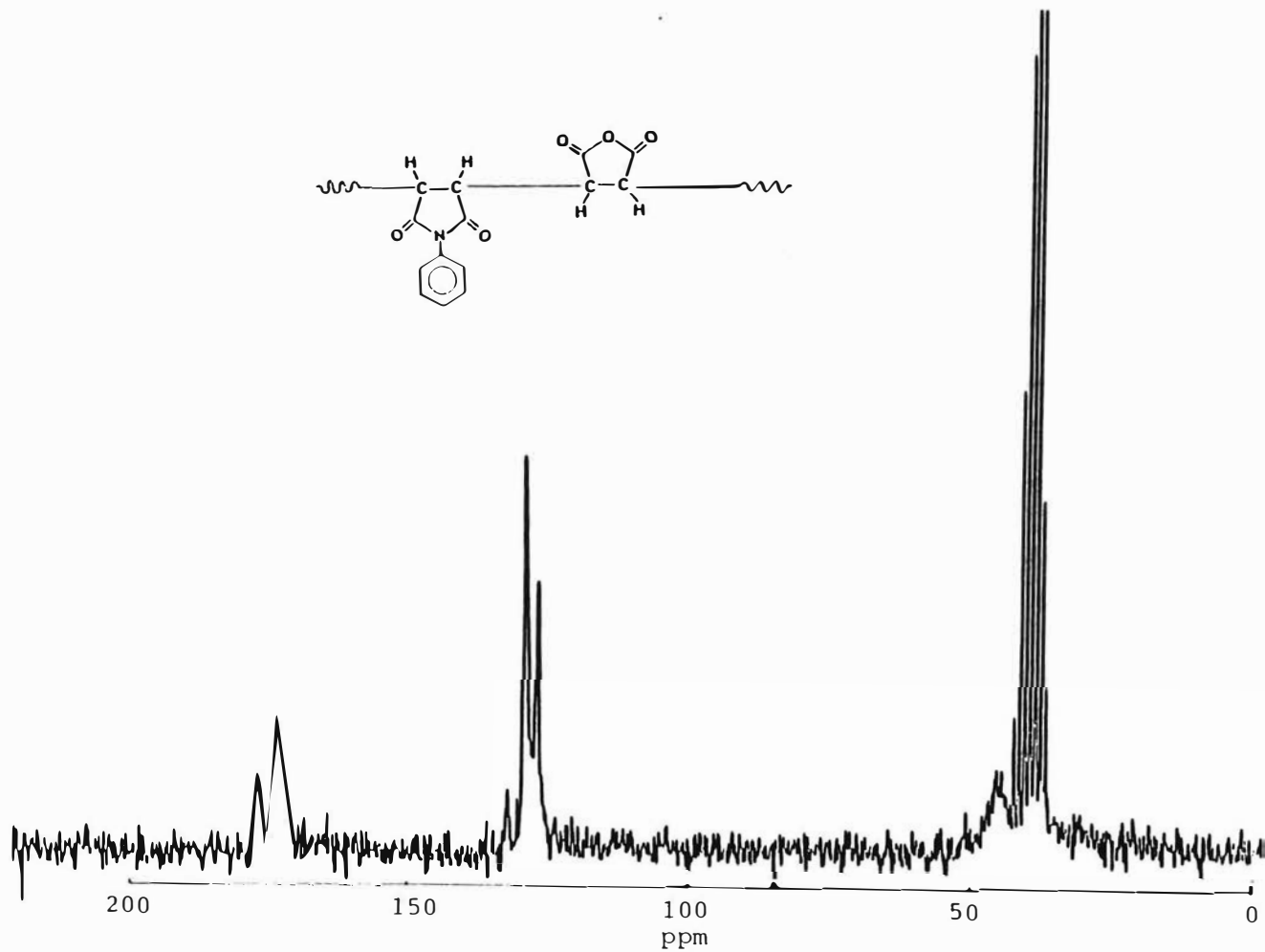
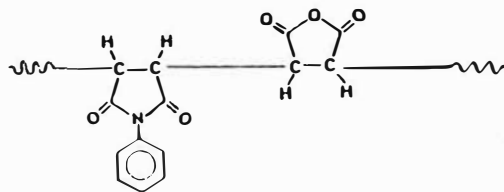


Figure 68.  $^{13}\text{C}$  NMR Spectrum of Poly(N-phenylmaleimide-co-maleic anhydride-10).

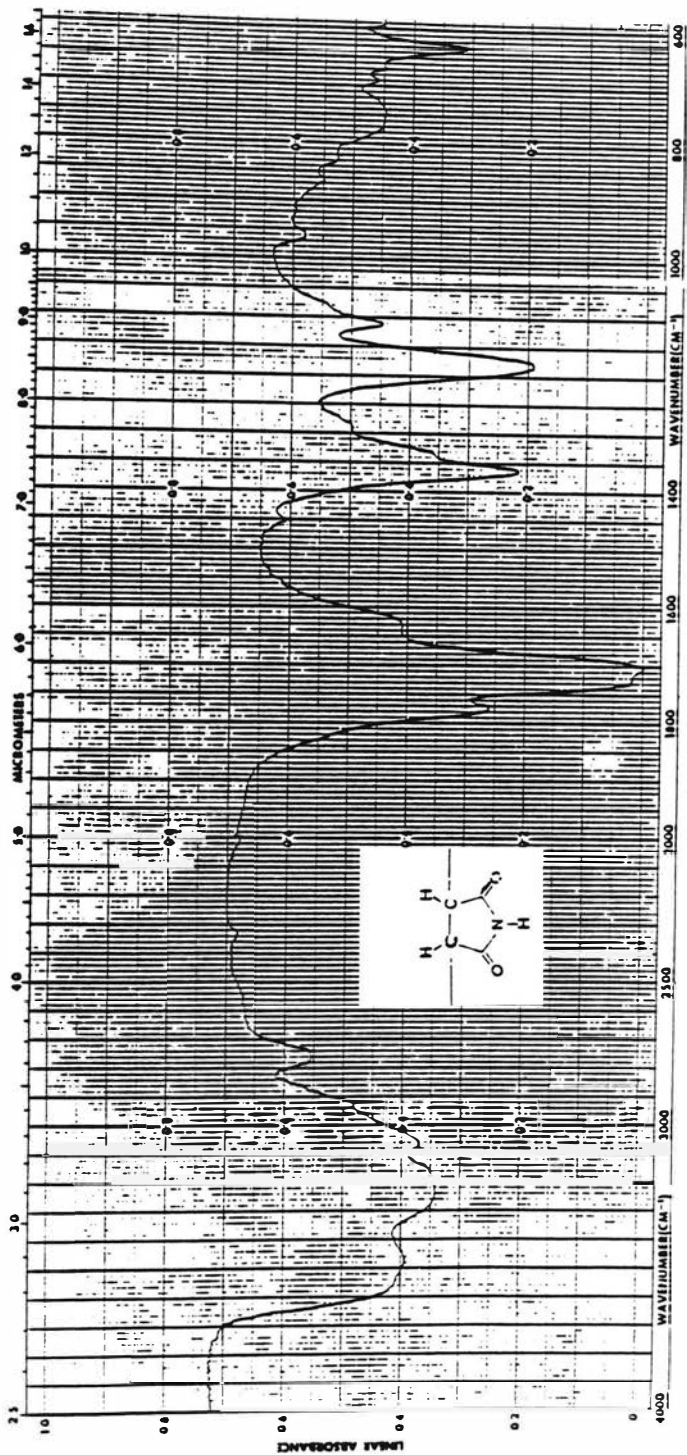


Figure 69. IR Spectrum of Polymaleimide.

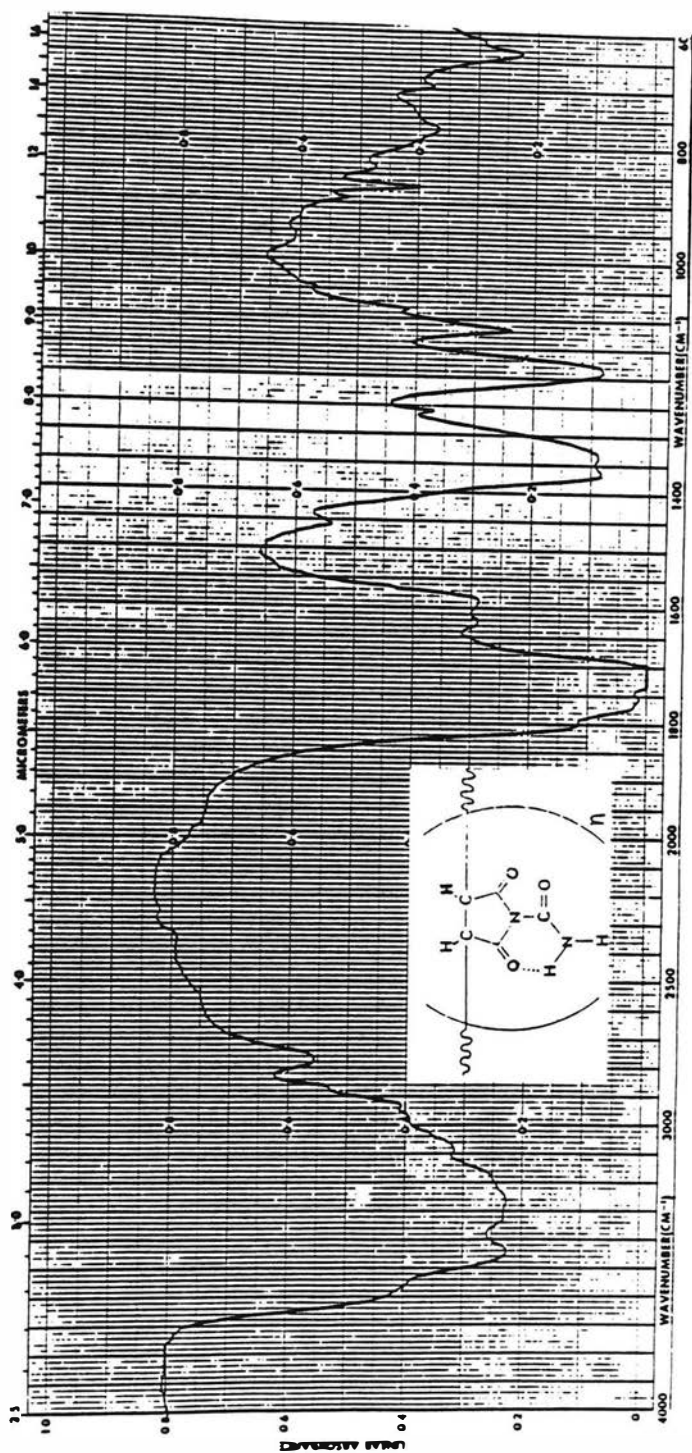


Figure 70. IR Spectrum of Poly(N-carbamylmaleimide).

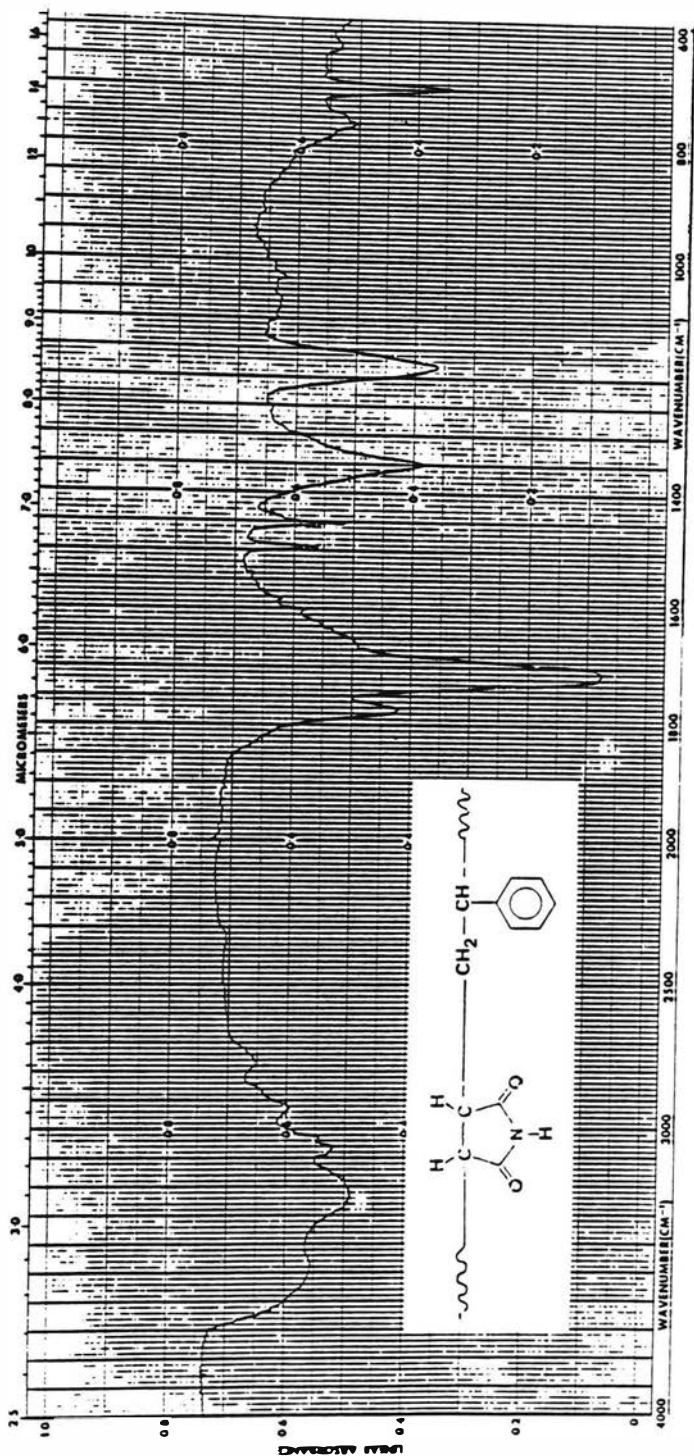


Figure 71. IR Spectrum of Poly(maleimide-co-styrene).

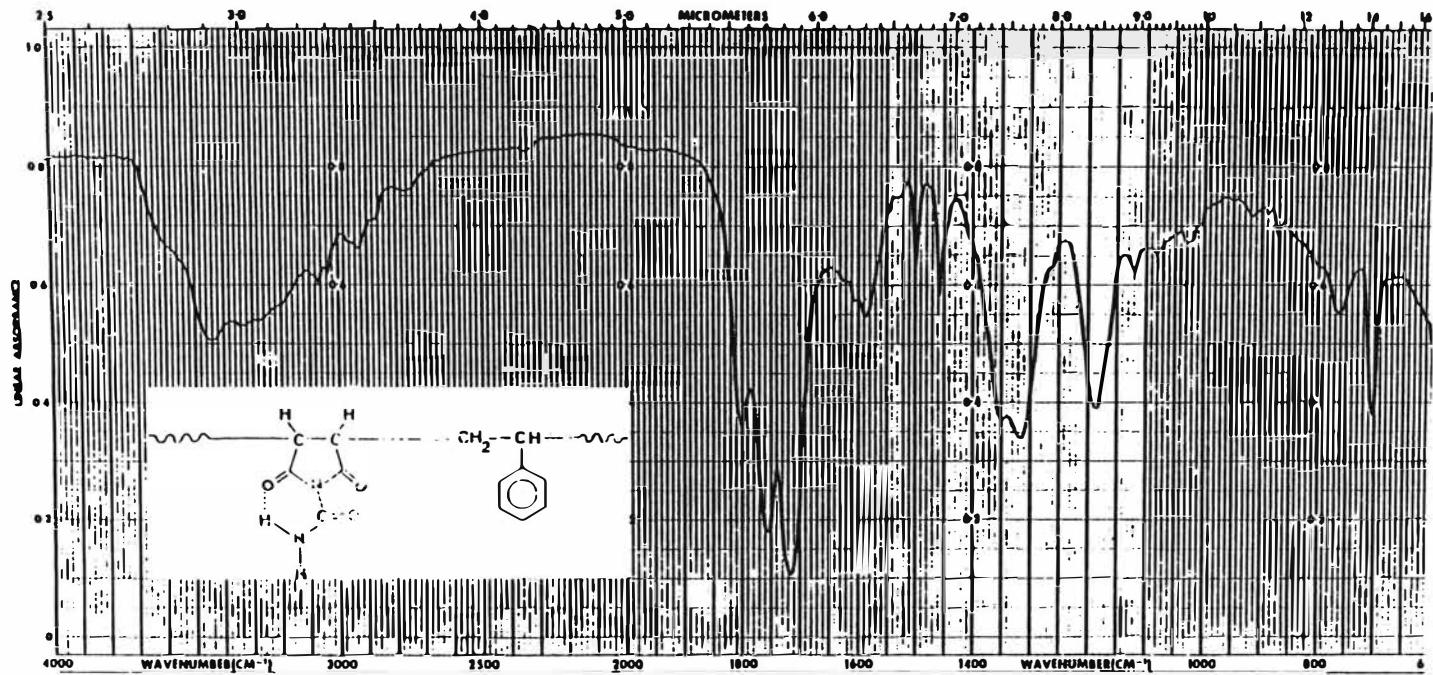


Figure 72. IR Spectrum of Poly(N-carbamylmaleimide-co-styrene).

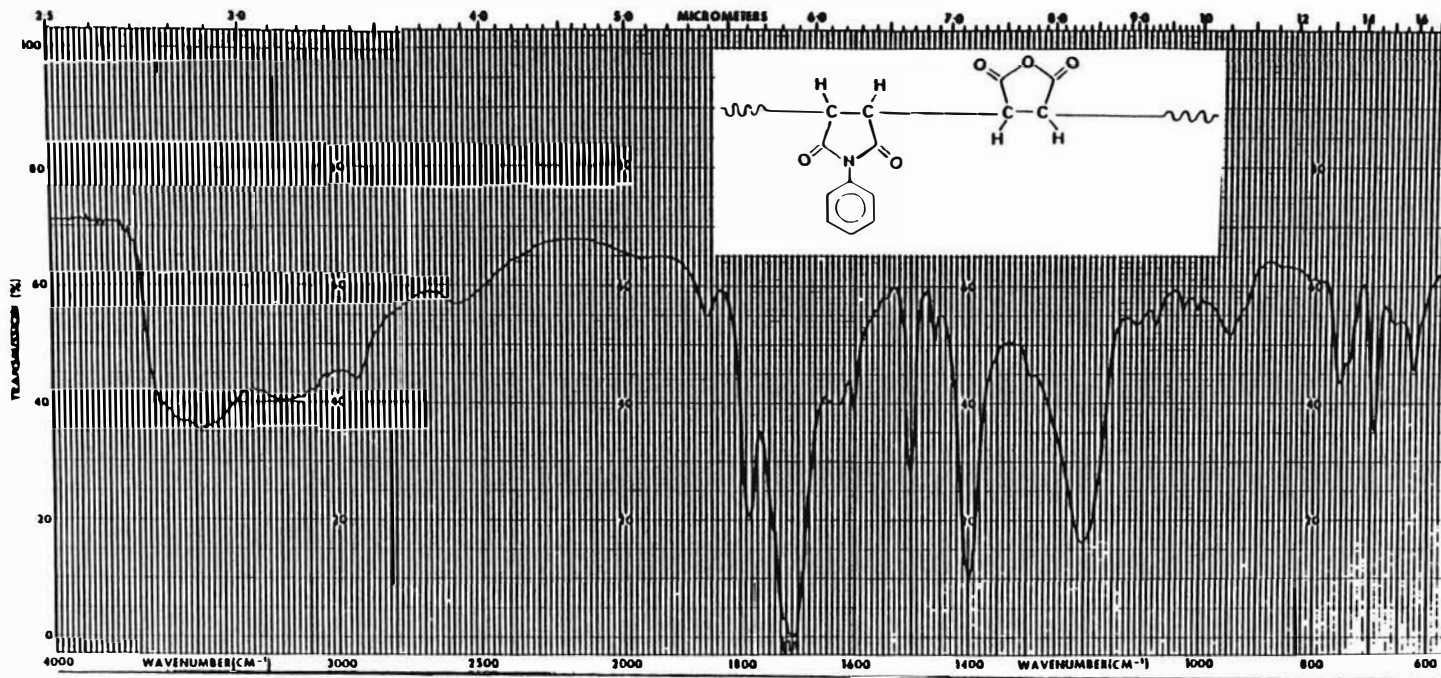


Figure 73 . IR Spectrum of Poly(N-phenylmaleimide-co-maleic anhydride-12).



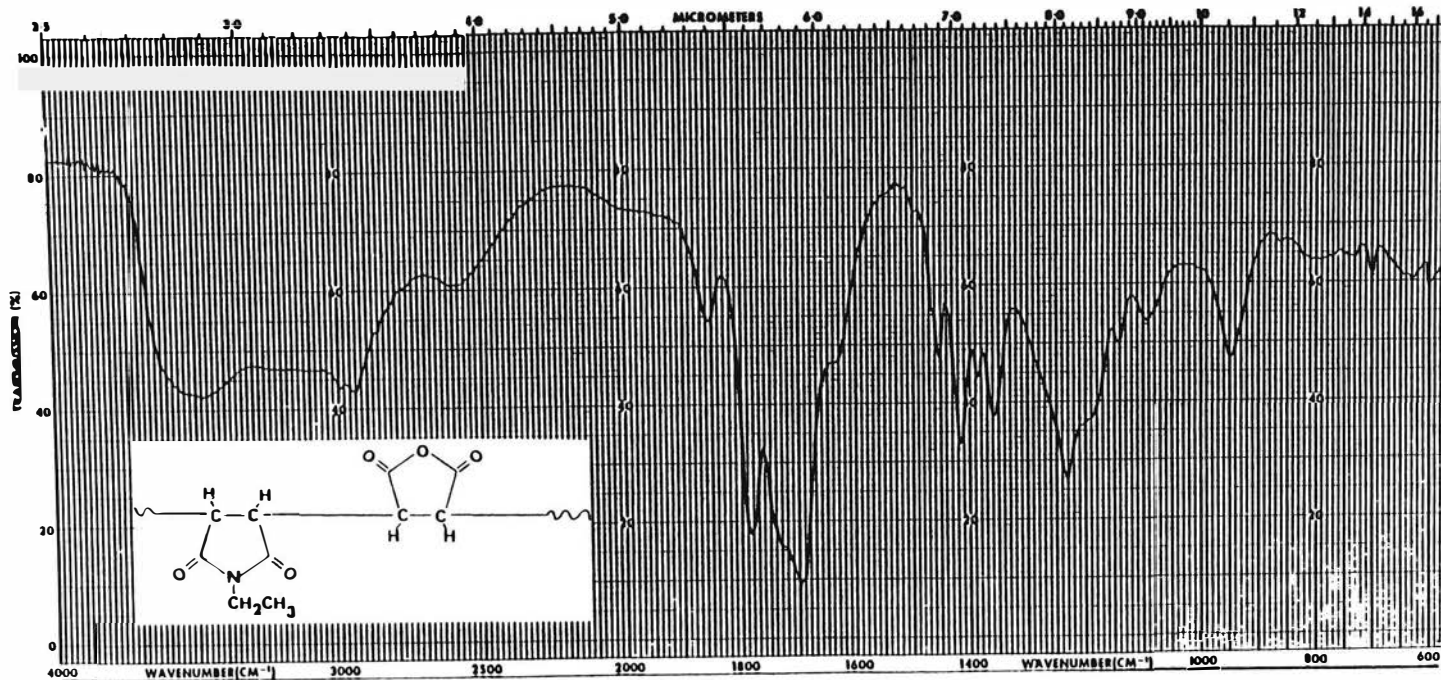


Figure 74. IR spectrum of Poly(N-ethylmaleimide-co-maleic anhydride-7).

VITA

[REDACTED]

[REDACTED]

[REDACTED]

[REDACTED]

[REDACTED]

[REDACTED]

[REDACTED]

[REDACTED]

[REDACTED]

[REDACTED]

[REDACTED]

[REDACTED]

[REDACTED]

[REDACTED]

[REDACTED]

[REDACTED]

[REDACTED]

[REDACTED]

[REDACTED]

[REDACTED]

[REDACTED]

[REDACTED]

[REDACTED]

[REDACTED]

[REDACTED]

[REDACTED]

[REDACTED]

[REDACTED]